2 Conservation of Momentum

The time rate for change in momentum of a body equals the net force exerted on it.

Isaac Newton, Philosophiae Naturalis Principia, 1687

2.1 Introduction

As in Chapter 1, from the large number of formulations of the conservation equations for multiphase flows, local volume averaging as founded by *Anderson* and *Jackson, Slattery*, and *Whitaker* was selected to derive rigorously the momentum equations for multiphase flows conditionally and divided into three velocity fields. The heterogeneous porous-media formulation introduced by *Gentry* et al., commented on by *Hirt*, and used by *Sha, Chao,* and *Soo*, is then implanted into the formalism as a geometrical skeleton. Beyond these concepts, I perform subsequent time averaging. This yields a working form that is applicable to a large variety of problems. All interfacial integrals are suitably transformed in order to enable practical application. Some minor simplifications are introduced in the finally obtained general equation and working equations for each of the three velocity fields are recommended for general use in multiphase fluid dynamic analysis.

This chapter is an improved and extended version of the work published in *Kolev* (1994b). The strategy followed is: We first apply the momentum equations for each of the velocity fields, excluding the interfaces by replacing their actions by forces. Then, we write a force balance at the interfaces, considering them as immaterial and therefore inertialess. This interfacial force balance links the momentum equations that are valid for the both sides of the interface.

2.2 Local volume-averaged momentum equations

2.2.1 Single-phase momentum equations

> The time rate for change in momentum of a body relative to an inertial frame of reference equals the net force exerted on it (*Newton*).

Applied to a single continuum, this principle results in *Euler*'s first law of continuum mechanics (*Truesdell,* 1968). When applied to each velocity field within the control volume, except the interface, this principle yields the well known local instantaneous momentum equation

$$\frac{\partial}{\partial \tau}\left(\rho_l \mathbf{V}_l^\tau\right) + \nabla \cdot \left(\rho_l \mathbf{V}_l^\tau \mathbf{V}_l^\tau - \mathbf{T}_l^\tau\right) + \nabla p_l^\tau + \rho_l \mathbf{g} = 0\,, \tag{2.1}$$

which is valid only inside the velocity field l excluding the interface. Here, the positive velocity direction gives the negative force direction – a commonly used definition. The total stress tensor is split into $p_l^\tau \mathbf{I}$ and $\mathbf{T}_l^\tau$. p_l^τ is the static pressure inside field l, $\mathbf{I}$ is the unit matrix, and $\mathbf{T}_l^\tau$ is the shear stress tensor. $\mathbf{V}_l^\tau \mathbf{V}_l^\tau$ is the dyadic product of two vectors $\mathbf{V}_l^\tau$ and $\mathbf{V}_l^\tau$ – see Appendix 1. It is a second-order tensor. $\mathbf{g}$ is the vector of the gravitational acceleration. Equation (2.1) is the generally accepted balance of momentum for the single phase for velocities that are much smaller than the velocity of light.

2.2.2 Interface force balance (momentum jump condition)

Next, we abstract a volume around the interface having thickness ε converging to zero. Mechanical decoupling of the control volume from the adjacent fields requires replacing the action of the forces on the volume by equivalent forces. In this case, *Cauchy*'s lemma holds:

> The stress vectors acting upon opposite sides of the same surface at a given point are equal in magnitude and opposite in direction, *Truesdell* (1968, p.32).

Characterization of the interface surface tension: Consider two fluids with different densities, fluid *m,* and fluid *l* as presented in Fig. 2.1.

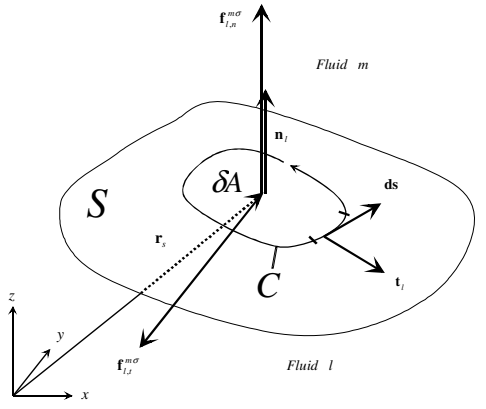

Fig. 2.1 Surface force – geometry definitions

Fluid *m* is a gas and fluid *l* is a liquid, $\rho_l > \rho_m$. A three-dimensional surface *S,* described by the position vector $\mathbf{r}_S(x, y, z)$, separates both fluids. We call such fluids *imiscible*. The unit normal vector of the liquid interface $\mathbf{n}_l$ points outside the liquid *l* and is an important local characteristic of this surface. It is defined from the spatial distribution of the volume fraction of the field *l* as follows:

$$\mathbf{n}_l = -\frac{\nabla(\alpha_l \gamma)}{\left|\nabla(\alpha_l \gamma)\right|}. \tag{2.2}$$

Due to different molecular attraction forces at the two sides of the surface a resulting attraction force with special properties arises at the surface. The force exists only at the surface and acts at the denser fluid *l*. This force is called *surface force*. The surface force per unit mixture volume is denoted by $\mathbf{f}_l^{m\sigma}$. The subscript *l* indicates that the force acts at the field *l*, and the subscript $m\sigma$ indicates that the surface is an interface with field *m*. From the surface *S* we extract an infinitesimal part δA around the point $\mathbf{r}_S(x, y, z)$ so that

$$\boldsymbol{\delta}\mathbf{A} = \mathbf{n}_l \delta A. \tag{2.3}$$

The closed curve *C* contains δA. The closed curve *C* is oriented counterclockwise. Consider the infinitesimal directed line element **ds** called the *arc length vector*. The unit tangent vector to the surface *S* at *C* that is perpendicular to **ds** is **t**. In this case, the following relation holds:

$$\mathbf{t}ds = \mathbf{ds} \times \mathbf{n}_l. \tag{2.4}$$

The surface force exerted on the surface δA by the surface outside of δA across the directed line element **ds** is equal to $\sigma_{lm}\mathbf{t}ds$. Here σ_{lm} is a material property being a force tangential to *S* per unit length called *surface tension*. It may vary

with surface properties such as temperature, concentration of the impurities of the liquid, etc. The net surface force on the element δA is then obtained by summing all forces $\sigma_{lm}\mathbf{t}ds$ exerted on each element of arc length *ds*, $\int_C \sigma_{lm}\mathbf{t}ds$. Using Eq. (2.4) gives

$$\int_C \sigma_{lm}\mathbf{t}ds = \int_C \sigma_{lm}\mathbf{ds}\times\mathbf{n}_l \,. \tag{2.5}$$

The *Stokes* theorem, see *Thomas* et al. (1998) for derivation, allows one to transfer the integral over a closed curve to an integral over the surface closed by this curve

$$\int_C \mathbf{ds}\times\mathbf{n}_l\sigma_{lm} = \iint_S (\mathbf{n}_l\times\nabla)\times\mathbf{n}_l\sigma_{lm}dA \,. \tag{2.6}$$

We see that for the *infinitesimal* surface δA the *surface force per unit interface* is

$$(\mathbf{n}_l\times\nabla)\times\mathbf{n}_l\sigma_{lm} = \sigma_{lm}\left[(\mathbf{n}_l\times\nabla)\times\mathbf{n}_l\right] + (\mathbf{n}_l\times\nabla\sigma_{lm})\times\mathbf{n}_l \,. \tag{2.7}$$

This force can be split into a normal and a tangential component by splitting the gradient into a sum of normal and tangential components

$$\nabla = \nabla_n + \nabla_t \,, \tag{2.8}$$

where

$$\nabla_n = (\nabla\cdot\mathbf{n}_l)\mathbf{n}_l \tag{2.9}$$

and

$$\nabla_t = \nabla - \nabla_n \,. \tag{2.10}$$

Using this splitting and after some mathematical manipulation, *Brackbill* et al. (1992) simplified Eq. (2.7) and finally obtained the very important result,

$$(\mathbf{n}_l\times\nabla)\times\mathbf{n}_l\sigma = -\mathbf{n}_l\sigma_{lm}(\nabla\cdot\mathbf{n}_l) + \nabla_t\sigma_{lm} = \mathbf{n}_l\sigma_{lm}\kappa_l + \nabla_t\sigma_{lm} \,, \tag{2.11}$$

where

$$\kappa_l = -(\nabla\cdot\mathbf{n}_l) = \nabla\cdot\left[\frac{\nabla(\alpha_l\gamma)}{|\nabla(\alpha_l\gamma)|}\right] \tag{2.12}$$

is the curvature of the interface defined only by the gradient of the interface unit vector. Equation (2.12) is used in Eq. (5.4) in *Drazin* and *Reid* (1981, p. 23). Note that the mathematical definition of curvature is the sum of the two principal curvatures which are magnitudes of two vectors. This sum is always positive. The expression resulting from Eq. (2.12) defines curvature with sign, which means with its orientation. The curvature is positive if the center of the curvature is in the fluid *m*. In other words, the positive curvature κ_l is oriented along the normal vector $\mathbf{n}_l$.

As an example, let us estimate the curvature of a liquid layer in stratified flow between two horizontal planes with a gap equal to H. The interface is described by the curve $z^* = \dfrac{z}{H} = \alpha_2(x)$ being in the plane y = const. As coordinates we use (x, y, z^*). The gradient of the liquid volume fraction is then

$$\nabla\alpha_2(x) = \frac{\partial\alpha_2(x)}{\partial x}\mathbf{i} + \frac{\partial\alpha_2(x)}{\partial z^*}\mathbf{k} = \frac{\partial\alpha_2(x)}{\partial x}\mathbf{i} + \frac{\partial z^*}{\partial z^*}\mathbf{k} = \frac{\partial\alpha_2(x)}{\partial x}\mathbf{i} + \mathbf{k}\,.$$

The magnitude of the gradient is then

$$\left|\nabla\alpha_2(x)\right| = \left\{1 + \left[\frac{\partial\alpha_2(x)}{\partial x}\right]^2\right\}^{1/2}.$$

The normal vector is

$$\mathbf{n}_2 = -\frac{\nabla\alpha_2(x)}{\left|\nabla\alpha_2(x)\right|} = -\left(\frac{\dfrac{\partial\alpha_2(x)}{\partial x}}{\left\{1 + \left[\dfrac{\partial\alpha_2(x)}{\partial x}\right]^2\right\}^{1/2}}\mathbf{i} + \frac{1}{\left\{1 + \left[\dfrac{\partial\alpha_2(x)}{\partial x}\right]^2\right\}^{1/2}}\mathbf{k}\right).$$

The curvature in accordance with Eq. (2.12) is then

$$\kappa_l = -(\nabla\cdot\mathbf{n}_l) = \nabla\cdot\left[\frac{\nabla(\alpha_l\gamma)}{\left|\nabla(\alpha_l\gamma)\right|}\right]$$

$$= \nabla\cdot\left(\frac{\dfrac{\partial\alpha_2(x)}{\partial x}}{\left\{1 + \left[\dfrac{\partial\alpha_2(x)}{\partial x}\right]^2\right\}^{1/2}}\mathbf{i} + \frac{1}{\left\{1 + \left[\dfrac{\partial\alpha_2(x)}{\partial x}\right]^2\right\}^{1/2}}\mathbf{k}\right)$$

$$= \frac{\partial}{\partial x}\frac{\dfrac{\partial\alpha_2(x)}{\partial x}}{\left\{1 + \left[\dfrac{\partial\alpha_2(x)}{\partial x}\right]^2\right\}^{1/2}} + \frac{\partial}{\partial z^*}\frac{1}{\left\{1 + \left[\dfrac{\partial\alpha_2(x)}{\partial x}\right]^2\right\}^{1/2}}.$$

Bearing in mind that

$$\frac{\partial}{\partial z^*}\frac{1}{\left\{1+\left[\frac{\partial \alpha_2(x)}{\partial x}\right]^2\right\}^{1/2}} = -\frac{\frac{\partial \alpha_2(x)}{\partial x}\frac{\partial^2 \alpha_2(x)}{\partial x \partial z^*}}{\left\{1+\left[\frac{\partial \alpha_2(x)}{\partial x}\right]^2\right\}^{3/2}} = 0\,,$$

one finally obtains the well known expression

$$\kappa_2 = \frac{\partial^2 \alpha_2(x)}{\partial x^2}\Bigg/\left\{1+\left[\frac{\partial \alpha_2(x)}{\partial x}\right]^2\right\}^{3/2}\,.$$

The higher pressure is in the fluid medium on the concave side of the interface, since surface force in case of constant surface tension is a net normal force directed toward the center of curvature of the interface.

Note that the term $\sigma_{lm}\kappa_l$ becomes important for

$$1/|\kappa_l| < 0.001m\,. \tag{2.13}$$

The term $\nabla_t \sigma_{lm}$ can be expressed as

$$\nabla_t \sigma_{lm} = (\nabla_t T_l)\frac{\partial \sigma_{lm}}{\partial T_l} + \sum_{i=1}^{i_{\max}} (\nabla_t C_{il})\frac{\partial \sigma_{lm}}{\partial C_{il}}\,. \tag{2.14}$$

These terms describe the well known *Marangoni* effect.

The grid density for computational analysis can be judged by comparing the size of the control volume Δx with the curvature. Obviously, if and only if the volume is small enough,

$$\Delta x|\kappa_l| < 1\,, \tag{2.15}$$

the curvature can be resolved by the computational analysis.

No velocity variation across the interface: Consider the case for which there is no velocity variation across the interface (e.g., stagnant fluids) – Fig. 2.2.

The interface pressure $p_l^{m\sigma,\tau}$ is the normal force per unit surface acting on field *l*. This force acts *inside* the field *l* in the immediate vicinity of the interface and in the opposite direction on the interface control volume. It is *different* from the surface force exerted by the pressure of the neighboring velocity field, $p_m^{l\sigma,\tau}$. If there are no other forces except pressure and surface tension, we have

$$p_l^{m\sigma,\tau}\mathbf{n}_l + p_m^{l\sigma,\tau}\mathbf{n}_m + \nabla_l \sigma_{lm} + \sigma_{lm}\kappa_l \mathbf{n}_l = 0\,. \tag{2.16}$$

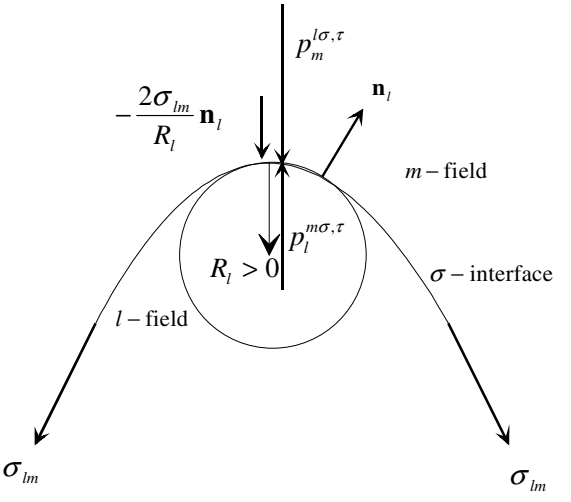

Fig. 2.2 Interface force equilibrium without mass transfer and Marangoni effect (Laplace)

This equation is known as the *Laplace* equation. If, in addition, we have viscous forces acting on the two sides the momentum balance is

$$\left(\mathbf{T}_l^{m\sigma,\tau} - p_l^{m\sigma,\tau}\mathbf{I}\right)\cdot\mathbf{n}_l + \left(\mathbf{T}_m^{l\sigma,\tau} - p_m^{l\sigma,\tau}\mathbf{I}\right)\cdot\mathbf{n}_m - \nabla_l\sigma_{lm} - \sigma_{lm}\kappa_l\mathbf{n}_l = 0\,. \qquad (2.17)$$

Velocity variation across the interface: If mass is transferred from one to the other fluid for whatever reason, the interface moves in space not only convectively but is also controlled by the amount of mass transferred between the fields – Fig. 2.3. In this case, the interface velocity $\mathbf{V}_{lm}^{\tau}$ is not equal to the neighboring field velocities. The mass flow rate

$$(\rho w)_{lm} = \rho_l\left(\mathbf{V}_l^{\tau} - \mathbf{V}_{lm}^{\tau}\right)\cdot\mathbf{n}_l$$

enters the interface control volume and exerts the force $\rho_l\mathbf{V}_l^{\tau}\left(\mathbf{V}_l^{\tau} - \mathbf{V}_{lm}^{\tau}\right)\cdot\mathbf{n}_l$ per unit surface on it. Note that this force has the same direction as the pressure force inside the field *l*. Similarly, we have a reactive force $\rho_m\mathbf{V}_m^{\tau}\left(\mathbf{V}_m^{\tau} - \mathbf{V}_{lm}^{\tau}\right)\cdot\mathbf{n}_m$ exerted per unit surface on the control volume by the leaving mass flow rate. Assuming that the control volume moves with the normal component of the interface velocity, $\mathbf{V}_{lm}^{\tau}\cdot\mathbf{n}_l$, we obtain the following force balance:

$$\begin{aligned}&-\rho_l\mathbf{V}_l^{\tau}\left(\mathbf{V}_l^{\tau} - \mathbf{V}_{lm}^{\tau}\right)\cdot\mathbf{n}_l + \left(\mathbf{T}_l^{m\sigma,\tau} - p_l^{m\sigma,\tau}\mathbf{I}\right)\cdot\mathbf{n}_l\\ &-\rho_m\mathbf{V}_m^{\tau}\left(\mathbf{V}_m^{\tau} - \mathbf{V}_{m\sigma}^{\tau}\right)\cdot\mathbf{n}_m + \left(-p_{m\sigma}^{\tau}\mathbf{I} + \mathbf{T}_{m\sigma}^{\tau}\right)\cdot\mathbf{n}_m - \nabla_l\sigma_{lm} - \sigma_{lm}\kappa_l\mathbf{n}_l = 0\,. \quad (2.18)\end{aligned}$$

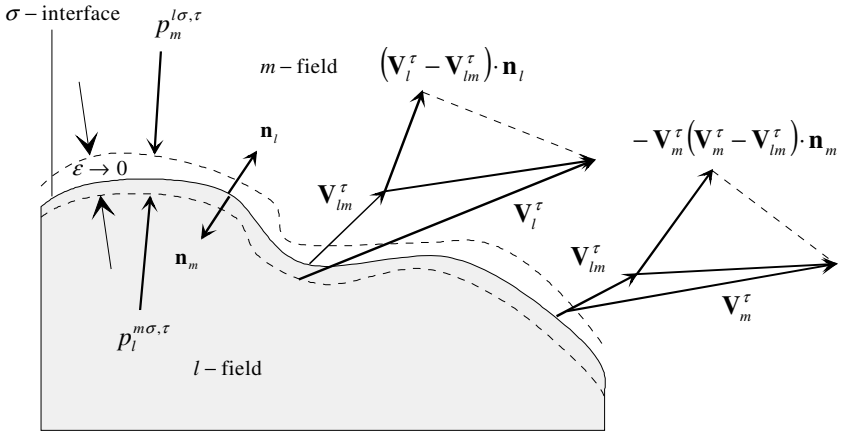

Fig. 2.3 Definition of the interface characteristics

This is the general form of the interfacial momentum jump condition. It is convenient to rewrite the above equation by using the mass jump condition at the interface

$$\rho_l(\mathbf{V}_l^\tau - \mathbf{V}_{lm}^\tau)\cdot\mathbf{n}_l + \rho_m(\mathbf{V}_m^\tau - \mathbf{V}_{lm}^\tau)\cdot\mathbf{n}_m = 0\,, \tag{2.19}$$

which is Eq. (1.42). The result is

$$\left[\rho_l(\mathbf{V}_l^\tau - \mathbf{V}_{lm}^\tau)\left(\mathbf{V}_m^\tau - \mathbf{V}_l^\tau\right) + \left(p_m^{l\sigma,\tau} - p_l^{m\sigma,\tau}\right)\mathbf{I} + \mathbf{T}_l^{m\sigma,\tau} - \mathbf{T}_m^{l\sigma,\tau} - \sigma_{lm}\kappa_l\right]\cdot\mathbf{n}_l - \nabla_l\sigma_{lm} = 0 \tag{2.20}$$

or

$$(\rho w)_{lm}\left(\mathbf{V}_m^\tau - \mathbf{V}_l^\tau\right) + \left(p_m^{l\sigma,\tau} - p_l^{m\sigma,\tau}\right)\mathbf{n}_l + \left[\mathbf{T}_l^{m\sigma,\tau} - \mathbf{T}_m^{l\sigma,\tau} - \sigma_{lm}\kappa_l\right]\cdot\mathbf{n}_l - \nabla_l\sigma_{lm} = 0\,. \tag{2.21}$$

The projection of this force to the normal direction is obtained by scalar multiplication of the above equation with the unit vector $\mathbf{n}_l$. The result is

$$(\rho w)_{lm}\left(\mathbf{V}_m^\tau - \mathbf{V}_l^\tau\right)\cdot\mathbf{n}_l + p_m^{l\sigma,\tau} - p_l^{m\sigma,\tau} - \sigma_{lm}\kappa_l + \left[\left(\mathbf{T}_l^{m\sigma,\tau} - \mathbf{T}_m^{l\sigma,\tau}\right)\cdot\mathbf{n}_l\right]\cdot\mathbf{n}_l$$
$$-\left(\nabla_l\sigma_{lm}\right)\cdot\mathbf{n}_l = 0\,. \tag{2.22}$$

Using the mass conservation at the interface we finally have an important force balance normal to the interface

$$(\rho w)_{lm}^2\left(\frac{1}{\rho_m} - \frac{1}{\rho_l}\right) + p_m^{l\sigma,\tau} - p_l^{m\sigma,\tau} - \sigma_{lm}\kappa_l + \left[\left(\mathbf{T}_l^{m\sigma,\tau} - \mathbf{T}_m^{l\sigma,\tau}\right)\cdot\mathbf{n}_l\right]\cdot\mathbf{n}_l$$
$$-\left(\nabla_l\sigma_{lm}\right)\cdot\mathbf{n}_l = 0\,. \tag{2.23}$$

Neglecting all forces except those caused by pressure and interfacial mass transfer results in the surprising conclusion that during the mass transfer the pressure in the denser fluid is always larger than the pressure in the lighter fluid independently of the direction of the mass transfer – *Delhaye* (1981, p. 52, Eq. (2.64)).

For the limiting case of no interfacial mass transfer and dominance of the pressure difference, the velocity of the interface can be expressed as a function of the pressure difference and the velocities in the bulk of the fields,

$$V_{lm}^{n,\tau} = V_l^{n,\tau} - \frac{p_m^{l\sigma,\tau} - p_l^{m\sigma,\tau}}{\rho_l \left(V_m^{n,\tau} - V_l^{n,\tau} \right)} . \tag{2.24}$$

This velocity is called contact discontinuity velocity. Replacing the discontinuity velocity with Eq. (1.42), we obtain

$$\left(V_l^{n,\tau} - V_m^{n,\tau} \right)^2 = \frac{\rho_l - \rho_m}{\rho_l \rho_m} \left(p_l^{m\sigma,\tau} - p_m^{l\sigma,\tau} \right) . \tag{2.25}$$

For the case $\rho_l >> \rho_m$, we have the expected result that the pressure difference equals the stagnation pressure at the side of the lighter medium

$$p_l^{m\sigma,\tau} - p_m^{l\sigma,\tau} = \rho_m \left(V_l^{n,\tau} - V_m^{n,\tau} \right)^2 . \tag{2.26}$$

2.2.3 Local volume averaging of the single-phase momentum equation

The aim here is to average Eq. (2.1) over the total control volume – see Fig. 2.4.

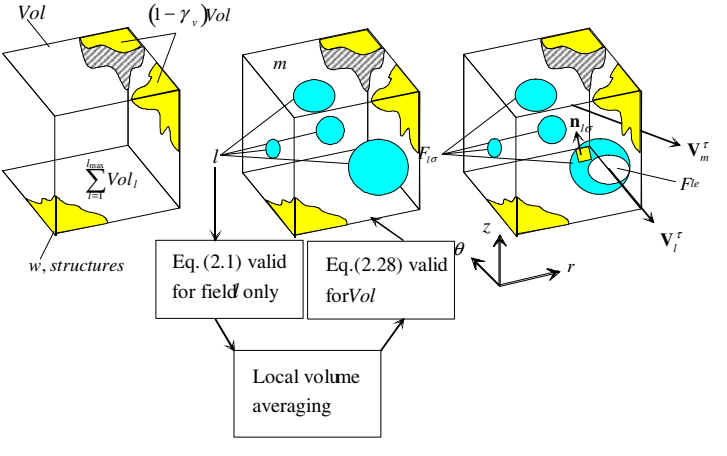

Fig. 2.4 Definition regions for single-phase instantaneous momentum balance and the local volume average balance

The mathematical tools used to derive local volume-averaged field conservation equations for the property being any scalar, vectorial, or tensorial function of time and location are once again *Slattery–Whitaker*'s spatial averaging theorem, together with the *Gauss–Ostrogradskii* theorem and the general transport equation (*Leibnitz* rule), see *Anderson* and *Jackson* (1967), *Slattery* (1967), *Whitaker* (1967, 1985, 1969), and *Gray* and *Lee* (1977). Applying the local volume average to Eq. (2.1), the following is obtained:

$$\left\langle \frac{\partial}{\partial \tau}\left(\rho_l \mathbf{V}_l^{\tau}\right)\right\rangle + \left\langle \nabla \cdot \left(\rho_l \mathbf{V}_l^{\tau}\mathbf{V}_l^{\tau}\right)\right\rangle - \left\langle \nabla \cdot \left(\mathbf{T}_l^{\tau}\right)\right\rangle + \left\langle \nabla p_l^{\tau}\right\rangle + \left\langle \rho_l \mathbf{g}\right\rangle = 0\,, \qquad (2.27)$$

or using Eqs. (1.28), (1.32), and (1.28), (*Kolev*, 1994),

$$\frac{\partial}{\partial \tau}\left\langle \rho_l \mathbf{V}_l^{\tau}\right\rangle + \nabla \cdot \left\langle \rho_l \mathbf{V}_l^{\tau}\mathbf{V}_l^{\tau}\right\rangle + \nabla \cdot \left\langle p_l^{\tau}\mathbf{I} - \mathbf{T}_l^{\tau}\right\rangle + \frac{1}{Vol}\int\limits_{F_{l\sigma}+F_{lw}} \rho_l \mathbf{V}_l^{\tau}\left(\mathbf{V}_l^{\tau} - \mathbf{V}_l^{\sigma,\tau}\right)\cdot \mathbf{n}_l dF$$

$$-\frac{1}{Vol}\int\limits_{F_{l\sigma}+F_{lw}} \left(-p_l^{\tau}\mathbf{I} + \mathbf{T}_l^{\tau}\right)\cdot \mathbf{n}_l dF + \mathbf{g}\rho_l = 0\,. \qquad (2.28)$$

The volume average momentum equation can be rewritten using the *weighted average*, see Eq. (1.19), *Kolev* (1994),

$$\left\langle \mathbf{V}_l^{\tau}\right\rangle^{le,\rho} = \left\langle \rho_l \mathbf{V}_l^{\tau}\right\rangle^{le} / \left\langle \rho_l \right\rangle^{l}, \qquad (2.29)$$

and

$$\left\langle \mathbf{V}_l^{\tau}\right\rangle^{le}\left\langle \mathbf{V}_l^{\tau}\right\rangle^{le} = \left\langle \rho_l \mathbf{V}_l^{\tau}\mathbf{V}_l^{\tau}\right\rangle^{le} / \left\langle \rho_l \right\rangle^{l}. \qquad (2.30)$$

The result is

$$\frac{\partial}{\partial \tau}\left(\alpha_l \gamma_v \left\langle \rho_l \right\rangle^{l}\left\langle \mathbf{V}_l^{\tau}\right\rangle^{le}\right) + \nabla \cdot \left(\alpha_l^{e}\gamma \left\langle \rho_l \right\rangle^{l}\left\langle \mathbf{V}_l^{\tau}\right\rangle^{le}\left\langle \mathbf{V}_l^{\tau}\right\rangle^{le}\right) - \nabla \cdot \left(\alpha_l^{e}\gamma \left\langle \mathbf{T}_l^{\tau}\right\rangle^{le}\right)$$

$$+\nabla\left(\alpha_l^{e}\gamma\left\langle p_l^{\tau}\right\rangle^{le}\right) + \alpha_l\gamma_v\left\langle \rho_l\right\rangle^{l}\mathbf{g} - \frac{1}{Vol}\int\limits_{F_{l\sigma}}\left[-p_l^{m\sigma,\tau}\mathbf{I} + \mathbf{T}_l^{m\sigma,\tau} - \rho_l \mathbf{V}_l^{\tau}\left(\mathbf{V}_l^{\tau} - \mathbf{V}_{lm}^{\tau}\right)\right]\cdot \mathbf{n}_l dF$$

$$-\frac{1}{Vol}\int\limits_{F_{lw}}\left[-p_l^{w\sigma,\tau}\mathbf{I} + \mathbf{T}_l^{w\sigma,\tau} - \rho_l \mathbf{V}_l^{\tau}\left(\mathbf{V}_l^{\tau} - \mathbf{V}_{lw}^{\tau}\right)\right]\cdot \mathbf{n}_l dF = 0\,. \qquad (2.31)$$

We assume that the weighted average of products can be replaced by the products of the average. This should be borne in mind when constructing a numerical algorithm for solving the final system and selecting the size of the finite volume so as to be not so large as to violate the validity of this assumption.

Note the differences between Eq. (2.31) and the final result obtained by *Ishii* (1975), Eq. (3.16):

(a) the directional permeability is used here instead of the volumetric porosity in the pressure gradient term, and

(b) as for the mass conservation equation in *Kolev* (1994a), the volumetric porosity is kept below the time differential since it can be a function of time in a number of interesting applications.

For the case $\gamma_v = \gamma = 1$ and one-dimensional flow, Eq. (2.31) reduces to Eq. (15) derived by *Delhaye* in *Hetstrony* (1982, p. 163).

Equation (2.31), the rigorously derived local volume average momentum equation, is not amenable to direct use in computational models without further transformation. In order to facilitate its practical use

(a) the integral expression must be evaluated, and
(b) the time averaging must be performed subsequently.

These steps, which go beyond *Sha* et al. (1984), are performed in Sects. 2.3 and 2.4.

2.3 Rearrangement of the surface integrals

The expression under the surface integral is replaced by its equivalent from the momentum jump condition, Eq. (2.18):

$$-\frac{1}{Vol}\int_{F_{l\sigma}}\left[-\rho_l \mathbf{V}_l^{\tau}\left(\mathbf{V}_l^{\tau}-\mathbf{V}_{lm}^{\tau}\right)+\mathbf{T}_l^{m\sigma,\tau}-p_l^{m\sigma,\tau}\mathbf{I}\right]\cdot\mathbf{n}_l dF$$

$$=-\frac{1}{Vol}\int_{F_{l\sigma}}\left\{\left[-\rho_m \mathbf{V}_m^{\tau}\left(\mathbf{V}_m^{\tau}-\mathbf{V}_{m\sigma}^{\tau}\right)+\mathbf{T}_m^{l\sigma,\tau}-p_m^{l\sigma,\tau}\mathbf{I}+\sigma_{lm}\kappa_l\right]\cdot\mathbf{n}_l+\nabla_l\sigma_{lm}\right\}dF \quad (2.32)$$

Note that there are no surface force terms in Eq. (2.31). Equation (2.32) reflects the action of the surface forces and the action of the stresses caused by the surrounding field *m* on *l*. Note also that if the momentum equations are written for two neighboring fields the interface forces will appear in both equations with opposite sign only if the equations are applied to a common dividing surface. Otherwise, the exchange terms in question will be nonsymmetric.

The *intrinsic surface-averaged* field pressure at the entrances and exits of the control volume crossing the field *m* is $\left\langle p_m^{\tau}\right\rangle^{me}$. We call it bulk pressure inside the velocity field *m* at this particular surface. The interfacial *m*-side pressure $p_m^{l\sigma,\tau}$ can be expressed as the sum of the intrinsic averaged pressure, $\left\langle p_m^{\tau}\right\rangle^{me}$, which is not a function of the position at the interface inside the control volume and can be taken outside of the integral sign, and a pressure difference $\Delta p_m^{l\sigma,\tau}$, which is a function of the position at the interface in the control volume

$$p_m^{l\sigma,\tau}=\left\langle p_m^{\tau}\right\rangle^{me}+\Delta p_m^{l\sigma,\tau}. \quad (2.33)$$

The same is performed for all other fields. Similarly, the surface pressure of the field structure interface is expressed as

$$p_l^{w\sigma,\tau} = \left\langle p_l^{\tau} \right\rangle^{le} + \Delta p_l^{w\sigma,\tau} . \tag{2.34}$$

The interfacial pressure differs from the bulk pressures of the corresponding fields $m\sigma$, and lw, $\Delta p_m^{l\sigma,\tau} \neq 0$ and $\Delta p_l^{w\sigma,\tau} \neq 0$. This occurs because obstacles to the continuous phase can cause local velocity decreases or increases at the interface velocity boundary layer, resulting in increased or decreased pressure relative to bulk pressure. In order to estimate the surface integrals the exact dependence of the pressure as a function of the position at the interface inside the control volume must be elaborated for each idealized flow pattern and form of the structure. The same is valid for the viscous shear stresses $\mathbf{T}_m^{l\sigma,\tau}$ and $\mathbf{T}_l^{w\sigma,\tau}$. Note that in order to estimate the interfacial pressure integrals for practical use of the momentum equations the time averaging must be performed first to make it admissible to use the real pressure distributions measured experimentally on bodies in turbulent flow.

Substituting Eqs. (2.32)–(2.34) into Eq. (2.31), we obtain

$$\begin{aligned}
&\frac{\partial}{\partial \tau}\left(\alpha_l \gamma_v \left\langle \rho_l \right\rangle^l \left\langle \mathbf{V}_l^{\tau} \right\rangle^{le}\right) + \nabla \cdot \left(\alpha_l^e \gamma \left\langle \rho_l \right\rangle^l \left\langle \mathbf{V}_l^{\tau} \right\rangle^{le} \left\langle \mathbf{V}_l^{\tau} \right\rangle^{le}\right) - \nabla \cdot \left(\alpha_l^e \gamma \left\langle \mathbf{T}_l^{\tau} \right\rangle^{le}\right) \\
&+ \nabla\left(\alpha_l^e \gamma \left\langle p_l^{\tau} \right\rangle^{le}\right) + \alpha_l \gamma_v \left\langle \rho_l \right\rangle^l \mathbf{g} + \frac{1}{Vol} \int_{F_{l\sigma}} \left\langle p_m^{\tau} \right\rangle^{me} \mathbf{n}_l dF + \frac{1}{Vol} \int_{F_{lw}} \left\langle p_l^{\tau} \right\rangle^{le} \mathbf{n}_l dF \\
&- \frac{1}{Vol} \int_{F_{l\sigma}} \left\{ \left[-\Delta p_m^{l\sigma,\tau} \mathbf{I} + \mathbf{T}_m^{l\sigma,\tau} - \rho_m \mathbf{V}_m^{\tau} \left(\mathbf{V}_m^{\tau} - \mathbf{V}_{lm}^{\tau} \right) + \sigma_{lm} \kappa_l \right] \cdot \mathbf{n}_l + \nabla_t \sigma_{lm} \right\} dF \\
&- \frac{1}{Vol} \int_{F_{lw}} \left[-\Delta p_l^{w\sigma,\tau} \mathbf{I} + \mathbf{T}_l^{w\sigma,\tau} - \rho_l \mathbf{V}_l^{\tau} \left(\mathbf{V}_l^{\tau} - \mathbf{V}_{lw}^{\tau} \right) \right] \cdot \mathbf{n}_l dF = 0 .
\end{aligned} \tag{2.35}$$

Keeping in mind that $\left\langle p_m^{\tau} \right\rangle^{me}$ and $\left\langle p_l^{\tau} \right\rangle^{le}$ are not functions of the interface position inside the control volume, and making use of Eq. (1.32) (see also *Kolev* (1994)), the bulk pressure integrals can then be rewritten as follows:

$$\begin{aligned}
&\left\langle p_m^{\tau} \right\rangle^{me} \frac{1}{Vol} \int_{F_{l\sigma}} \mathbf{n}_l dF + \left\langle p_l^{\tau} \right\rangle^{le} \frac{1}{Vol} \int_{F_{lw}} \mathbf{n}_{lw} dF \\
&= -\left\langle p_m^{\tau} \right\rangle^{me} \nabla\left(\alpha_l^e \gamma\right) + \left(\left\langle p_l^{\tau} \right\rangle^{le} - \left\langle p_m^{\tau} \right\rangle^{me} \right) \frac{1}{Vol} \int_{F_{lw}} \mathbf{n}_l dF .
\end{aligned} \tag{2.36}$$

Rearranging the surface tension integrals: The surface force per unit volume of the mixture is, in fact, the local volume average of the surface tension force

$$\mathbf{f}_l^{m\sigma} = -\frac{1}{Vol} \iint_{F_{l\sigma}} \left(\mathbf{n}_l \sigma_{lm} \kappa + \nabla_t \sigma_{lm} \right) dF . \tag{2.37}$$

Note that the orientation of this force is defined with respect the coordinate system given in Fig. 2.1. Using Eq. (1.29) we have

$$\mathbf{f}_l^{m\sigma} = -\sigma_{lm}\kappa_l \frac{1}{Vol}\iint_{F_{l\sigma}} \mathbf{n}_l \sigma_{lm}\kappa dF - \frac{1}{Vol}\iint_{F_{l\sigma}} (\nabla_t \sigma_{lm}) dF$$

$$= \sigma_{lm}\kappa_l \left[\nabla\left(\alpha_l^e \gamma\right) + \frac{1}{Vol}\int_{F_{lw}} \mathbf{n}_l dF \right] - \frac{1}{Vol}\iint_{F_{l\sigma}} (\nabla_t \sigma_{lm}) dF \,, \tag{2.38}$$

with normal

$$\mathbf{f}_{l,n}^{m\sigma} = \sigma_{lm}\kappa_l \left[\nabla\left(\alpha_l^e \gamma\right) + \frac{1}{Vol}\int_{F_{lw}} \mathbf{n}_l dF \right] = \sigma_{lm} \nabla \cdot \left[\frac{\nabla(\alpha_l \gamma)}{\left|\nabla(\alpha_l \gamma)\right|} \right] \left[\nabla\left(\alpha_l^e \gamma\right) + \frac{1}{Vol}\int_{F_{lw}} \mathbf{n}_l dF \right]$$

for $\alpha_l > 0$ (2.39)

and tangential

$$\mathbf{f}_{l,t}^{m\sigma} = -\frac{1}{Vol}\iint_{F_{l\sigma}} (\nabla_t \sigma_{lm}) dF \approx -a_{lm} \nabla_t \sigma_{lm} \tag{2.40}$$

surface force components per unit volume of the mixture, respectively. Here a_{lm} is the interfacial area density. In the literature, the local volume averaged surface force is sometimes called the *continuum surface force* or abbreviated as CSF, see *Brackbill* et al. (1992).

Note that if the surface tension is a constant in space there is no resulting tangential force component. At plane surfaces the curvature is zero and therefore there is no normal force acting at the liquid. If the liquid consists of clouds of spheres the local surface force creates only a difference in pressures inside and outside the sphere, but there is no net force influencing the total movement either of a single droplet or of the cloud of the droplets in the space due to this force. We express this fact by multiplying the surface force by the function δ_l being 1 for the continuum and 0 for the disperse field.

Using Eqs. (2.36) and (2.38) the pressure and the surface tension terms can be rearranged as follows:

$$\nabla \cdot \left(\alpha_l^e \gamma \left\langle p_l^\tau \right\rangle^{le} \right) + \frac{1}{Vol}\int_{F_{l\sigma}} \left\langle p_m^\tau \right\rangle^{me} \mathbf{n}_l dF + \frac{1}{Vol}\int_{F_{lw}} \left\langle p_l^\tau \right\rangle^{le} \mathbf{n}_l dF$$

$$-\frac{1}{Vol}\iint_{F_{l\sigma}} \left(\mathbf{n}_l \sigma_{lm}\kappa + \nabla_t \sigma_{lm}\right) dF$$

$$= \nabla \cdot \left(\alpha_l^e \gamma \left\langle p_l^\tau \right\rangle^{le} \right) - \left\langle p_m^\tau \right\rangle^{me} \nabla\left(\alpha_l^e \gamma\right) + \left(\left\langle p_l^\tau \right\rangle^{le} - \left\langle p_m^\tau \right\rangle^{me} \right) \frac{1}{Vol}\int_{F_{lw}} \mathbf{n}_l dF$$

$$+\delta_l \sigma_{lm}\kappa_l \left[\nabla\left(\alpha_l^e \gamma\right) + \frac{1}{Vol}\int_{F_{lw}} \mathbf{n}_l dF \right] - \delta_l \frac{1}{Vol}\iint_{F_{l\sigma}} (\nabla_t \sigma_{lm}) dF$$

$$= \alpha_l^e \gamma \nabla \left\langle p_l^\tau \right\rangle^{le} + \left(\left\langle p_l^\tau \right\rangle^{le} - \left\langle p_m^\tau \right\rangle^{me} + \delta_l \sigma_{lm} \kappa_l \right) \left(\nabla \left(\alpha_l^e \gamma \right) + \frac{1}{Vol} \int_{F_{lw}} \mathbf{n}_l dF \right)$$

$$- \delta_l \frac{1}{Vol} \iint_{F_{l\sigma}} \left(\nabla_t \sigma_{lm} \right) dF \,. \tag{2.41}$$

Note that in Eq. (2.41)

$$\alpha_l^e \gamma \nabla \cdot \left\langle p_l^\tau \right\rangle^{le}$$

stands for

$$\nabla \cdot \left(\alpha_l^e \gamma \left\langle p_l^\tau \right\rangle^{le} \right) - \left\langle p_l^\tau \right\rangle^{le} \nabla \cdot \left(\alpha_l^e \gamma \right).$$

Rearranging the integrals defining interfacial momentum transfer due to mass transfer: Again using the mass jump condition at the interface, which is Eq. (1.42),

$$\rho_m \mathbf{V}_m^\tau \left(\mathbf{V}_m^\tau - \mathbf{V}_{lm}^\tau \right) = \rho_l \mathbf{V}_m^\tau \left(\mathbf{V}_l^\tau - \mathbf{V}_{lm}^\tau \right), \tag{2.42}$$

the surface integral is rearranged as follows:

$$-\frac{1}{Vol} \int_{F_{l\sigma}} \left[-\rho_m \mathbf{V}_m^\tau \left(\mathbf{V}_m^\tau - \mathbf{V}_{lm}^\tau \right) \right] \cdot \mathbf{n}_l dF = \frac{1}{Vol} \int_{F_{l\sigma}} \left[\rho_l \mathbf{V}_m^\tau \left(\mathbf{V}_l^\tau - \mathbf{V}_{lm}^\tau \right) \right] \cdot \mathbf{n}_l dF \,. \tag{2.43}$$

For practical applications, the mass source term is split into nonnegative components, as has already been explained in Chap. 1 (see also *Kolev* (1994a)). In addition, it is assumed that the mass emitted from a field has the velocity of the donor field. As a result, the local volume-averaged interfacial forces related to mass transfer through the interfaces can be rewritten as follows:

(a) The components related to mass injection into, or suction from, the field through the field structure interface are replaced by the "donor" hypothesis

$$-\frac{1}{Vol} \int_{F_{lw}} \left[\rho_l \mathbf{V}_m^\tau \left(\mathbf{V}_l^\tau - \mathbf{V}_{lw}^\tau \right) \right] \cdot \mathbf{n}_l dF = \gamma_v \left(\mu_{wl}^\tau \left\langle \mathbf{V}_w^\tau \right\rangle^{we} - \mu_{lw}^\tau \left\langle \mathbf{V}_l^\tau \right\rangle^{le} \right). \tag{2.44}$$

(b) The components due to evaporation, condensation, entrainment, and deposition are replaced by the "donor" hypothesis

$$-\frac{1}{Vol} \int_{F_{l\sigma}} \left[\rho_l \mathbf{V}_l^\tau \left(\mathbf{V}_l^\tau - \mathbf{V}_{l\sigma}^\tau \right) \right] \cdot \mathbf{n}_l dF = \gamma_v \sum_{m=1}^{3} \left(\mu_{ml}^\tau \left\langle \mathbf{V}_m^\tau \right\rangle^{me} - \mu_{lm}^\tau \left\langle \mathbf{V}_l^\tau \right\rangle^{le} \right). \tag{2.45}$$

The sum of all interface mass transfer components is then

$$\gamma_v \sum_{m=1}^{3,w} \left(\mu_{ml}^\tau \left\langle \mathbf{V}_m^\tau \right\rangle^{me} - \mu_{lm}^\tau \left\langle \mathbf{V}_l^\tau \right\rangle^{le} \right). \tag{2.46}$$

Thus, the final form obtained for the local volume average momentum equation is as follows:

$$\frac{\partial}{\partial\tau}\left(\alpha_l\gamma_v\left\langle\rho_l\right\rangle^l\left\langle\mathbf{V}_l^\tau\right\rangle^{le}\right)+\nabla\cdot\left(\alpha_l^e\gamma\left\langle\rho_l\right\rangle^l\left\langle\mathbf{V}_l^\tau\right\rangle^{le}\left\langle\mathbf{V}_l^\tau\right\rangle^{le}\right)-\nabla\cdot\left(\alpha_l^e\gamma\left\langle\mathbf{T}_l^\tau\right\rangle^{le}\right)+\alpha_l\gamma_v\left\langle\rho_l\right\rangle^l\mathbf{g}$$
$$+\alpha_l^e\gamma\nabla\left\langle p_l^\tau\right\rangle^{le}+\left(\left\langle p_l^\tau\right\rangle^{le}-\left\langle p_m^\tau\right\rangle^{me}+\delta_l\sigma_{lm}\kappa_l\right)\left(\nabla\left(\alpha_l^e\gamma\right)+\frac{1}{Vol}\int\limits_{F_{lw}}\mathbf{n}_l dF\right)$$
$$-\delta_l\frac{1}{Vol}\int\limits_{F_{l\sigma}}\left(\nabla_t\sigma_{lm}\right)dF+\frac{1}{Vol}\int\limits_{F_{l\sigma}}\left(\Delta p_m^{l\sigma,\tau}\mathbf{I}-\mathbf{T}_m^{l\sigma,\tau}\right)\cdot\mathbf{n}_l dF$$
$$+\frac{1}{Vol}\int\limits_{F_{lw}}\left(\Delta p_l^{w\sigma,\tau}\mathbf{I}-\mathbf{T}_l^{w\sigma,\tau}\right)\cdot\mathbf{n}_l dF=\gamma_v\sum_{m=1}^{3,w}\left(\mu_{ml}^\tau\left\langle\mathbf{V}_m^\tau\right\rangle^{me}-\mu_{lm}^\tau\left\langle\mathbf{V}_l^\tau\right\rangle^{le}\right),\qquad(2.47)$$

and is independent of whether the field is structured or nonstructured. Before we continue with the estimation of the remaining integrals, we will first perform a time averaging of Eq. (2.47).

2.4 Local volume average and time average

The instantaneous surface-averaged velocity of the field l, $\left\langle\mathbf{V}_l^\tau\right\rangle^{le}$, can be expressed as the sum of the surface-averaged velocity, which is subsequently time-averaged,

$$V_l=\overline{\left\langle\mathbf{V}_l^\tau\right\rangle^{le}}\qquad(2.48)$$

and a pulsation component V_l',

$$\left\langle\mathbf{V}_l^\tau\right\rangle^{le}=V_l+V_l',\qquad(2.49)$$

as proposed by *Reynolds*. The fluctuation of the velocity is the predominant fluctuation component relative to, say, the fluctuation of α_l or ρ_l. Introduction of Eq. (2.49) into the momentum conservation equation and time averaging yields

$$\frac{\partial}{\partial\tau}\left(\alpha_l\rho_l\mathbf{V}_l\gamma_v\right)+\nabla\cdot\left(\alpha_l^e\rho_l\mathbf{V}_l\mathbf{V}_l\gamma\right)+\nabla\cdot\left[\alpha_l^e\gamma\left(\rho_l\overline{\mathbf{V}_l'\mathbf{V}_l'}-\delta_l\mathbf{T}_l\right)\right]+\alpha_l^e\gamma\nabla p_l+\alpha_l\gamma_v\rho_l\mathbf{g}$$
$$+\left(p_l-p_m+\delta_l\sigma_{lm}\kappa_l\right)\left(\nabla\left(\alpha_l^e\gamma\right)+\frac{1}{Vol}\int\limits_{F_{lw}}\mathbf{n}_l dF\right)-\delta_l\frac{1}{Vol}\int\limits_{F_{l\sigma}}\left(\nabla_t\sigma_{lm}\right)dF$$
$$+\frac{1}{Vol}\int\limits_{F_{l\sigma}}\left(\Delta p_m^{l\sigma}\mathbf{I}-\mathbf{T}_m^{l\sigma}\right)\cdot\mathbf{n}_l dF+\frac{1}{Vol}\int\limits_{F_{lw}}\left(\Delta p_l^{w\sigma}\mathbf{I}-\mathbf{T}_l^{w\sigma}\right)\cdot\mathbf{n}_l dF$$

$$= \gamma_v \sum_{\substack{k=1 \\ k\neq l}}^{3,w} \left(\mu_{kl} \mathbf{V}_k - \mu_{lk} \mathbf{V}_l \right), \tag{2.50a}$$

see also Appendix 2.1. It is evident from Eq. (2.50a) that the products of the pulsation velocity components, called *Reynolds* stresses, act on the flow, introducing additional macroscopic cohesion inside the velocity field. Equation (2.50a) is applied on the field l including the surface up to the m-side interface.

For dispersed flows it is convenient to have also the momentum equation of the continuum in a primitive form without using the momentum jump condition. In this case, the time average of Eq. (2.31) for field m after introducing Eq. (2.33) is

$$\frac{\partial}{\partial \tau}\left(\alpha_m \rho_m \mathbf{V}_m \gamma_v\right) + \nabla \cdot \left(\alpha_m^e \rho_m \mathbf{V}_m \mathbf{V}_m \gamma\right) + \nabla \cdot \left[\alpha_m^e \gamma \left(\rho_m \overline{\mathbf{V}_m' \mathbf{V}_m'} - \delta_m \mathbf{T}_m\right)\right] + \alpha_m \gamma_v \rho_m \mathbf{g}$$
$$+ \alpha_m^e \gamma \nabla p_m - \frac{1}{Vol} \int_{F_{m\sigma}} \left(\Delta p_m^{l\sigma} \mathbf{I} - \mathbf{T}_m^{l\sigma}\right) \cdot \mathbf{n}_l dF + \frac{1}{Vol} \int_{F_{mw}} \left(\Delta p_m^{w\sigma} \mathbf{I} - \mathbf{T}_m^{w\sigma}\right) \cdot \mathbf{n}_m dF$$
$$= \gamma_v \sum_{\substack{k=1 \\ k\neq m}}^{3,w} \left(\mu_{km} \mathbf{V}_k - \mu_{mk} \mathbf{V}_m\right). \tag{2.50b}$$

Comparing Eq. (2.50a) with Eq. (2.50b) we realize that the term

$$-\frac{1}{Vol} \int_{F_{m\sigma}} \left(\Delta p_m^{l\sigma} \mathbf{I} - \mathbf{T}_m^{l\sigma}\right) \cdot \mathbf{n}_l dF$$

appears in both equations with opposite sign. For practical computation we recommend the use of a couple of equations having common interface in order to easily control the momentum conservation at the selected common interface.

2.5 Dispersed phase in a laminar continuum – pseudo turbulence

It is known that even low-velocity potential flow over a family of spheres is associated with natural fluctuations of the continuum. The produced oscillations of the laminar continuum are called *pseudo turbulence* by some authors. The averaged pressure over the dispersed particles surface is smaller than the volume averaged pressure. Therefore, in flows with spatially changing concentration of the disperse

phase, an additional force acts towards the concentration gradients. For bubbly flow, *Nigmatulin* (1979) obtained the analytical expression

$$\overline{-\mathbf{V}_c'\mathbf{V}_c'} = \left|\Delta\mathbf{V}_{cd}\right|^2 \begin{vmatrix} \frac{4}{20} & 0 & 0 \\ 0 & \frac{3}{20} & 0 \\ 0 & 0 & \frac{3}{20} \end{vmatrix}.$$

Van Wijngaarden (1982) used this expression multiplied by α_d.

2.6 Viscous and *Reynolds* stresses

The solid body rotation and translation of the fluid element does not cause any deformation and, therefore, no internal viscous stresses in the fluid. Only the deformation of the fluid element causes viscous stress resisting this deformation. For estimation of the relationship between deformation and viscous stress, the heuristic approach proposed by *Helmholtz* and *Stokes* (1845a and b) can be used for the continuous, intrinsic isotropic, nonstructured field, see *Schlichting* (1959, p. 58). The background conditions behind this approach will now be recalled: (a) the field is a continuum, (b) small velocity changes are considered, (c) only the linear part of the *Taylor* series is taken into account, and (d) linear dependence between stresses and velocity deformations (*Newtonian* continuum). The mathematical notation for this hypothesis is

$$\mathbf{T}_\eta = \eta\left[\nabla\mathbf{V} + (\nabla\mathbf{V})^T - \frac{2}{3}(\nabla\cdot\mathbf{V})\mathbf{I}\right] = \eta\left[2\mathbf{D} - \frac{2}{3}(\nabla\cdot\mathbf{V})\mathbf{I}\right]$$

$$= \eta\begin{pmatrix} 2\left(\frac{\partial u}{\partial x} - \frac{1}{3}\nabla\cdot\mathbf{V}\right) & \frac{\partial v}{\partial x} + \frac{\partial u}{\partial y} & \frac{\partial w}{\partial x} + \frac{\partial u}{\partial z} \\ \frac{\partial u}{\partial y} + \frac{\partial v}{\partial x} & 2\left(\frac{\partial v}{\partial y} - \frac{1}{3}\nabla\cdot\mathbf{V}\right) & \frac{\partial w}{\partial y} + \frac{\partial v}{\partial z} \\ \frac{\partial u}{\partial z} + \frac{\partial w}{\partial x} & \frac{\partial v}{\partial z} + \frac{\partial w}{\partial y} & 2\left(\frac{\partial w}{\partial z} - \frac{1}{3}\nabla\cdot\mathbf{V}\right) \end{pmatrix}, \qquad (2.51)$$

where $\mathbf{T}$ is the second-order tensor for the viscous momentum flux, $\nabla\mathbf{V}$ is the dyadic product of the *nabla* operator and the velocity vector (a second-order tensor), and ^{T} designates the transposed tensor. Note that the *nabla* operator of the velocity vector,

$$\nabla\mathbf{V} = \mathbf{D} + \mathbf{W}$$

consists of a symmetric part

$$\mathbf{D} = \frac{1}{2}\left[\nabla\mathbf{V} + (\nabla\mathbf{V})^T\right],$$

called *deformation rate,* and a skew part

$$\mathbf{W} = \frac{1}{2}\left[\nabla\mathbf{V} - (\nabla\mathbf{V})^T\right]$$

called *spin* or *vortices tensor.*

$$\nabla\cdot\mathbf{V} = \frac{\partial u}{\partial x} + \frac{\partial v}{\partial y} + \frac{\partial w}{\partial z}$$

is the divergence of the velocity vector. *Stokes* called the term containing the divergence of the velocity vector the *rate of cubic dilatation*. The hypothesis says that the relation between viscous stresses and the deformation rate of a control volume is linear and the proportionality factor is the dynamic viscosity η, that solid body translations and rotations do not contribute to the viscous forces, that the share stresses are symmetric, and that the relation between volumetric and the share viscosity is such that the pressure always equals one third of the sum of the normal stresses. *Stokes* ingeniously argues each of these points in his paper. In the multiphase continuous field models, as long as they are resolved with very fine grids this stress tensor reflects the real one.
I recommend to anyone having the serious intention to understand flows to study this paper. Alternatively, see *Schliching* (1959, p.60), where it is explained that Eq. (2.51) contains the *Stoke*s result for the relation of the bulk viscosity equal to −2/3 dynamic viscosity. From the mechanical equilibrium condition for all angular momenta around an axis for vanishing dimensions of the control volume, one obtains the symmetry of the components of the viscous stress tensor, see *Schlichting* (1959, p. 50) for the *Cartesian* coordinates.

For practical use it is convenient to write the viscous stress tensor for Cartesian and cylindrical coordinates as follows:

$$\mathbf{T}_\eta = \eta\begin{pmatrix} 2\left[\dfrac{\partial u}{\partial r} - \dfrac{1}{3}(\nabla\cdot\mathbf{V})\right] & \dfrac{1}{r^\kappa}\dfrac{\partial u}{\partial\theta} - \kappa\dfrac{v}{r^\kappa} + \dfrac{\partial v}{\partial r} & \dfrac{\partial u}{\partial z} + \dfrac{\partial w}{\partial r} \\ \dfrac{1}{r^\kappa}\dfrac{\partial u}{\partial\theta} - \kappa\dfrac{v}{r^\kappa} + \dfrac{\partial v}{\partial r} & 2\left(\dfrac{1}{r^\kappa}\dfrac{\partial v}{\partial\theta} + \kappa\dfrac{v}{r^\kappa} - \dfrac{1}{3}(\nabla\cdot\mathbf{V})\right) & \dfrac{\partial v}{\partial z} + \dfrac{1}{r^\kappa}\dfrac{\partial w}{\partial\theta} \\ \dfrac{\partial u}{\partial z} + \dfrac{\partial w}{\partial r} & \dfrac{\partial v}{\partial z} + \dfrac{1}{r^\kappa}\dfrac{\partial w}{\partial\theta} & 2\left[\dfrac{\partial w}{\partial z} - \dfrac{1}{3}(\nabla\cdot\mathbf{V})\right] \end{pmatrix},$$

where

$$\nabla\cdot\mathbf{V} = \frac{1}{r^\kappa}\frac{\partial}{\partial r}\left(r^\kappa u\right) + \frac{1}{r^\kappa}\frac{\partial v}{\partial\theta} + \frac{\partial w}{\partial z}.$$

For cylindrical coordinates $\kappa = 1$. For Cartesian coordinates set $\kappa = 0$ and replace r, θ, z with x, y, z, respectively.

Now let us step to the turbulence stress tensor $-\rho_l \overline{\mathbf{V}_l' \mathbf{V}_l'}$ called the *Reynolds* stress tensor. The search for a quantitative estimation of the *Reynolds* stresses for multiphase flows is in its initial stage. A possible step in the right direction, in analogy to single-phase turbulence, is the use of the *Boussinesq* hypothesis (1877) for the viscosity of turbulent eddies inside the velocity field. *Boussinesq* introduced the idea of turbulent eddy viscosity inside the velocity field,

$$-\rho_l \overline{\mathbf{V}_l' \mathbf{V}_l'} = \eta_l^t \left[2\mathbf{D}_l - \frac{2}{3}(\nabla \cdot \mathbf{V}_l)\mathbf{I} \right]$$

$$= \eta_l^t \begin{pmatrix} 2\left(\frac{\partial u}{\partial x} - \frac{1}{3}\nabla \cdot \mathbf{V}\right) & \frac{\partial v}{\partial x} + \frac{\partial u}{\partial y} & \frac{\partial w}{\partial x} + \frac{\partial u}{\partial z} \\ \frac{\partial u}{\partial y} + \frac{\partial v}{\partial x} & 2\left(\frac{\partial v}{\partial y} - \frac{1}{3}\nabla \cdot \mathbf{V}\right) & \frac{\partial w}{\partial y} + \frac{\partial v}{\partial z} \\ \frac{\partial u}{\partial z} + \frac{\partial w}{\partial x} & \frac{\partial v}{\partial z} + \frac{\partial w}{\partial y} & 2\left(\frac{\partial w}{\partial z} - \frac{1}{3}\nabla \cdot \mathbf{V}\right) \end{pmatrix}_l, \qquad (2.52)$$

so that it has the same structure as the *Stokes* hypothesis. The corresponding *Reynolds* stresses are

$$-\rho_l u_l' u_l' = \tau_{l,xx}' = \eta_l^t 2\left(\frac{\partial u_l}{\partial x} - \frac{1}{3}\nabla \cdot \mathbf{V}_l\right),$$

$$-\rho_l v_l' v_l' = \tau_{l,yy}' = \eta_l^t 2\left(\frac{\partial v_l}{\partial y} - \frac{1}{3}\nabla \cdot \mathbf{V}_l\right),$$

$$-\rho_l w_l' w_l' = \tau_{l,zz}' = \eta_l^t 2\left(\frac{\partial w_l}{\partial y} - \frac{1}{3}\nabla \cdot \mathbf{V}_l\right),$$

$$-\rho_l u_l' v_l' = \tau_{l,xy}' = \eta_l^t \left(\frac{\partial v_l}{\partial x} + \frac{\partial u_l}{\partial y}\right),$$

$$-\rho_l u_l' w_l' = \tau_{l,xz}' = \eta_l^t \left(\frac{\partial w_l}{\partial x} + \frac{\partial u_l}{\partial z}\right),$$

$$-\rho_l v_l' w_l' = \tau_{l,yz}' = \eta_l^t \left(\frac{\partial w_l}{\partial y} + \frac{\partial v_l}{\partial z}\right).$$

The dynamic turbulent viscosity now is a flow property and remains to be estimated. Note that at a given point this is a single value for all directions. Strictly speaking, this approach is valid for isotropic turbulence because there is a single eddy viscosity assumed to be valid for all directions.

An alternative notation of the term $\nabla\cdot\left[\alpha_l^e\left(\rho_l\overline{\mathbf{V}_l'\mathbf{V}_l'}\right)\gamma\right]$ is given here for isotropic turbulence, for which

$$u_l'u_l' = v_l'v' = w_l'w_l' = \frac{2}{3}k_l : \tag{2.53}$$

$$\nabla\cdot\left[\left(\alpha_l^e\rho_l\mathbf{V}_l'\mathbf{V}_l'\right)\gamma\right] = \begin{pmatrix} \dfrac{\partial\gamma_x\alpha_l^e\rho_l u_l'u_l'}{\partial x}+\dfrac{\partial\gamma_y\alpha_l^e\rho_l u_l'v_l'}{\partial y}+\dfrac{\partial\gamma_z\alpha_l^e\rho_l u_l'w_l'}{\partial z} \\ \dfrac{\partial\gamma_x\alpha_l^e\rho_l v_l'u_l'}{\partial x}+\dfrac{\partial\gamma_y\alpha_l^e\rho_l v_l'v_l'}{\partial y}+\dfrac{\partial\gamma_z\alpha_l^e\rho_l v_l'w_l'}{\partial z} \\ \dfrac{\partial\gamma_x\alpha_l^e\rho_l w_l'u_l'}{\partial x}+\dfrac{\partial\gamma_y\alpha_l^e\rho_l w_l'v_l'}{\partial y}+\dfrac{\partial\gamma_z\alpha_l^e\rho_l w_l'w_l'}{\partial z} \end{pmatrix}$$

$$= \begin{pmatrix} \dfrac{\partial\gamma_y\alpha_l^e\rho_l u_l'v_l'}{\partial y}+\dfrac{\partial\gamma_z\alpha_l^e\rho_l u_l'w_l'}{\partial z} \\ \dfrac{\partial\gamma_x\alpha_l^e\rho_l v_l'u_l'}{\partial x}+\dfrac{\partial\gamma_z\alpha_l^e\rho_l v_l'w_l'}{\partial z} \\ \dfrac{\partial\gamma_x\alpha_l^e\rho_l w_l'u_l'}{\partial x}+\dfrac{\partial\gamma_y\alpha_l^e\rho_l w_l'v_l'}{\partial y} \end{pmatrix} + \frac{2}{3}\nabla\left(\gamma\alpha_l^e\rho_l k_l\right)$$

$$= -\tilde{\mathbf{S}}_l + \frac{2}{3}\nabla\left(\gamma\alpha_l^e\rho_l k_l\right), \tag{2.54}$$

where

$$\tilde{\mathbf{S}}_l = \begin{pmatrix} \dfrac{\partial}{\partial y}\left[\gamma_y\alpha_l^e\rho_l\nu_l^t\left(\dfrac{\partial v_l}{\partial x}+\dfrac{\partial u_l}{\partial y}\right)\right]+\dfrac{\partial}{\partial z}\left[\gamma_z\alpha_l^e\rho_l\nu_l^t\left(\dfrac{\partial w_l}{\partial x}+\dfrac{\partial u_l}{\partial z}\right)\right] \\ \dfrac{\partial}{\partial x}\left[\gamma_x\alpha_l^e\rho_l\nu_l^t\left(\dfrac{\partial v_l}{\partial x}+\dfrac{\partial u_l}{\partial y}\right)\right]+\dfrac{\partial}{\partial z}\left[\gamma_z\alpha_l^e\rho_l\nu_l^t\left(\dfrac{\partial w_l}{\partial y}+\dfrac{\partial v_l}{\partial z}\right)\right] \\ \dfrac{\partial}{\partial x}\left[\gamma_x\alpha_l^e\rho_l\nu_l^t\left(\dfrac{\partial w_l}{\partial x}+\dfrac{\partial u_l}{\partial z}\right)\right]+\dfrac{\partial}{\partial y}\left[\gamma_y\alpha_l^e\rho_l\nu_l^t\left(\dfrac{\partial w_l}{\partial y}+\dfrac{\partial v_l}{\partial z}\right)\right] \end{pmatrix}. \tag{2.55}$$

Here the diagonal symmetric term $\frac{2}{3}\nabla\left(\gamma\alpha_l^e\rho_l k_l\right)$ is considered as a dispersion force and is directly computed from the turbulent kinetic energy delivered by the turbulence model.

It is important to emphasize that, in spite of the fact that several processes in single-phase fluid dynamics can be successfully described by the *Helmholtz–Stokes* and by the *Boussinesq* hypotheses; these hypotheses have never been derived from experiments or proven by abstract arguments. This limitation of the hypotheses should be borne in mind when they are applied.

While the heuristic approach proposed by *Helmholtz* and *Stokes*, Eq. (2.51), is valid only for the continuous part of each velocity field, the *Boussinesq* hypothesis is useful for continuous and disperse velocity fields. This behavior is again described here by introducing for each velocity field the multiplier δ_l in Eq. (2.50), where $\delta_l = 0$ for dispersed field and $\delta_l = 1$ for continuous nonstructured fields.

For a single field, $\delta_l = 1$, the description of the viscous and *Reynolds* stresses reduces to the widely accepted expression.

It is plausible to define the turbulent pressure as

$$p_l' = \rho_l \frac{2}{3} k_l = \rho_l \frac{1}{3}\left(u'u' + v'v' + w'w'\right), \tag{2.56}$$

and to consider the term $-\alpha_l^e \gamma \nabla p_l'$ as absorbed from the pressure term $\alpha_l^e \gamma \nabla p_l$ and the term

$$-p_l' \nabla\left(\alpha_l^e \gamma\right) = \frac{1}{Vol} \int_{F_{l\sigma}} p_l' \mathbf{n}_l dF + \frac{1}{Vol} \int_{F_{lw}} p_l' \mathbf{n}_l dF \tag{2.57}$$

as included in the pressure differences between the bulk pressure and boundary layer pressure. This could mean that p_l' no longer needs to appear in the notation. Until the correctness of this agglomeration of the terms is not strictly proven I do not recommend it.

It is interesting to note that from the kinetic theory for two colliding particles plus their added mass the following is obtained:

$$\nabla\left(\alpha_l^e \gamma\, p_l'\right) \approx \nabla\left[\alpha_l^e \gamma \left(\rho_l + c_l^{vm} \rho_m\right) \frac{1}{3} \mathbf{V}_l'^2\right]. \tag{2.58}$$

2.7 Nonequal bulk and boundary layer pressures

2.7.1 Continuous interface

2.7.1.1 3D flows

Examples for the existence of continuous interfaces are the stratified pool, see Fig. 2.5, and annular pipe flow.

The treatment of the interface depends very much on the numerical method used. If the numerical method is able to resolve the interface itself and the two attached boundary layers (see, for instance, *Hirt* and *Nichols* (1981) for more information), the interface momentum jump condition is the only information needed to close the mathematical description of the interface. If this is not the case, special treatment of the processes at the interface is necessary. In this section we discuss some possibilities.

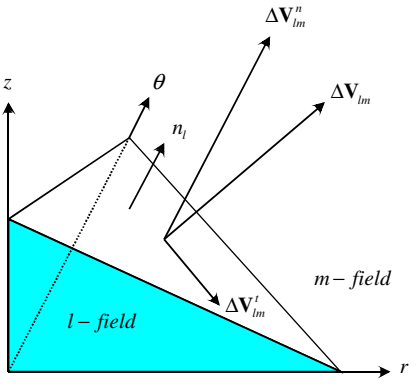

Fig. 2.5 Continuous interface

Consider a liquid (l)-gas (m) flow without mass transfer. The computational cells are so large that the surface is at best represented by piecewise planes at which the surface tension is neglected. The compressibility of the gas is much larger than the compressibility of the liquid. In this case, we can assume that there is almost no difference between the bulk and liquid side interface pressure

$$\Delta p_l^{m\sigma} = 0\,. \tag{2.59}$$

The pressure change across the gas side boundary layer is then approximated by the stagnation pressure

$$\Delta p_m^{l\sigma} = \rho_m \left(V_l^n - V_m^n\right)^2 = \rho_m \left|\Delta\mathbf{V}_{lm}^n\right|^2 sign\left(V_l^n - V_m^n\right), \tag{2.60}$$

see Fig. 2.6. The normal velocity difference required in the above expression can be obtained by splitting the relative velocity vector at the interface $\Delta\mathbf{V}_{lm}$ into a component that is parallel to $\mathbf{n}_l$

$$\Delta\mathbf{V}_{lm}^n = proj_{\mathbf{n}_l}\Delta\mathbf{V}_{lm} = \left(\frac{\Delta\mathbf{V}_{lm}\cdot\mathbf{n}_l}{\mathbf{n}_l\cdot\mathbf{n}_l}\right)\mathbf{n}_l = \left(\Delta\mathbf{V}_{lm}\cdot\mathbf{n}_l\right)\mathbf{n}_l\,, \tag{2.61}$$

with a magnitude

$$\left|\Delta\mathbf{V}_{lm}^n\right| = \left|\Delta\mathbf{V}_{lm}\cdot\mathbf{n}_l\right| = \sqrt{\left[n_{lx}\left(u_l-u_m\right)\right]^2+\left[n_{ly}\left(v_l-v_m\right)\right]^2+\left[n_{lz}\left(w_l-w_m\right)\right]^2} \tag{2.62}$$

and a component orthogonal to $\mathbf{n}_l$,

$$\begin{aligned}\Delta\mathbf{V}_{lm}^t &= \Delta\mathbf{V}_{lm} - proj_{\mathbf{e}_l}\Delta\mathbf{V}_{lm} = \Delta\mathbf{V}_{lm} - \left(\Delta\mathbf{V}_{lm}\cdot\mathbf{n}_l\right)\mathbf{n}_l \\ &= \left[\Delta u_{lm} - n_{lx}\left(\Delta\mathbf{V}_{lm}\cdot\mathbf{n}_l\right)\right]\mathbf{i} + \left[\Delta v_{lm} - n_{ly}\left(\Delta\mathbf{V}_{lm}\cdot\mathbf{n}_l\right)\right]\mathbf{j} + \left[\Delta w_{lm} - n_{lz}\left(\Delta\mathbf{V}_{lm}\cdot\mathbf{n}_l\right)\right]\mathbf{k}\,.\end{aligned} \tag{2.63}$$

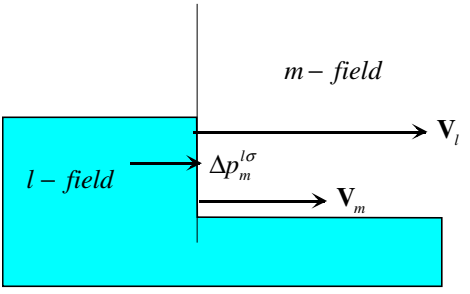

Fig. 2.6 Stagnation pressure in stratified flow

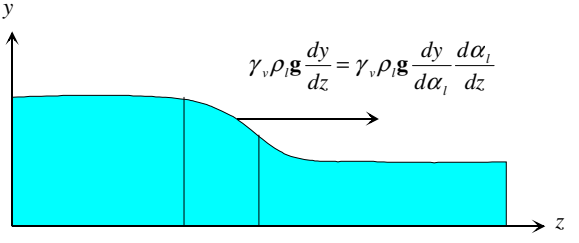

Fig. 2.7 Geodesic pressure force

In a similar way, the stagnation pressure difference at the field-structure interface can be estimated,

$$\Delta p_l^{w\sigma} = \rho_l \left(V_l^n - V_w^n\right)^2 sign\left(V_l^n - V_w^n\right). \tag{2.64}$$

For the case of $\Delta p_m^{l\sigma} \approx const$ within *Vol* the following can be written:

$$\frac{1}{Vol}\int\limits_{F_{l\sigma}} \Delta p_m^{l\sigma}\mathbf{n}_l dF = \Delta p_m^{l\sigma}\frac{1}{Vol}\int\limits_{F_{l\sigma}} \mathbf{n}_l dF = -\Delta p_m^{l\sigma}\left[\nabla\left(\alpha_l^e\gamma\right) + \frac{1}{Vol}\int\limits_{F_{lw}} \mathbf{n}_l dF\right]. \tag{2.65}$$

For $\mathbf{V}_l^n > \mathbf{V}_m^n$ and decreasing $\alpha_l^e\gamma$ in space, this force resists the field *l*. If there is no difference in the average normal velocities at the interface the above term is zero.

If the tangential average velocity difference differs from zero, there is a tangential viscous shear force

$$-\frac{1}{Vol}\int\limits_{F_{l\sigma}} \mathbf{T}_{m\sigma}\cdot\mathbf{n}_{l\sigma} dF = c_{ml}\left|\Delta\mathbf{V}_{lm}^t\right|\Delta\mathbf{V}_{lm}^t. \tag{2.66}$$

Here c_{ml} has to be computed using empirical correlation in the case of the large scale of the cells not resolving the details of the boundary layer. For a wavy sur-

face, the interface share coefficient should be increased by a component for form drag caused by the nonuniform pressure distribution, which results in an additional tangential force. Similarly, the viscous shear stress of the wall is

$$-\frac{1}{Vol}\int_{F_{lw}} \mathbf{T}_{lw}\cdot\mathbf{n}_{lw}dF = c_{wl}\left|\mathbf{V}_l^t\right|\mathbf{V}_l^t\,, \tag{2.67}$$

where, like in the previous case, c_{wl} has to be computed using empirical correlation. Note that in the case of stratified rectangular duct flow in the z direction, see Fig. 2.7, the change in the liquid thickness causes a lateral geodesic pressure force

$$\gamma_v\rho_l\mathbf{g}\frac{dy}{dz} = \gamma_v\rho_l\mathbf{g}\frac{dy}{d\alpha_l}\frac{d\alpha_l}{dz}\,. \tag{2.68}$$

Here y is the distance between the bottom of the duct and the center of mass of the liquid. In three-dimensional models this force automatically arises due to differences in the local bulk pressure having the geodesic pressure as a component. This force should be taken into account in one-dimensional models. If this force is neglected, the one-dimensional model will not be able to predict water flow in a horizontal pipe with negligible gas-induced shear. In the next section we consider this problem in more detail.

2.7.1.2 Stratified flow in horizontal or inclined rectangular channels

Geometrical characteristics: Stratified flow may exist in regions with such relative velocities between the liquid and the gas which does not cause instabilities leading to slugging.

Some important geometrical characteristics are specified here – compare with Fig. 2.8. The perimeter of the pipe is then

$$Per_{1w} = 2\left(a+H\right), \tag{2.69}$$

and the wetted perimeters for the gas and the liquid parts are

$$Per_{1w} = a + 2\left(H-\delta_{2F}\right) = a + 2\alpha_1 H\,, \tag{2.70}$$

$$Per_{2w} = a + 2\delta_{1F} = a + 2\alpha_2 H\,. \tag{2.71}$$

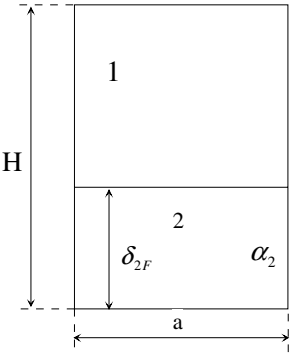

Fig. 2.8 Definition of the geometrical characteristics of the stratified flow

The gas-–liquid interface median is then a, and the liquid level

$$\delta_{2F} = \alpha_2 H \ . \tag{2.72}$$

The hydraulic diameters for the gas and the liquid for computation of the pressure drop due to friction with the wall are, therefore,

$$D_{h1} = 4\alpha_1 F / Per_{1w} = \frac{4\alpha_1 aH}{a + 2H\alpha_1}, \tag{2.73}$$

$$D_{h2} = 4\alpha_2 F / Per_{2w} = \frac{4\alpha_2 aH}{a + 2H\alpha_2}, \tag{2.74}$$

and the corresponding *Reynolds* numbers

$$\mathrm{Re}_1 = \frac{\alpha_1 \rho_1 w_1}{\eta_1} \frac{4\alpha_1 aH}{a + 2H\alpha_1}, \tag{2.75}$$

$$\mathrm{Re}_2 = \frac{\alpha_2 \rho_2 w_2}{\eta_2} \frac{4\alpha_2 aH}{a + 2H\alpha_2}. \tag{2.76}$$

Here F is the channel cross-section and Per_{1w} and Per_{2w} are the perimeters wet by gas and film, respectively. If one considers the gas-core of the flow, the hydraulic diameter for computation of the pressure loss component due to the gas-liquid friction is then

$$D_{h12} = 4\alpha_1 F / \left(Per_{1w} + a\right) = \frac{2\alpha_1 aH}{a + H\alpha_1} \tag{2.77}$$

and the corresponding *Reynolds* number

$$\mathrm{Re}_1 = \frac{\alpha_1 \rho_1 \left|w_1 - w_2\right|}{\eta_1} \frac{2\alpha_1 aH}{a + H\alpha_1}. \tag{2.78}$$

The gas-wall, liquid-wall, and gas-liquid interfacial area densities are

$$a_{1w} = \frac{Per_{1w}}{F} = \frac{a + 2\alpha_1 H}{aH}, \tag{2.79}$$

$$a_{2w} = \frac{Per_{2w}}{F} = \frac{a + 2\alpha_2 H}{aH}, \tag{2.80}$$

$$a_{12} = \frac{a}{F} = \frac{1}{H}. \tag{2.81}$$

For the estimation of the flow pattern transition criterion, the following expression is sometimes required:

$$\frac{d\alpha_2}{d\delta_{2F}} = \frac{1}{H}. \tag{2.82}$$

Using the geometric characteristics and the Reynolds numbers the interfacial interaction coefficients can be computed by means of empirical correlations as discussed in Volume II of this monograph.

Gravitational (hydrostatic) pressure variation across the flow cross-section of horizontal pipe: In stratified flow the gravitation is a dominant force. The cross-section averaged gas gravity pressure difference with respect to the interface is

$$\Delta p_1^{2\sigma} = \rho_1 g \alpha_1 \frac{H}{2}. \tag{2.83}$$

The cross-section averaged liquid gravity pressure difference with respect to the interface is

$$\Delta p_2^{1\sigma} = -\rho_2 g \alpha_2 \frac{H}{2}. \tag{2.84}$$

The cross-section averaged field pressures in terms of the interfacial pressure are then

$$p_1 = p_1^{2\sigma} - \Delta p_1^{2\sigma} = p_1^{2\sigma} - \rho_1 g \alpha_1 \frac{H}{2}, \tag{2.85}$$

$$p_2 = p_2^{1\sigma} - \Delta p_2^{1\sigma} = p_2^{1\sigma} + \rho_2 g \alpha_2 \frac{H}{2}, \tag{2.86}$$

recalling the definition in Eqs. (2.33) and (2.34). The averaged pressure in the cross-section can be expressed as the cross-section weighted averaged pressures inside the fields

$$p = \alpha_1 p_1 + \alpha_2 p_2 = \alpha_1 p_1^{2\sigma} + \alpha_2 p_2^{1\sigma} + g \frac{H}{2}\left(\alpha_2^2 \rho_2 - \alpha_1^2 \rho_1\right). \tag{2.87}$$

Neglecting the surface tension, we obtain

$$p \approx p_\sigma + g\frac{H}{2}\left(\alpha_2^2\rho_2 - \alpha_1^2\rho_1\right), \tag{2.88}$$

or

$$p_\sigma \approx p - g\frac{H}{2}\left(\alpha_2^2\rho_2 - \alpha_1^2\rho_1\right). \tag{2.89}$$

The averaged pressure in the gas and in the liquid phase can be then expressed as a function of the system averaged pressure and geometrical characteristics by replacing p_σ in Eqs. (2.85) and (2.86)

$$p_1 = p - \frac{H}{2} g\alpha_2\rho \quad \text{for} \quad \alpha_1 > 0\ , \tag{2.90}$$

$$p_2 = p + \frac{H}{2} g\alpha_1\rho \quad \text{for} \quad \alpha_2 > 0\,, \tag{2.91}$$

where $\rho = \alpha_1\rho_1 + \alpha_2\rho_2$ is the homogeneous mixture density. The check $\alpha_1 p_1 + \alpha_2 p_2 = p$ proves the correctness of the computation. The difference between both averaged pressures is then

$$\Delta p_{21} = p_2 - p_1 = \frac{H}{2} g\rho \ \text{ for } \ \alpha_1 > 0 \ \text{ and } \ \alpha_2 > 0\,, \tag{2.92}$$

Delhaye (1981, p.89). Therefore

$$p_1 = p - \alpha_2\Delta p_{21}\,, \tag{2.93}$$

$$p_2 = p + \alpha_1\Delta p_{21}\,, \tag{2.94}$$

and consequently

$$\frac{\partial p_1}{\partial z} = \frac{\partial p}{\partial z} - \Delta p_{21}\frac{\partial \alpha_2}{\partial z} - \alpha_2\frac{\partial \Delta p_{21}}{\partial z}\,, \tag{2.95}$$

$$\frac{\partial p_2}{\partial z} = \frac{\partial p}{\partial z} + \Delta p_{21}\frac{\partial \alpha_1}{\partial z} + \alpha_1\frac{\partial \Delta p_{21}}{\partial z}\,. \tag{2.96}$$

Now we can write the specific form of the following general terms of the momentum equation:

$$\begin{aligned} &\ldots + \alpha_l^e\gamma_z\frac{\partial p_l}{\partial z} + \left(p_l - p_m - \delta_l\sigma_{lm}\kappa_l - \Delta p_m^{l\sigma}\right)\left[\frac{\partial}{\partial z}\left(\alpha_l^e\gamma_z\right) - \delta_l\frac{\partial \gamma_z}{\partial z}\right] \\ &- \Delta p_l^{w\sigma}\delta_l\frac{\partial \gamma_z}{\partial z} + \gamma_v\alpha_l\rho_l g\cos\varphi \ldots \end{aligned} \tag{2.97}$$

Note that both fields are continuous and, therefore, $\delta_l = 1$ and the effect of the surface tension is neglected

$$... + \alpha_1 \gamma_z \frac{\partial p_1}{\partial z} - \gamma_z \left(\Delta p_{21} + \Delta p_2^{1\sigma} \right) \frac{\partial \alpha_1}{\partial z} - \Delta p_1^{w\sigma} \frac{\partial \gamma_z}{\partial z} ... \tag{2.98}$$

$$... + \alpha_2 \gamma_z \frac{\partial p_2}{\partial z} + \gamma_z \left(\Delta p_{21} - \Delta p_1^{2\sigma} \right) \frac{\partial \alpha_2}{\partial z} - \Delta p_2^{w\sigma} \frac{\partial \gamma_z}{\partial z} ... \tag{2.99}$$

Substituting the field pressures, we finally obtain

$$... + \gamma_z \left[\alpha_1 \frac{\partial p}{\partial z} - \alpha_1 \alpha_2 \frac{\partial \Delta p_{21}}{\partial z} - \left(\alpha_2 \Delta p_{21} + \Delta p_2^{1\sigma} \right) \frac{\partial \alpha_1}{\partial z} \right] - \Delta p_1^{w\sigma} \frac{\partial \gamma_z}{\partial z} ... \tag{2.100}$$

$$... + \gamma_z \left[\alpha_2 \frac{\partial p}{\partial z} + \alpha_1 \alpha_2 \frac{\partial \Delta p_{21}}{\partial z} - \left(\alpha_1 \Delta p_{21} - \Delta p_1^{2\sigma} \right) \frac{\partial \alpha_1}{\partial z} \right] - \Delta p_2^{w\sigma} \frac{\partial \gamma_z}{\partial z} ... \tag{2.101}$$

Assuming that the change of the densities contributes much less to the change of

$$\frac{\partial \Delta p_{21}}{\partial z} \approx \frac{\partial \Delta p_{21}}{\partial \alpha_1} \frac{\partial \alpha_1}{\partial z} = g \frac{H}{2} \left(\rho_1 - \rho_2 \right) \frac{\partial \alpha_1}{\partial z} \tag{2.102}$$

then the change of the local volume fraction becomes

$$... + \gamma_z \left[\alpha_1 \frac{\partial p}{\partial z} - gH \alpha_1 \alpha_2 \left(\rho_1 - \rho_2 \right) \frac{\partial \alpha_1}{\partial z} \right] - \Delta p_1^{w\sigma} \frac{\partial \gamma_z}{\partial z} ... \tag{2.103}$$

$$... + \gamma_z \left[\alpha_2 \frac{\partial p}{\partial z} + gH \alpha_1 \alpha_2 \left(\rho_1 - \rho_2 \right) \frac{\partial \alpha_1}{\partial z} \right] - \Delta p_2^{w\sigma} \frac{\partial \gamma_z}{\partial z} ... \tag{2.104}$$

As a plausibility check note that for $\alpha_1 \to 0$ or $\alpha_2 \to 0$ the term containing the derivative of the volume fraction of velocity field 1 converges to zero and the momentum equations take the expected form. The sum of the two momentum equations gives

$$... + \gamma_z \frac{\partial p}{\partial z} - \left(\Delta p_1^{w\sigma} + \Delta p_2^{w\sigma} \right) \frac{\partial \gamma_z}{\partial z} ... \tag{2.105}$$

Note that the gravitational force is already taken into account in Eqs. (2.103) and (2.104) and there is no need for an additional term $\gamma_v \alpha_l \rho_l g \cos \varphi$. Stability criteria for the stratified flow can be obtained from the eigenvalue analysis. For simplicity, assuming incompressible flow the mass and momentum equations of stratified flow in a straight pipe with constant cross-section section are

$$\alpha_1 \frac{\partial w_1}{\partial z} + \alpha_2 \frac{\partial w_2}{\partial z} + \left(w_1 - w_2 \right) \frac{\partial \alpha_1}{\partial z} = 0 , \tag{2.106}$$

$$\frac{\partial \alpha_1}{\partial \tau} + \alpha_1 \frac{\partial w_1}{\partial z} + w_1 \frac{\partial \alpha_1}{\partial z} = 0 , \tag{2.107}$$

$$\frac{\partial w_1}{\partial \tau} + w_1 \frac{\partial w_1}{\partial z} + \frac{1}{\rho_1}\frac{\partial p}{\partial z} + gH \frac{\alpha_2(\rho_2 - \rho_1)}{\rho_1}\frac{\partial \alpha_1}{\partial z} = 0\,, \tag{2.108}$$

$$\frac{\partial w_2}{\partial \tau} + w_2 \frac{\partial w_2}{\partial z} + \frac{1}{\rho_2}\frac{\partial p}{\partial z} - gH \frac{\alpha_1(\rho_2 - \rho_1)}{\rho_2}\frac{\partial \alpha_1}{\partial z} = 0\,, \tag{2.109}$$

or in matrix notation

$$\begin{pmatrix} 0 & 0 & 0 & 0 \\ 0 & 1 & 0 & 0 \\ 0 & 0 & 1 & 0 \\ 0 & 0 & 0 & 1 \end{pmatrix} \frac{\partial}{\partial \tau} \begin{pmatrix} p \\ \alpha_1 \\ w_1 \\ w_2 \end{pmatrix} + \begin{pmatrix} 0 & (w_1 - w_2) & \alpha_1 & \alpha_2 \\ 0 & w_1 & \alpha_1 & 0 \\ \frac{1}{\rho_1} & gH\frac{\alpha_2(\rho_2 - \rho_1)}{\rho_1} & w_1 & 0 \\ \frac{1}{\rho_2} & -gH\frac{\alpha_1(\rho_2 - \rho_1)}{\rho_2} & 0 & w_2 \end{pmatrix} \frac{\partial}{\partial z} \begin{pmatrix} p \\ \alpha_1 \\ w_1 \\ w_2 \end{pmatrix} = 0\,. \tag{2.110}$$

For the reader who is not familiar with the analysis of the type of a system of partial differential equations by first computing the eigenvalues, eigenvectors, and canonical forms it is recommended to first read Section 11 before continuing here.

The eigenvalues are defined by the characteristics equations

$$\begin{pmatrix} 0 & (w_1 - w_2) & \alpha_1 & \alpha_2 \\ 0 & w_1 - \lambda & \alpha_1 & 0 \\ \frac{1}{\rho_1} & gH\frac{\alpha_2(\rho_2 - \rho_1)}{\rho_1} & w_1 - \lambda & 0 \\ \frac{1}{\rho_2} & -gH\frac{\alpha_1(\rho_2 - \rho_1)}{\rho_2} & 0 & w_2 - \lambda \end{pmatrix} = 0\,, \tag{2.111}$$

or

$$\frac{\alpha_1}{\rho_1}(w_1 - w_2)(w_2 - \lambda) - \frac{\alpha_1}{\rho_1}(w_1 - \lambda)(w_2 - \lambda) - \frac{\alpha_2}{\rho_2}(w_1 - \lambda)^2 + gH\frac{\alpha_1\alpha_2(\rho_2 - \rho_1)}{\rho_1\rho_2} = 0\,, \tag{2.112}$$

or

$$\left(\frac{\alpha_1}{\rho_1} + \frac{\alpha_2}{\rho_2}\right)\lambda^2 - 2\left(\frac{\alpha_1}{\rho_1}w_2 + \frac{\alpha_2}{\rho_2}w_1\right)\lambda + \frac{\alpha_1}{\rho_1}w_2^2 + \frac{\alpha_2}{\rho_2}w_1^2 - gH\frac{\alpha_1\alpha_2(\rho_2 - \rho_1)}{\rho_1\rho_2} = 0\,. \tag{2.113}$$

This equation is, in fact, consistent with the long wave gravity theory by *Milne-Thomson* (1968). There are two eigenvalues

$$\lambda_{1,2} = \frac{\frac{\alpha_1}{\rho_1} w_2 + \frac{\alpha_2}{\rho_2} w_1 \pm \sqrt{\left(\frac{\alpha_1}{\rho_1} w_2 + \frac{\alpha_2}{\rho_2} w_1\right)^2 - \left(\frac{\alpha_1}{\rho_1} + \frac{\alpha_2}{\rho_2}\right)\left(\frac{\alpha_1}{\rho_1} w_2^2 + \frac{\alpha_2}{\rho_2} w_1^2 - gH \frac{\alpha_1 \alpha_2 (\rho_2 - \rho_1)}{\rho_1 \rho_2}\right)}}{\left(\frac{\alpha_1}{\rho_1} + \frac{\alpha_2}{\rho_2}\right)}, \tag{2.114}$$

or after rearranging

$$\lambda_{1,2} = \frac{\frac{\alpha_1}{\rho_1} w_2 + \frac{\alpha_2}{\rho_2} w_1 \pm \sqrt{\left[gH(\rho_2 - \rho_1)\left(\frac{\alpha_1}{\rho_1} + \frac{\alpha_2}{\rho_2}\right) - (w_1 - w_2)^2\right] \frac{\alpha_1 \alpha_2}{\rho_1 \rho_2}}}{\left(\frac{\alpha_1}{\rho_1} + \frac{\alpha_2}{\rho_2}\right)}, \tag{2.115}$$

which are real and different from each other if

$$(w_1 - w_2)^2 < gH(\rho_2 - \rho_1)\left(\frac{\alpha_1}{\rho_1} + \frac{\alpha_2}{\rho_2}\right). \tag{2.116}$$

In fact this is the *Kelvin–Helmholtz* stability criterion. If the above condition is satisfied the system describing the flow is hyperbolic. In nature, violation of the above condition results in flow patterns that are different from the stratified one. Condition (2.116) is equivalent to Eq. (2.216) derived by *Delhaye* (1981, p. 90). In 1992 *Brauner* and *Maron* included the surface tension effect in their stability analysis and obtained

$$(w_1 - w_2)^2 < H\left(\frac{\alpha_1}{\rho_1} + \frac{\alpha_2}{\rho_2}\right)\left[g(\rho_2 - \rho_1) + \sigma_{12} k^2\right],$$

see Eq. (28a) in *Brauner* and *Maron* (1992), which for neglected surface tension results in Eq. (2.116). Here k is the real wave number.

2.7.1.3 Stratified flow in horizontal or inclined pipes

Geometrical characteristics: The geometric flow characteristics for round pipes are nonlinearly dependent on the liquid level, which makes the computation somewhat more complicated.

Some important geometrical characteristics are specified here – compare with Fig. 2.9. The angle with the origin of the pipe axis defined between the upwards oriented vertical and the liquid-gas-wall triple point is defined as a function of the liquid volume fraction by the equation

$$f(\theta) = -(1-\alpha_2)\pi + \theta - \sin\theta\cos\theta = 0\,. \tag{2.117}$$

The derivative

$$\frac{d\theta}{d\alpha_1} = \frac{\pi}{2\sin^2\theta} \tag{2.118}$$

will be used later. Bearing in mind that

$$\frac{df}{d\theta} = 2\sin^2\theta\,, \tag{2.119}$$

the solution with respect to the angle can be obtained by using the *Newton* iteration method as follows:

$$\theta = \theta_0 - \frac{f_0}{df/d\theta} = \theta_0 + \frac{(1-\alpha_2)\pi - \theta_0 + \sin\theta_0\cos\theta_0}{2\sin^2\theta_0}\,, \tag{2.120}$$

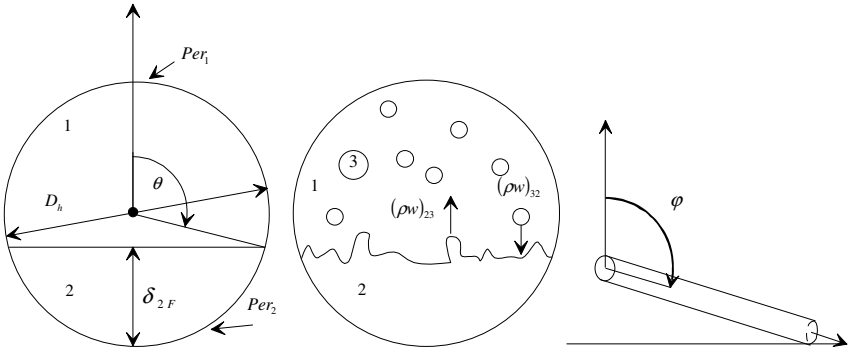

Fig. 2.9 Definition of the geometrical characteristics of the stratified flow

where subscript *0* indicates the previous guess in the iteration. The iteration starts with an initial value of $\pi/2$ (*Kolev* 1977). In 1999 *Biberg* proposed an accurate direct approximation

$$\theta = \pi\alpha_2 + \left(\frac{3\pi}{2}\right)^{1/3}\left[1 - 2\alpha_2 + \alpha_2^{1/3} - (1-\alpha_2)^{1/3}\right] \tag{2.120b}$$

with an error of less than $\pm 0.002 rad$ or

$$\theta = \pi\alpha_2 + \left(\frac{3\pi}{2}\right)^{1/3}\left[1 - 2\alpha_2 + \alpha_2^{1/3} - (1-\alpha_2)^{1/3}\right]$$
$$-\frac{1}{200}\alpha_2(1-\alpha_2)(1-2\alpha_2)\left\{1 + 4\left[\alpha_2^2 + (1-\alpha_2)^2\right]\right\}, \tag{2.120c}$$

with an error less then $\pm 0.00005 rad$. The perimeter of the pipe is then

$$Per_{1w} = \pi D_h , \tag{2.121}$$

and the wetted perimeters for the gas and the liquid parts are

$$Per_{1w} = \theta D_h , \tag{2.122}$$

$$Per_{2w} = (\pi - \theta) D_h . \tag{2.123}$$

The gas-liquid interface median is then

$$b = D_h \sin(\pi - \theta) = D_h \sin\theta , \tag{2.124}$$

and the liquid level is

$$\delta_{2F} = \frac{1}{2} D_h (1 + \cos\theta) . \tag{2.125}$$

The hydraulic diameters for the gas and the liquid for computation of the pressure drop due to friction with the wall are, therefore,

$$D_{h1} = 4\alpha_1 F / Per_{1w} = \frac{\pi}{\theta} \alpha_1 D_h , \tag{2.126}$$

$$D_{h2} = 4\alpha_2 F / Per_{2w} = \frac{\pi}{\pi - \theta} \alpha_2 D_h , \tag{2.127}$$

and the corresponding *Reynolds* numbers are

$$\mathrm{Re}_1 = \frac{\alpha_1 \rho_1 w_1 D_h}{\eta_1} \frac{\pi}{\theta} , \tag{2.128}$$

$$\mathrm{Re}_2 = \frac{\alpha_2 \rho_2 w_2 D_h}{\eta_2} \frac{\pi}{\pi - \theta} . \tag{2.129}$$

Here F is the channel cross-section section and Per_1 and Per_2 are the wet perimeters of gas and film, respectively.

If one considers the core of the flow the hydraulic diameter for computation of the friction pressure loss component at the gas-liquid interface is then

$$D_{h12} = 4\alpha_1 F / (Per_{1w} + b) = \frac{\pi}{\theta + \sin\theta} \alpha_1 D_h , \tag{2.130}$$

and the corresponding *Reynolds* number is

$$\mathrm{Re}_1 = \frac{\alpha_1 \rho_1 |w_1 - w_2| D_h}{\eta_1} \frac{\pi}{\theta + \sin\theta} . \tag{2.131}$$

The gas-wall, liquid-wall, and gas-liquid interfacial area densities are

$$a_{1w} = \frac{Per_{1w}}{F} = \frac{4\alpha_1}{D_{h1}} = \frac{\theta}{\pi}\frac{4}{D_h}, \tag{2.132}$$

$$a_{2w} = \frac{Per_{2w}}{F} = \frac{4\alpha_2}{D_{h2}} = \frac{\pi-\theta}{\pi}\frac{4}{D_h}, \tag{2.133}$$

$$a_{12} = \frac{b}{F} = \frac{\sin\theta}{\pi}\frac{4}{D_h}. \tag{2.134}$$

Some authors approximated this relation for a smooth interface with

$$a_{12} \cong \frac{8}{\pi D_h}\sqrt{\alpha_2\left(1-\alpha_2\right)}, \tag{2.135}$$

which in view of the accurate computation presented above is no longer necessary. For the estimation of the flow pattern transition criterion, the following expression is sometimes required:

$$\frac{d\alpha_2}{d\delta_{2F}} = \frac{4}{D_h}\frac{\sin\theta}{\pi}. \tag{2.136}$$

Gravitational (hydrostatic) pressure variation across the flow cross-section section of a horizontal pipe: In stratified flow the gravitation is a dominant force. The cross-section section averaged gas gravity pressure difference with respect to the interface is

$$\Delta p_1^{2\sigma} = \rho_1 g D_h\left(\frac{\sin^3\theta}{3\pi\alpha_1} - \frac{1}{2}\cos\theta\right). \tag{2.137}$$

The cross-section averaged liquid gravity pressure difference with respect to the bottom of the pipe is

$$\Delta p_2^{1\sigma} = -\rho_2 g D_h\left(\frac{\sin^3\theta}{3\pi\alpha_2} + \frac{1}{2}\cos\theta\right). \tag{2.138}$$

With respect to the interfacial pressure we have

$$p_1 = p_1^{2\sigma} - \Delta p_1^{2\sigma} = p_1^{2\sigma} - \rho_1 g D_h\left(\frac{\sin^3\theta}{3\pi\alpha_1} - \frac{1}{2}\cos\theta\right), \tag{2.139}$$

$$p_2 = p_2^{1\sigma} - \Delta p_2^{1\sigma} = p_2^{1\sigma} + \rho_2 g D_h\left(\frac{\sin^3\theta}{3\pi\alpha_2} + \frac{1}{2}\cos\theta\right), \tag{2.140}$$

which are, in fact, Eqs. (55) and (60) in *Ransom* et al. (1987 , p. 30). The averaged pressure in the cross-section section can be expressed as the cross-section section weighted averaged pressures inside the fields

$$p = \alpha_1 p_1 + \alpha_2 p_2 = \alpha_1 p_1^{2\sigma} + \alpha_2 p_2^{1\sigma} + gD_h \left[\frac{\sin^3 \theta}{3\pi} (\rho_2 - \rho_1) + (\alpha_2 \rho_2 + \alpha_1 \rho_1) \frac{1}{2} \cos\theta \right]. \tag{2.141}$$

Neglecting the surface tension we obtain

$$p \approx p_\sigma + gD_h \left[\frac{\sin^3 \theta}{3\pi} (\rho_2 - \rho_1) + (\alpha_2 \rho_2 + \alpha_1 \rho_1) \frac{1}{2} \cos\theta \right], \tag{2.142}$$

or

$$p_\sigma \approx p - gD_h \left[\frac{\sin^3 \theta}{3\pi} (\rho_2 - \rho_1) + (\alpha_2 \rho_2 + \alpha_1 \rho_1) \frac{1}{2} \cos\theta \right]. \tag{2.143}$$

The averaged pressure in the gas phase and in the liquid phase can then be expressed as a function of the system's averaged pressure and geometrical characteristics:

$$p_1 = p - gD_h \left[\frac{\sin^3 \theta}{3\pi\alpha_1} (\alpha_1 \rho_2 + \alpha_2 \rho_1) + \alpha_2 (\rho_2 - \rho_1) \frac{1}{2} \cos\theta \right] \quad \text{for} \quad \alpha_1 > 0, \tag{2.144}$$

$$p_2 = p + gD_h \left[\frac{\sin^3 \theta}{3\pi\alpha_2} (\alpha_1 \rho_2 + \alpha_2 \rho_1) + \alpha_1 (\rho_2 - \rho_1) \frac{1}{2} \cos\theta \right] \quad \text{for} \quad \alpha_2 > 0. \tag{2.145}$$

The check $\alpha_1 p_1 + \alpha_2 p_2 = p$ proves the correctness of the computation. The difference between both averaged pressures is then

$$\Delta p_{21} = p_2 - p_1 = gD_h \left[\frac{\sin^3 \theta}{3\pi} \left(\frac{\rho_2}{\alpha_2} + \frac{\rho_1}{\alpha_1} \right) + (\rho_2 - \rho_1) \frac{1}{2} \cos\theta \right]$$
$$\text{for} \quad \alpha_1 > 0 \text{ and } \alpha_2 > 0, \tag{2.146}$$

and, therefore ,Eqs. (2.93)–(2.96) are valid also for a circular pipe. Assuming that the change of the densities contributes much less to the change of Δp_{21}, the change of the local volume fraction results in

$$\frac{\partial \Delta p_{21}}{\partial z} \approx \frac{\partial \Delta p_{21}}{\partial \alpha_1} \frac{\partial \alpha_1}{\partial z}$$
$$= gD_h \left[\frac{\sin^3 \theta}{3\pi} \left(\frac{\rho_2}{\alpha_2^2} - \frac{\rho_1}{\alpha_1^2} \right) + \left(\frac{\rho_2}{\alpha_2} + \frac{\rho_1}{\alpha_1} \right) \frac{1}{2} \cos\theta - (\rho_2 - \rho_1) \frac{\pi}{4 \sin\theta} \right] \frac{\partial \alpha_1}{\partial z}. \tag{2.147}$$

This equation was obtained by taking into account that θ is also an implicit function of α_1 through Eq. (2.117) and using Eq. (2.118). Using Eqs. (2.156), (2.146), (2.137), and (2.138) and substituting into the momentum equations (2.100) and (2.101), we finally obtain

$$... + \gamma_z \left[\alpha_1 \frac{\partial p}{\partial z} + \alpha_1 \alpha_2 (\rho_2 - \rho_1) \frac{\pi g D_h}{4 \sin\theta} \frac{\partial \alpha_1}{\partial z} \right] - \Delta p_1^{w\sigma} \frac{\partial \gamma_z}{\partial z} ... \tag{2.148}$$

$$... + \gamma_z \left[\alpha_2 \frac{\partial p}{\partial z} - \alpha_1 \alpha_2 (\rho_2 - \rho_1) \frac{\pi g D_h}{4 \sin\theta} \frac{\partial \alpha_1}{\partial z} \right] - \Delta p_2^{w\sigma} \frac{\partial \gamma_z}{\partial z} ... \tag{2.149}$$

As a plausibility check note that for $\alpha_1 \to 0$ the term containing the derivative of the volume fraction of velocity field 1 converges to zero and the momentum equation for field 2 takes the expected form. The sum of the two equations is then

$$... + \gamma_z \frac{\partial p}{\partial z} - \left(\Delta p_1^{w\sigma} + \Delta p_2^{w\sigma} \right) \frac{\partial \gamma_z}{\partial z} ... \tag{2.150}$$

Comparing with the momentum equations for the rectangular channel we find instead of H the length $\frac{\pi D_h}{4 \sin\theta} = \frac{\pi D_h^2}{4b}$, which is the height of the rectangular channel having the same cross-section section as the pipe and a base equal to the gas-liquid median from Eq. (2.124). Therefore, the stability condition for stratified flow in a pipe is

$$\left(w_1 - w_2 \right)^2 < g \frac{\pi D_h}{4 \sin\theta} (\rho_2 - \rho_1) \left(\frac{\alpha_1}{\rho_1} + \frac{\alpha_2}{\rho_2} \right), \tag{2.151a}$$

or in an alternative form

$$\left(w_1 - w_2 \right)^2 < g (\rho_2 - \rho_1) \left(\frac{\alpha_1}{\rho_1} + \frac{\alpha_2}{\rho_2} \right) \frac{d\delta_{2F}}{d\alpha_2}, \tag{2.151b}$$

which is a generalized *Kelvin–Helmholtz* stability criterion valid for pipes with arbitrary cross-section section. Substituting Eq. (2.82) in the above equation we obtain Eq. (2.116) for rectangular channels. This result is, in fact, Eq. (26) in *Barnea* and *Taitel* (1994) for the inviscid case. It is identical with Eq. (6.9), p. 313, obtained by *de Crecy* in 1986.

Dividing the momentum equations by $\alpha_1 \rho_1$ and $\alpha_2 \rho_2$, respectively, and subtracting the second from the first, we obtain

$$... + \gamma_z \left[\left(\frac{1}{\rho_1} - \frac{1}{\rho_2} \right) \frac{\partial p}{\partial z} + \frac{\rho}{\rho_1 \rho_2} (\rho_2 - \rho_1) \frac{\pi g D_h}{4 \sin\theta} \frac{\partial \alpha_1}{\partial z} \right] - \left(\frac{\Delta p_1^{w\sigma}}{\alpha_1 \rho_1} - \frac{\Delta p_2^{w\sigma}}{\alpha_2 \rho_2} \right) \frac{\partial \gamma_z}{\partial z} ... \tag{2.152}$$

The second term in the first brackets is exactly Eq. (58) obtained by *Ransom* et al. (1987, p. 30).

Note the general notation of the coefficients of $\partial\alpha_1/\partial z$ in Eqs. (2.103) and (2.104) and Eqs. (2.148) and (2.149)

$$\alpha_1\alpha_2(\rho_2-\rho_1)g\frac{F}{b}\frac{\partial\alpha_1}{\partial z},$$

where F is the channel cross-section section and b is the gas-liquid interface median. This result was obtained by *de Crecy* (1986, p. 312) in his Eq. (6.3).

Teletov and *Mamaev* et al., see *Mamaev* et al. (1969), presented analytical solutions for stratified flow between two parallel plates and stratified flow in circular tubes, respectively. The gas and liquid phases are considered incompressible. No heat and mass transfer is considered. The pressure gradient is assumed constant and the flow is considered to be stationary and fully developed. The velocities at the wall are assumed to be zero and the velocity at the interface is assumed to be equal for both phases. The solution for the circular tube is found after introducing a bipolar coordinate transformation and integration, and is expressed as cross-section section averaged velocities as a function of the flow parameter in the form

$$w_1=\frac{\pi R^4}{8\eta_1}\left[\frac{dp}{dz}-\rho_1 g\cos(\mathbf{g},z)\right]\varphi_1(\alpha_1,\eta_2/\eta_1),$$

$$w_2=\frac{\pi R^4}{8\eta_2}\left[\frac{dp}{dz}-\rho_2 g\cos(\mathbf{g},z)\right]\varphi_2(\alpha_1,\eta_2/\eta_1).$$

$\varphi_1(\alpha_1,\eta_2/\eta_1)$ and $\varphi_2(\alpha_1,\eta_2/\eta_1)$ are complicated integral functions. For practical use they are presented in graphical form.

2.7.2 Dispersed interface

2.7.2.1 General

In this section, we provide a guide for derivation of a constitutive relation for mechanical interaction between a dispersed field l and the surrounding continuum m. An example for such flow is bubbly flow. In other words, we discuss a possible simplification of the surface integrals in Eq. (2.50). For a dispersed phase l, the viscous shear at the interface is negligible for non-*Stokes* flows:

$$-\frac{1}{Vol}\int_{F_{l\sigma}}\mathbf{T}_l^{m\sigma}\cdot\mathbf{n}_l dF\approx 0. \tag{2.153}$$

The viscous effects in the continuum at the interface are also neglected,

$$-\frac{1}{Vol}\int_{F_{m\sigma}}\mathbf{T}_m^{l\sigma}\cdot\mathbf{n}_m dF\approx 0. \tag{2.154}$$

Note that a 1 cm bubble in water having a relative velocity of 10 cm/s has a *Reynolds* number of about 100. For Reynolds numbers less than 24 the viscous effect in the continuum is important. For larger Reynolds numbers, which is often the case in nature, the viscous effects can be neglected. The force of the *Marangoni* effect,

$$\delta_l \frac{1}{Vol} \int_{F_{l\sigma}} (\nabla_t \sigma_{lm}) dF = 0 , \tag{2.155}$$

can be neglected for the majority of macroscopic processes. If the dispersed phase is assumed to have no wall contact, $F_{lw} = 0$, the following results:

$$\frac{1}{Vol} \int_{F_{lw}} \left(\Delta p_l^{w\sigma} \mathbf{I} - \mathbf{T}_l^{w\sigma} \right) \cdot \mathbf{n}_l dF = 0 . \tag{2.156}$$

The difference between the bubble bulk pressure and the bubble interface pressure is also negligible,

$$+\frac{1}{Vol} \int_{F_{m\sigma}} \Delta p_l^{m\sigma} \mathbf{n}_m dF \approx 0 . \tag{2.157}$$

The momentum equation for the dispersed field is

$$\begin{aligned} &\frac{\partial}{\partial \tau}\left(\alpha_l \rho_l \mathbf{V}_l \gamma_v\right) + \nabla \cdot \left(\alpha_l^e \rho_l \mathbf{V}_l \mathbf{V}_l \gamma\right) + \nabla \cdot \left[\alpha_l^e \left(\rho_l \overline{\mathbf{V}_l' \mathbf{V}_l'}\right) \gamma\right] + \alpha_l^e \gamma \nabla p_l + \alpha_l \gamma_v \rho_l \mathbf{g} \\ &+ \left(p_l - p_m + \delta_l \sigma_{lm} \kappa_l\right) \nabla \left(\alpha_l^e \gamma\right) + \frac{1}{Vol} \int_{F_{l\sigma}} \Delta p_m^{l\sigma} \mathbf{n}_l dF = \gamma_v \sum_{\substack{k=1 \\ k \neq l}}^{3,w} \left(\mu_{kl} \mathbf{V}_k - \mu_{lk} \mathbf{V}_l\right) . \end{aligned} \tag{2.158}$$

The dispersed equation for the continuum (2.50b) is

$$\begin{aligned} &\frac{\partial}{\partial \tau}\left(\alpha_m \rho_m \mathbf{V}_m \gamma_v\right) + \nabla \cdot \left(\alpha_m^e \rho_m \mathbf{V}_m \mathbf{V}_m \gamma\right) + \nabla \cdot \left[\alpha_m^e \gamma \left(\rho_m \overline{\mathbf{V}_m' \mathbf{V}_m'} - \delta_m \mathbf{T}_m\right)\right] + \alpha_m \gamma_v \rho_m \mathbf{g} \\ &+ \alpha_m^e \gamma \nabla p_m - \frac{1}{Vol} \int_{F_{m\sigma}} \Delta p_m^{l\sigma} \mathbf{n}_l dF + \frac{1}{Vol} \int_{F_{mw}} \left(\Delta p_m^{w\sigma} \mathbf{I} - \mathbf{T}_m^{w\sigma}\right) \cdot \mathbf{n}_m dF \\ &= \gamma_v \sum_{\substack{k=1 \\ k \neq m}}^{3,w} \left(\mu_{km} \mathbf{V}_k - \mu_{mk} \mathbf{V}_m\right) \end{aligned} \tag{2.159}$$

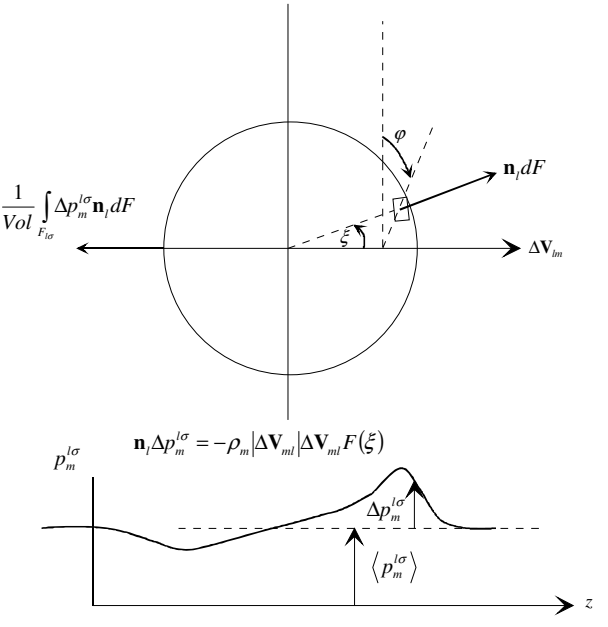

Fig. 2.10 Difference between the bulk pressure and interfacial pressure inside the velocity field *m* for steady state flow

The term in the momentum equation for the dispersed field that remains to be estimated is

$$\frac{1}{Vol}\int_{F_{l\sigma}} \Delta p_m^{l\sigma}\mathbf{n}_l dF \,.$$

For this, information is needed about the pressure distribution over the surface of a single particle, see Fig. 2.10. For illustration of the estimation of this integral we assume a family of monodisperse spheres. For dispersed flow with a small concentration of the dispersed phase, the flow about each sphere can be considered as unaffected by its neighbors. The interface pressure distribution along the surface can be generally represented by the following expression:

$$\Delta p_m^{l\sigma}\mathbf{n}_l = -\frac{1}{2}\rho_m R_l \left[\frac{\partial}{\partial\tau}\Delta\mathbf{V}_{ml} + \left(\mathbf{V}_l \cdot \nabla\right)\Delta\mathbf{V}_{ml}\right]\cos\xi + \rho_m \left|\Delta\mathbf{V}_{ml}\right|^2 F\left(\xi\right), \tag{2.160}$$

see, for example, *Stuhmiller* (1977). Here a spherical coordinate system is used with the main axis along $\Delta\mathbf{V}_{lm}$. The polar angle ξ is measured with respect to the direction of $\Delta\mathbf{V}_{lm}$. The azimuthal angle is φ. The force per unit surface is split into a component parallel to $\Delta\mathbf{V}_{lm}$ and a component perpendicular to $\Delta\mathbf{V}_{lm}$. The integration is then performed. Note that Eq. (2.160) does not depend on φ and,

therefore, the perpendicular component for the symmetric body is **0**. Note also that the pressure distribution in Eq. (2.160) does not take into account the spatial variation of the continuum velocity. The latter will give rise to a force component perpendicular to $\Delta\mathbf{V}_{lm}$ even for a symmetric body. For the integration we need the following relations. The differential surface element of the sphere (rotational body) is $dF = R_l^2 \sin\xi \, d\xi \, d\varphi$. The projection of the interfacial pressure force on direction $\Delta\mathbf{V}_{lm}$ for a single particle is, therefore,

$$\frac{1}{Vol}\int_{F_{l\sigma}} \Delta p_m^{l\sigma}\mathbf{n}_l \cos\xi dF = R_l^2 \int_0^{2\pi}\int_0^{\pi} \Delta p_m^{l\sigma}\mathbf{n}_l \cos\xi \sin\xi \, d\xi \, d\varphi, \tag{2.161}$$

and on the plane normal to $\Delta\mathbf{V}_{lm}$

$$\frac{1}{Vol}\int_{F_{l\sigma}} \Delta p_m^{l\sigma}\mathbf{n}_l \sin\xi dF = R_l^2 \int_0^{2\pi}\int_0^{\pi} \Delta p_m^{l\sigma}\mathbf{n}_l \sin^2\xi \, d\xi \, d\varphi. \tag{2.162}$$

For our case of a rotational body, the above integral gives **0**. The collective force acting on the cloud of $n_l \sum_{l=1}^{3} Vol_l$ spheres in the control volume *Vol* per unit control volume in the axial direction is, therefore,

$$\frac{\sum_{l=1}^{3} Vol_l}{Vol} n_l R_l^2 \int_0^{2\pi}\int_0^{\pi} \Delta p_m^{l\sigma}\mathbf{n}_l \cos\xi \sin\xi \; d\xi \, d\varphi = \gamma_v n_l R_l^2 \int_0^{2\pi}\int_0^{\pi} \Delta p_m^{l\sigma}\mathbf{n}_l \cos\xi \sin\xi \, d\xi \, d\varphi, \tag{2.163}$$

and in the plane normal to $\Delta\mathbf{V}_{ml}$

$$\frac{\sum_{l=1}^{3} Vol_l}{Vol} n_l R_l^2 \int_0^{2\pi}\int_0^{\pi} \Delta p_m^{l\sigma} \, \mathbf{n}_l \sin^2\xi \, d\xi \, d\varphi = \gamma_v n_l R_l^2 \int_0^{2\pi}\int_0^{\pi} \Delta p_m^{l\sigma} \, \mathbf{n}_l \sin^2\xi \, d\xi \, d\varphi. \tag{2.164}$$

Estimation of the integrals (2.163) and (2.164) provides a practical approach for computing the interfacial forces. What remains after the integration and some rearrangements given in the next section is

$$\begin{aligned}
&\frac{1}{Vol}\int_{F_{l\sigma}} \Delta p_m^{l\sigma}\mathbf{n}_l dF = -\gamma_v \alpha_l \frac{1}{2}\rho_m \left[\frac{\partial}{\partial\tau}\Delta\mathbf{V}_{ml} + \left(\mathbf{V}_l \cdot \nabla\right)\Delta\mathbf{V}_{ml}\right] \\
&+0.37 c_{ml}^d \rho_m \left|\Delta\mathbf{V}_{ml}\right|^2 \nabla\left(\alpha_l^e \gamma\right) - \gamma_v \alpha_l \rho_m \frac{1}{D_l}\frac{3}{4} c_{ml}^d \left|\Delta\mathbf{V}_{ml}\right| \Delta\mathbf{V}_{ml} \\
&= \gamma_v \left(\mathbf{f}_l^{vm} + \mathbf{f}_l^d\right) + \Delta p_m^{l\sigma *} \frac{1}{Vol}\int_{F_l^{m\sigma}} \mathbf{n}_l dF.
\end{aligned} \tag{2.165}$$

This result for one-dimensional flow was obtained by *Stuhmiller* (1977). If we take the nonisotropy of the continuum velocity field into account in Eq. (2.160), we obtain the general form

$$\frac{1}{Vol}\int\limits_{F_{l\sigma}} \Delta p_m^{l\sigma}\mathbf{n}_l dF = \gamma_v\left(\mathbf{f}_l^{vm}+\mathbf{f}_l^{d}+\mathbf{f}_l^{L}\right)+\Delta p_m^{l\sigma *}\frac{1}{Vol}\int\limits_{F_l^{m\sigma}}\mathbf{n}_l dF\,. \tag{2.166}$$

The force components $\mathbf{f}_l^{vm}$, $\mathbf{f}_l^{d}$, $\mathbf{f}_l^{L}$, and $\Delta p_m^{l\sigma *}\frac{1}{Vol}\int\limits_{F_l^{m\sigma}}\mathbf{n}_l dF$ are called virtual mass force, drag force, lift force, and stagnation pressure force, respectively. A detailed discussion of these is given below. Empirical information on how to compute these forces is given in Volume II.

The pressure distribution around a particle may influence the local mass transfer. In the case of strong thermodynamic nonequilibrium, the larger pressure difference across the interface at the stagnation point may lead to lower evaporation compared to the rear point. It may lead to a reactive resulting force at the droplet, which manifests itself as an effective drag reduction. A strong condensation may lead to the opposite effect. Although such arguments may sound reasonable, one should be careful because there is no accurate theoretical or experimental treatment of this problem.

2.7.2.2 Virtual mass force

Consider the integral defined by Eq. (2.161) taking over the first term of Eq. (2.160)

$$\begin{aligned}\gamma_v\mathbf{f}_l^{vm} &= -\gamma_v n_l\frac{1}{2}\rho_m\left[\frac{\partial}{\partial\tau}\Delta\mathbf{V}_{ml}+\left(\mathbf{V}_l\cdot\nabla\right)\Delta\mathbf{V}_{ml}\right]R_l^3\int_0^{2\pi}d\varphi\int_0^{\pi}\cos^2\xi\sin\xi d\xi\\ &= -\gamma_v n_l\frac{4}{3}\pi R_l^3\frac{1}{2}\rho_m\left[\frac{\partial}{\partial\tau}\Delta\mathbf{V}_{ml}+\left(\mathbf{V}_l\cdot\nabla\right)\Delta\mathbf{V}_{ml}\right]\\ &= -\gamma_v\alpha_l\frac{1}{2}\rho_m\left[\frac{\partial}{\partial\tau}\Delta\mathbf{V}_{ml}+\left(\mathbf{V}_l\cdot\nabla\right)\Delta\mathbf{V}_{ml}\right].\end{aligned} \tag{2.167}$$

The force $\mathbf{f}_l^{vm}$ is the *virtual mass force* per unit mixture volume. Here, the virtual mass coefficient is $c_{ml}^{vm}=1/2$. The general form of the virtual mass force with the accuracy of an empirical coefficient was first proposed first *Prandtl* (1952), *Lamb* (1945), and *Milne-Thomson* (1968) in the same form

$$\mathbf{f}_d^{vm}=-\alpha_d\rho_c c_d^{vm}\left[\frac{\partial}{\partial\tau}\Delta\mathbf{V}_{cd}+\left(\mathbf{V}_d\cdot\nabla\right)\Delta\mathbf{V}_{cd}\right], \tag{2.168}$$

where the subscripts *c* and *d* mean continuous and disperse, respectively. The scalar force components in *Cartesian* and in *cylindrical* coordinates are

$$f_{d,r}^{vm} = -\alpha_d \rho_c c_d^{vm} \left\{ \begin{array}{l} \dfrac{\partial}{\partial \tau}(u_c - u_d) + u_d \dfrac{\partial}{\partial r}(u_c - u_d) \\ \\ +v_d \dfrac{1}{r^\kappa} \dfrac{\partial}{\partial \theta}(u_c - u_d) + w_d \dfrac{\partial}{\partial z}(u_c - u_d) \end{array} \right\}, \tag{2.169}$$

$$f_{d,\theta}^{vm} = -\alpha_d \rho_c c_d^{vm} \left\{ \begin{array}{l} \dfrac{\partial}{\partial \tau}(v_c - v_d) + u_d \dfrac{\partial}{\partial r}(v_c - v_d) \\ \\ +v_d \dfrac{1}{r^\kappa} \dfrac{\partial}{\partial \theta}(v_c - v_d) + w_d \dfrac{\partial}{\partial z}(v_c - v_d) \end{array} \right\}, \tag{2.170}$$

$$f_{d,z}^{vm} = -\alpha_d \rho_c c_d^{vm} \left\{ \begin{array}{l} \dfrac{\partial}{\partial \tau}(w_c - w_d) + u_d \dfrac{\partial}{\partial r}(w_c - w_d) \\ \\ +v_d \dfrac{1}{r^\kappa} \dfrac{\partial}{\partial \theta}(w_c - w_d) + w_d \dfrac{\partial}{\partial z}(w_c - w_d) \end{array} \right\}. \tag{2.171}$$

The virtual mass force is experienced by the body as if it were to have an additional mass during its translation relative to the continuum. This explains the other name used for this force, *added mass force*. For larger particle concentrations, c_d^{vm} is a function of α_l. Expressions for practical computation of the virtual mass coefficient for dispersed fields with larger concentration can be found in *Biesheuvel* and *van Wijngaarden* (1984), *Biesheuvel* and *Spollstra* (1989), *Cook* and *Harlow* (1983, 1984), *Ishii* and *Michima* (1984), *Lahey* (1991), *Lamb* (1945), *Milne-Thomson* (1968), *Mokeyev* (1977), *No* and *Kazimi* (1985), *Prandtl* (1952), *Ruggles* et al. (1988), *van Wijngaarden* (1976), *Winatabe* et al. (1990), *Wallis* (1969), and *Zuber* (1964). These references represent the state of the art in this field. *Winatabe* et al. (1990) proposed the use of only the transient part of the virtual mass force for the case of strong transients.

Lamb (1945) computed the virtual mass coefficient for partials in potential flow with ellipsoidal shape defined by

$$\frac{x^2}{R_x} + \frac{y^2}{R_y} + \frac{z^2}{R_z} = 1,$$

where the lengths of the principal axis are R_x, R_y and R_z, and the relative velocity is parallel to the x-axis as follows:

$$c_{cd}^{vm} = \frac{a_0}{2 - a_0},$$

$$a_0 = R_x R_y R_z \int_0^\infty \frac{d\lambda}{\left(R_x^2+\lambda\right)\sqrt{\left(R_x^2+\lambda\right)\left(R_y^2+\lambda\right)\left(R_z^2+\lambda\right)}}.$$

Bournaski (1992) evaluated some values as given in Table 2.1.

Table 2.1. Virtual mass coefficients for an ellipsoid

Shape of particles	Translation parallel to axis		
	x	y	z
	$c_{cd,x}^{vm}$	$c_{cd,y}^{vm}$	$c_{cd,z}^{vm}$
$R_x = R_y = R_z$, sphere	1/2	1/2	1/2
$R_x = R_y = R_z/2$, rotary ellipsoid	0.704	0.704	0.210
$R_x = R_y = R_z/3$, rotary ellipsoid	0.803	0.803	0.122
$R_x = R_y = R_z/4$, rotary ellipsoid	0.859	0.859	0.081
$R_x = (2/3)R_y = R_z/2$, unrotary ellipsoid	0.936	0.439	0.268
$R_x = R_y/2 = R_z/4$, unrotary ellipsoid	1.516	0.398	0.126

For a single ellipsoid bubble with axis aspect ratio χ

$$c_{21}^{vm} = \frac{\left(\chi^2-1\right)^{1/2} - \cos^{-1}\chi^{-1}}{\cos^{-1}\chi^{-1} - \left(\chi^2-1\right)^{1/2}/\chi^2},$$

van Wijngaarden (1998).

Lance and *Bataille* (1991) reported experiments showing that for a 5mm deforming bubble the virtual mass coefficient is in the region: $1.2 < c_{21}^{vm} < 3.4$. For a family of spherical bubbles:

$$c_{21}^{vm} = \frac{1}{2}\left(1+2.78\alpha_1\right),$$

dilute bubble dispersion, interaction between two equally sized bubbles, *van Wijngaarden* (1976);

$$c_{21}^{vm} = \frac{1}{2}\frac{1+2\alpha_1}{1-\alpha_1},$$

no interaction with the neighboring bubbles, *Zuber* (1964);

$$c_{21}^{vm} = \frac{1}{2}\left(1+3\alpha_1\right),\ \alpha \to 0,$$

Zuber (1964);

$$c_{21}^{vm} = \frac{1}{2}\left(1+3.32\alpha_1\right),$$

analogously to thermal conductivity in composite material, *Jeffrey* (1973);

$$c_{21}^{vm} = \frac{1}{2}\left[\frac{1}{2}-1.98\ln\left(0.62-\alpha_1\right)\right],$$

the approximation for $\alpha_1 \le 0.35$, *Biesheuvel* and *Spoelstra* (1989). *Laurien* and *Niemann* (2004) used direct numerical simulation and come to

$$c_{21}^{vm} = 0.5+1.63\alpha_1+3.85\alpha_1^2.$$

Kendoush (2006) considered the separation of the velocity profile around a single sphere and obtained a virtual mass coefficient depending on the separation angle. *Pougatch*, *Salcudean*, *Chan,* and *Knapper* (2008) concluded that the virtual mass force cannot be larger than the inertia force for accelerating the remaining liquid and, therefore, the coefficient is naturally limited by

$$c_{21}^{vm} \le \alpha_2/\alpha_1.$$

2.7.2.3 Form drag and stagnation pressure force

For inviscid (ideal) potential flow we have in Eq. (2.160)

$$F\left(\xi\right) = \frac{1}{8}\left(9\cos^2\xi-5\right), \tag{2.172}$$

see *Lamb* (1945). This profile does not give any resulting force component (*d'Alembert's* paradox).

In nature $F\left(\xi\right)$ gives a nonsymmetric profile, as indicated in Fig. 2.10. For an idealized nonsymmetric fore-aft profile, *Nigmatulin* (1979) estimated the integrals of Eqs. (2.160) and (2.161) for the second term of the right-hand side of Eq. (2.159) for bubbles in bubble-liquid flows. *Biesheuvel* and *van Wijngaarden* (1984) analytically computed the coefficients for spherical bubbles for *Nigmatuli's* derivation.

A more general approach was proposed by *Hwang* and *Schen* (1992). For the general case, $F\left(\xi\right)$ is determined experimentally, see *Schlichting* (1959, p.21, Fig. 1.11). *Hwang* and *Schen* (1992) provided a method for computing the pressure distribution around a sphere for Reynolds numbers greater than 3000, where

$$F\left(\xi\right) = \frac{1}{4}\left\{\frac{2\lambda^2-1}{\lambda^2+4}+\frac{9}{2}\frac{e^{-\lambda\xi}}{\lambda^2+4}\left[2\lambda\sin\left(2\xi\right)+\cos\left(2\xi\right)\right]\right\}, \tag{2.173}$$

see Eq. (12) in *Hwang* and *Schen* (1992). When the drag coefficient c_{ml}^{d} is known and the equation

$$c_{ml}^{d} = 45\frac{1-e^{-\pi\lambda}}{\left(\lambda^2+4\right)\left(\lambda^2+16\right)} \tag{2.174}$$

is solved for the smaller real root of λ, there is a method for estimating the integrals analytically. The reader can find the final result of this derivation, characterized by anisotropic forces in *Hwang* and *Schen* (1992).

Before *Hwang* and *Schen* published their work, *Stuhmiller* (1977) had already rewritten the term $F(\xi)$ as follows:

$$F(\xi) = \left\langle F(\xi)\right\rangle^{l\sigma} + F(\xi) - \left\langle F(\xi)\right\rangle^{l\sigma}, \tag{2.175}$$

where $\left\langle F(\xi)\right\rangle^{l\sigma}$ represents the surface average over a single sphere. For a *turbulent pressure distribution* around a sphere as given by *Schlichting* (1959), the interface average of the function $F(\xi)$ is

$$\left\langle F(\xi)\right\rangle^{l\sigma} = -0.37c_{ml}^{d}, \tag{2.176}$$

where c_{ml}^{d} is the form drag coefficient for single particles. In the literature sometimes $\left\langle F(\xi)\right\rangle^{l\sigma}$ is set to the constant value ¼ – see, for instance, *Lamb* (1945). This means that the integral over the second term of Eq. (2.160) can be split into two parts. The first part can be estimated directly exploiting the fact that $\left\langle F(\xi)\right\rangle^{l\sigma}$ does not depend on the position at the interface. The result is

$$\begin{aligned}\rho_m\left|\Delta\mathbf{V}_{ml}\right|^2 \int\limits_{F_{l\sigma}} \left\langle F(\xi)\right\rangle^{l\sigma}\mathbf{n}_l dF &= -\rho_m\left|\Delta\mathbf{V}_{ml}\right|^2\left\langle F(\xi)\right\rangle^{l\sigma}\left[\nabla\left(\alpha_l^e\gamma\right)+\frac{1}{Vol}\int\limits_{F_{lw}}\mathbf{n}_l dF\right]\\ = 0.37c_{ml}^{d}\rho_m\left|\Delta\mathbf{V}_{ml}\right|^2\left[\nabla\left(\alpha_l^e\gamma\right)+\frac{1}{Vol}\int\limits_{F_{lw}}\mathbf{n}_l dF\right] &= 0.37c_{ml}^{d}\rho_m\left|\Delta\mathbf{V}_{ml}\right|^2\nabla\left(\alpha_l^e\gamma\right),\end{aligned} \tag{2.177}$$

which results in an effective stagnation pressure difference

$$\Delta p_m^{l\sigma *} = -0.37c_{ml}^{d}\rho_m\left|\Delta\mathbf{V}_{ml}\right|^2 \tag{2.178}$$

similar to that discussed for stratified flow (Eq. (2.64)). To derive Eq. (2.177), Eq. (29) from *Kolev* (1994b) is also used together with the fact that there is no contact between the dispersed field and the wall, $F_{lw} = 0$.

The second part is the net force experienced by the particle due to nonuniform pressure distribution around the particle, the so-called form drag force:

$$\gamma_v \mathbf{f}_l^d = -\gamma_v n_l \rho_m \left|\Delta\mathbf{V}_{ml}\right| \Delta\mathbf{V}_{ml} R_l^2 \int_0^{2\pi} d\varphi \int_0^{\pi} \left[F(\xi) - \left\langle F(\xi) \right\rangle^{l\sigma} \right] \cos\xi \sin\xi d\xi$$

$$= -\gamma_v n_l \rho_m \left|\Delta\mathbf{V}_{ml}\right| \Delta\mathbf{V}_{ml} c_{ml}^d \frac{1}{2} \pi R_l^2 = -\gamma_v \left[\alpha_l / \left(\frac{4}{3} \pi R_l^3 \right) \right] \rho_m \left|\Delta\mathbf{V}_{ml}\right| \Delta\mathbf{V}_{ml} c_{ml}^d \frac{1}{2} \pi R_l^2$$

$$= -\gamma_v \alpha_l \rho_m \frac{1}{D_l} \frac{3}{4} c_{ml}^d \left|\Delta\mathbf{V}_{ml}\right| \Delta\mathbf{V}_{ml} . \qquad (2.179)$$

The form drag force per unit mixture volume is, therefore,

$$\mathbf{f}_l^d = -\alpha_l \rho_m \frac{1}{D_l} \frac{3}{4} c_{ml}^d \left|\Delta\mathbf{V}_{ml}\right| \Delta\mathbf{V}_{ml} . \qquad (2.180)$$

For larger volume fractions α_l one should take into account the dependence of the drag force on the volume fraction – also see *Ishii* and *Mishima* (1984) and *Zuber* (1964), for example. For drag forces in two-phase flows, the study by *Ishii* and *Mishima* (1984) is recommended.

2.7.2.4 Lift force

Note on particle rotation: A rotating sphere obeys the law of conservation of momentum

$$I_d \frac{d\omega_d}{d\tau} = -C_d^{\omega} \left(\frac{D_d}{2} \right)^5 \frac{1}{2} \rho_d \left|\omega_d\right| \omega_d .$$

Here, the particle rotation velocity is ω_d and I_d is the particle's moment of inertia.

$$C_d^{\omega} = \frac{c_1}{\left(\mathrm{Re}_{cd}^{\omega}\right)^{1/2}} + \frac{c_2}{\mathrm{Re}_{cd}^{\omega}} + c_3 \, \mathrm{Re}_{cd}^{\omega}$$

is a coefficient depending on the rotational *Reynolds* number

$$\mathrm{Re}_{cd}^{\omega} = \left(\frac{D_d}{2} \right) \left|\omega_d\right| \Big/ \nu_c .$$

The *c* coefficients are given by *Yamamotto* et al. (2001) in the following table:

$\mathrm{Re}_{cd}^{\omega}$	0 to 1	1 to 10	10 to 20	20 to 50	>50
c_1	0	0	5.32	6.44	6.45
c_2	50.27	50.27	37.2	32.2	32.1
c_3	0	0.0418	5.32	6.44	6.45

We learn from this dependence that small and light particles can be more easily put in rotation compared to heavy and large particles. The following three main idealizations give an idea of the origin of the so-called lift force:

a) A rotating symmetric particle in symmetric flow of continuum experiences a lift force called the *Magnus* force (named after the Berlin physicist *Gustav Magnus*, 1802–1870). The curiosity of Lord *Rayleigh* in regard to the trajectory of the tennis ball led him in 1877 to the corresponding explanation. The force was analytically estimated by *Jukowski* and independently by *Kutta*, see *Albring* (1970, p. 75).
b) A nonrotating symmetric particle in nonsymmetric continuum flow as presented in Fig. 2.11 experiences lift force, *Jukowski*.
c) A nonrotating asymmetric particle in symmetric continuum flow experiences lift force, *Jukowski*.

The force component perpendicular to the relative velocity direction is called the lateral or *lift force*. The lift force is zero for symmetric bodies exposed to symmetrical flow

$$\mathbf{f}_l^L = 0\,. \tag{2.181}$$

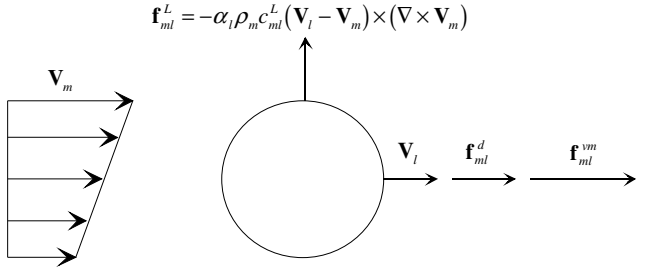

Fig. 2.11 Drag, virtual mass, and lift forces acting simultaneously on the field *l*

A symmetric body exposed to asymmetrical flow experiences a lateral force – see Fig. 2.11. The lift force is similar in nature to the aerodynamic lift of an airfoil, but differs in that it is a result of the gradient in the continuum velocity field over a symmetric body rather than a uniform flow over an asymmetric airfoil. The general form of the lateral lift force for inviscid flows is given by *Drew* and *Lahey* (1987)

$$\mathbf{f}_{cd}^L = -\alpha_d \rho_c c_{cd}^L \left(\mathbf{V}_d - \mathbf{V}_c\right) \times \left(\nabla \times \mathbf{V}_c\right). \tag{2.182}$$

The scalar components for *Cartesian* and *cylindrical* coordinates are

$$f_{cd,r}^L = -\alpha_d \rho_c c_{cd}^L \left\{ \left(v_d - v_c\right) \left[\frac{1}{r^\kappa} \frac{\partial}{\partial r} \left(r^\kappa v_c \right) - \frac{1}{r^\kappa} \frac{\partial u_c}{\partial \theta} \right] - \left(w_d - w_c\right) \left(\frac{\partial u_c}{\partial z} - \frac{\partial w_c}{\partial r} \right) \right\}, \tag{2.183}$$

$$f_{cd,\theta}^{L} = -\alpha_d \rho_c c_{cd}^{L} \left\{ \left(w_d - w_c \right) \left[\frac{1}{r^{\kappa}} \frac{\partial w_c}{\partial \theta} - \frac{\partial v_c}{\partial z} \right] - \left(u_d - u_c \right) \left(\frac{1}{r^{\kappa}} \frac{\partial}{\partial r} \left(r^{\kappa} v_c \right) - \frac{1}{r^{\kappa}} \frac{\partial u_c}{\partial \theta} \right) \right\} , \tag{2.184}$$

$$f_{cd,z}^{L} = -\alpha_d \rho_c c_{cd}^{L} \left\{ \left(u_d - u_c \right) \left[\frac{\partial u_c}{\partial z} - \frac{\partial w_c}{\partial r} \right] - \left(v_d - v_c \right) \left(\frac{1}{r^{\kappa}} \frac{\partial w_c}{\partial \theta} - \frac{\partial v_c}{\partial z} \right) \right\} . \tag{2.185}$$

The lift coefficient must be derived experimentally. The reader will find information on modeling of the lift force in *Deich* and *Philipoff* (1981), *Staffman* (1965), *Bernemann* et al. (1991), *Soo* and *Tung* (1972), *Ho* and *Leal* (1976), *Vasseur* and *Cox* (1976), *Drew* and *Lahey* (1987, 1990), *Erichhorn* and *Small* (1969), and *Bataille* et al. (1990).

For negligible particle rotation, *Staffman* (1965, 1968) derived a negligible particle *Reynolds* number and small gradients of the continuum velocity the analytical expression for the shear lift force

$$c_{21}^{L} = 3.084 \nu_2^{1/2} \Bigg/ \left(D_1 \left| \frac{dw_2}{dr} \right|^{1/2} \right) .$$

Inside the boundary layer of bubbly flow having $w_1 > w_2$ and $\partial w_2 / \partial r < 0$, the lift force pushes the bubbles towards the wall. Note that the spatial resolution in discrete analyses must be fine enough in order to accurately compute the rotation of the continuous velocity field. Bad resolution, such in so-called subchannel analyses, produces only useless noise that makes the use of this force meaningless.

Mei (1992) proposed an expression that can be used for larger particle *Reynolds* numbers

$$c_{21}^{L} = Mei \; 3.084 \nu_2^{1/2} \Bigg/ \left(D_1 \left| \frac{dw_2}{dr} \right|^{1/2} \right) ,$$

where

$$Mei = \left(1 - 0.3314 \omega_2^{1/2} \right) \exp\left(-0.1 \mathrm{Re}_{12} \right) + 0.3314 \omega_2^{1/2} , \quad \mathrm{Re}_{12} \le 40 ,$$

$$Mei = 0.0524 \left(\omega_2 \, \mathrm{Re}_{12} \right)^{1/2} , \quad \mathrm{Re}_{12} > 40 ,$$

and $\mathrm{Re}_{12} = \Delta w_{12} D_1 / \nu_2$, $\omega_2 = \dfrac{D_1 / 2}{w_2 - w_1} \left| \dfrac{dw_2}{dr} \right|$. In a later work, *Klausner* et al. (1993) found that the lift force on a bubble attached to a wall can be computed using

$$c_{21}^{L} = \frac{16}{3} 3.877 \omega_2^{3/2} \left(0.014 \beta^2 + \mathrm{Re}_{12}^{-2} \right)^{1/4} ,$$

which is valid for larger Reynolds numbers than the previous relation. In a later work *Mei* and *Klausner* (1995) proposed to use interpolation between the *Staffman*'s results for small *Reynolds* numbers and *Auton*'s (1987) results for large *Reynolds* numbers:

$$c_{21}^{L} = \frac{3}{8\omega_2^{1/2}}\left\{\frac{16}{9}\omega_2 + \left[\frac{1.72J\sqrt{2\omega_2/\mathrm{Re}_{12}}}{\mathrm{Re}_{12}^{1/2}}\right]^2\right\}^{1/2},$$

$$J = 0.6765\left\{1+\tanh\left[2.5\left(\log_{10}\sqrt{2\beta/\mathrm{Re}_{12}}+0.191\right)\right]\right\}$$

$$\times\left\{0.667+\tanh\left[6\left(\log_{10}\sqrt{2\beta/\mathrm{Re}_{12}}-0.32\right)\right]\right\}$$

There are other expressions for the lift force on a single bubble. *Tomiyama* et al. (2002) measured trajectories of single bubbles in simple share flows of glycerol–water solution. They obtained the following empirical correlation:

$$c_{21}^{L} = \min\left[0.288\tanh\left(0.121\mathrm{Re}_{12}\right), f\left(E\ddot{o}_{1m}\right)\right] \quad \text{for} \quad E\ddot{o}_{1m} < 4,$$

$$c_{21}^{L} = f\left(E\ddot{o}_{1m}\right) = 0.00105E\ddot{o}_{1m}^{3} - 0.0159E\ddot{o}_{1m}^{2} - 0.0204E\ddot{o}_{1m} + 0.474$$

$$\text{for} \quad 4 \le E\ddot{o}_{1m} \le 10.7,$$

$$c_{21}^{L} = -0.29 \ \text{for} \ 10.7 < E\ddot{o}_{1m},$$

based on experiments within the region of parameters defined by $1.39 \le E\ddot{o}_{1m} \le 5.74$, $-5.5 \le \log_{10} Mo_{12} \le -2.8$, and $0 < \left|\nabla\times\mathbf{V}_2\right| \le 8.3s^{-1}$. The lift coefficient varied in this region between about 0.3 and −0.3. Here a modified *Eötvös* and *Morton* numbers are computed using the horizontal bubble size

$$E\ddot{o}_{1m} = g\left(\rho_2-\rho_1\right)D_{1,\max}^{2}/\sigma_{12},$$

$$Mo_{12} = g\left(\rho_2-\rho_1\right)\eta_2^{4}/\left(\rho_2^{2}\sigma_{12}\right).$$

The aspect ratio of the bubble is computed by using the *Wellek* et al. (1966) correlation

$$D_{1,\max}/D_{1,\min} = 1+0.163E\ddot{o}_{1m}^{0.757}.$$

In accordance with the *Tomiyama* et al. correlation, the lift coefficient for a bubble with a diameter of 3 mm in an air–water system is equal to 0.288. *Zun* (1980) performed measurements and estimated a value for small bubbles of about 0.3. *Naciri* et al. (1992) experimentally measured the lift coefficient of a bubble in a vortex to be 0.25.

It should be emphasized that the above reviewed considerations are for a single object in shear flow. The presence of multiple objects in share flow is found to influence this force too.

The importance of the findings by *Tomiyama* et al. (2002) is in the observation that for large bubbles the lift force changes sign. *Krepper* et al. (2005) observed experimentally that in vertical bubbly flow the void profile depends on the bubble size spectrum. For a spectrum with predominantly small sized bubbles a wall void peaking is observed. The level of the wall peaking depends on the turbulence in the liquid and on the stagnation pressure force. For spectra having predominantly large bubbles the central void, peaking is observed. This effect was reproduced by *Krepper* et al. (2005) by using lift force applied on multiple groups with $c_{21}^L = 0.05$ for $D_1 < 0.006m$ and $c_{21}^L = -0.05$ for $D_1 \geq 0.006m$. The improvement going from 1 to 2 groups was considerable. No substantial change was reported if more then 8 size groups were used.

Using a combination of the radial liquid and gas momentum equations

$$p(r) = p(R) - (1-\alpha_1)\rho_2 \overline{u'^2} - \int_R^r \frac{(1-\alpha_1)\rho_2\left(\overline{u'^2} - \overline{v'^2}\right)}{r^*} dr^* \ .$$

and the measured fluctuation velocities in the radial and in the azimuthal direction, *Wang* et al. (1987) explained why the bubble peaking for upwards flows is observed close to the wall. Later it was found that this is valid for bubbles with small sizes. Close to the wall the authors observed that a) the velocity gradient has a maximal, b) the velocity fluctuations have maximum, and c) the static pressure has a minimum. Using the radial momentum equations for gas and liquids

$$-\alpha_1 \frac{dp}{dr} + \frac{1}{r}\frac{d}{dr}\left(\alpha_1 r \tau_{1,rr}\right) - \frac{1}{r}\alpha_1 \tau_{1,\theta\theta} + f_{21}^L = 0$$

$$-(1-\alpha_1)\frac{dp}{dr} + \frac{1}{r}\frac{d}{dr}\left[r(1-\alpha_1)\tau_{2,rr}\right] - \frac{1}{r}(1-\alpha_1)\tau_{2,\theta\theta} - f_{21}^L = 0\,,$$

it is possible to estimate the radial pressure distribution and the lift force, knowing from measurements the void and the velocity profiles with their fluctuations $\tau_{1,rr} \approx 0$ $\tau_{1,\theta\theta} \approx 0$, $\tau_{2,rr} = -\rho_2 \overline{u_2'^2}$, $\tau_{2,\theta\theta} = -\rho_2 \overline{v_2'^2}$. This is the approach used by *Wang* et al. to gain expression for the lift force in bubbly flow based on groups of variables that come from the theory of the lift force on a single object. *Wang* et al. introduced the influence of the local volume fraction into the lift coefficient

$$c_{21}^L(\xi) = 0.01 + \frac{0.49}{\pi}\cot^{-1}\frac{\log\xi + 9.3168}{0.1963}\,,$$

as a function of

$$\xi = \exp(-\alpha_1)\, 2\omega_2 \left(\frac{D_1}{D_{hyd}} \frac{1}{\mathrm{Re}_{12}} \right)^2 \left(\frac{w_1}{\Delta w_{12\infty}} \right)^2 ,$$

where $\Delta w_{12\infty} = 1.18 \left(g\sigma/\rho_2 \right)^{1/4}$. This coefficient varies within 0.01 and 0.1 in accordance to *Wang*'s et al. data. The disadvantage of this approach is that due to the dependence $\xi = \xi\left(D_{hyd}\right)$ the correlation depends on one global geometry characteristic and cannot be applied locally.

For a down flow of buoyant bubbles the lift-force is directed toward the center of the pipe. As a result, no wall peaking of the void fraction is experimentally observed in turbulent bubbly flow. The level of the wall peaking depends of the turbulence in the liquid and on the stagnation pressure force.

Conclusions: (a) The spatial resolution in finite volume analyses must be fine enough in order to accurately compute the rotation of the continuous velocity field. Bad resolution such as in the so-called subchannel analyses produces only useless noise that makes the use of this force meaningless. (b) There is no method known to me that is based on local conditions and that allows taking into account the effect of multiple objects on the lift force. (c) The other problem is that small bubbles will probably rotate and the application of lift force derived for nonrotating objects in shear flows is questionable. (d) Heavy solid particles carried by gas are rather subject to lift force than to Magnus force because due to their inertia they will hardly take the rotation of the surrounding continuum.

2.7.2.5 Interfacial structure forces

The continuous field interacts with the wall structures. Careful estimation of the surface integral

$$\frac{1}{Vol} \int_{F_{mw}} \Delta p_m^{w\sigma} \mathbf{n}_m dF$$

is required, especially in the case of variable geometry of the structure in space. The discussion of flow on immersed bodies given in Sections 2.6.2.2 through 2.6.2.4 is also valid for the case of a porous solid structure with a characteristic size of D_w. This means that the stagnation pressure force, form drag, virtual mass force, and lift force must also be incorporated,

$$\frac{1}{Vol} \int_{F_{mw}} \left(\Delta p_m^{w\sigma} \mathbf{I} - \mathbf{T}_m^{w\sigma} \right) \cdot \mathbf{n}_m dF = \gamma_v \left(f_{wm}^d + f_{wm}^{vm} + f_{wm}^L \right) + \Delta p_m^{w\sigma *} \frac{1}{Vol} \int_{F_{mw}} \mathbf{n}_m dF \, . \tag{2.186}$$

For a continuous velocity field wetting the total structure, $F_{mw} = F_w$ and, therefore,

$$\frac{1}{Vol}\int\limits_{F_{mw}} \mathbf{n}_m dF = \frac{1}{Vol}\int\limits_{F_w} \mathbf{n}_m dF = \nabla(1-\gamma) = -\nabla\gamma\,. \tag{2.187}$$

which is in fact Eq. (1.29) with $\mathbf{n}_l = -\mathbf{n}_w$ and $\alpha_l^e = 1$. Consequently

$$\frac{1}{Vol}\int\limits_{F_{mw}} \left(\Delta p_m^{w\sigma}\mathbf{I} - \mathbf{T}_m^{w\sigma}\right)\cdot\mathbf{n}_m dF = \gamma_v\left(f_{wm}^d + f_{wm}^{vm} + f_{wm}^L\right) - \Delta p_m^{w\sigma^*}\nabla\gamma\,. \tag{2.188}$$

Here the following applies for a disperse structure (flow through porous media):

$$\mathbf{f}_{wm}^{vm} = \rho_m c_w^{vm}\left[\frac{\partial}{\partial\tau}\Delta\mathbf{V}_{mw} + (\mathbf{V}_w\cdot\nabla)\Delta\mathbf{V}_{mw}\right] = \overline{c_w^{vm}}\left[\frac{\partial}{\partial\tau}\Delta\mathbf{V}_{mw} + (\mathbf{V}_w\cdot\nabla)\Delta\mathbf{V}_{mw}\right], \tag{2.189}$$

$$\mathbf{f}_{wm}^{d} = \rho_m\frac{1}{D_w}\frac{3}{4}c_{mw}^d\left|\Delta\mathbf{V}_{mw}\right|\Delta\mathbf{V}_{mw} = \overline{c_{mw}^d}\left|\Delta\mathbf{V}_{mw}\right|\Delta\mathbf{V}_{mw}\,, \tag{2.190}$$

$$\mathbf{f}_{wm}^{L} = \rho_m c_{mw}^L(\mathbf{V}_w - \mathbf{V}_m)\times(\nabla\times\mathbf{V}_m) = \overline{c_{mw}^L}(\mathbf{V}_w - \mathbf{V}_m)\times(\nabla\times\mathbf{V}_m)\,. \tag{2.191}$$

For the case of a wall at rest we have

$$\mathbf{f}_{wm}^{vm} = \rho_m c_w^{vm}\frac{\partial\mathbf{V}_m}{\partial\tau} = \overline{c_w^{vm}}\frac{\partial\mathbf{V}_m}{\partial\tau}\,, \tag{2.192}$$

$$\mathbf{f}_{wm}^{d} = \rho_m\frac{1}{D_w}\frac{3}{4}c_{mw}^d\left|\mathbf{V}_m\right|\mathbf{V}_m = \overline{c_{mw}^d}\left|\mathbf{V}_m\right|\mathbf{V}_m\,, \tag{2.193}$$

$$\mathbf{f}_{wm}^{L} = -\rho_m c_{mw}^L\mathbf{V}_m\times(\nabla\times\mathbf{V}_m) = -\overline{c_{mw}^L}\mathbf{V}_m\times(\nabla\times\mathbf{V}_m)\,. \tag{2.194}$$

The shear (friction) force for channels is usually incorporated into $\overline{c}_{mw}^d$. The same is performed for the drag resulting from local changes in the flow cross-section for the specific flow direction.

2.7.2.6 Force in the wall boundary layer

Note that no bubbles are observed at the wall for adiabatic flows. This led *Antal* et al. (1991) to the conclusion that there is a special force at the wall similar to the lubrication force that pushes the bubbles away from the surface,

$$\mathbf{f}_{cd}^{Lw} = \frac{\alpha_d\rho_c\left|\hat{\mathbf{V}}\right|^2}{R_d}\left(-0.104 - 0.06\left|\Delta V_{cd}\right| + 0.147\frac{R_d}{y_0}\right)\mathbf{n}_w\,,$$

where y_0 is the distance between the bubble and the wall, $\mathbf{n}_w$ is the unit outward normal vector on the surface of the wall, and

$$\hat{\mathbf{V}} = \mathbf{V}_d - \mathbf{V}_c - \left[\mathbf{n}_w \cdot \left(\mathbf{V}_d - \mathbf{V}_c\right)\right]\mathbf{n}_w .$$

2.7.2.7 Force causing turbulent diffusion

It is experimentally observed that turbulence in the continuous phase tends to smooth the volumetric concentrations of the dispersed phase. In other words, the pulsation in the continuum producing the force $\nabla \cdot \left[\alpha_l^e \left(\rho_l \overline{\mathbf{V}_l' \mathbf{V}_l'}\right)\gamma\right]$ forces the particles to move from the places with higher concentration to the places with lower concentration. For homogeneous turbulence

$$\nabla \cdot \left[\alpha_d^e \left(\rho_d \overline{\mathbf{V}_d' \mathbf{V}_d'}\right)\gamma\right] = \nabla\left[\alpha_d^e \left(\rho_d 2k_d\right)\gamma\right] .$$

For bubbly flow $\nabla\left[\alpha_d^e \left(\rho_d 2k_d\right)\gamma\right] \approx \nabla\left[\alpha_d^e \left(\rho_d 2k_c\right)\gamma\right]$. Here, k_c is the specific turbulent kinetic energy of the continuous phase. For bubbly flow, *Lopez de Bertodano* (1992) proposed the following form of this force:

$$\mathbf{f}_{cd}^t = \nabla \cdot \left[\alpha_d^e \left(\rho_d \overline{\mathbf{V}_d' \mathbf{V}_d'}\right)\gamma\right] \approx -c_{cd}^t \rho_c k_c \nabla \alpha_d ,$$

with $c_{cd}^t = 0.1$ proposed by *Lahey* et al. (1993). *Shi* et al. (2005) performed a *Favre* (mass-weighted) averaging of the classical form of the drag form. His final expression for the dispersed form is

$$\mathbf{f}_{cd}^t = -\frac{3}{4}\frac{c_{cd}^d}{D_d}\frac{\nu_c^t}{\left(1-\alpha_d\right) Sh_c^t}\rho_c \left|\mathbf{V}_c - \mathbf{V}_d\right| \nabla \alpha_d ,$$

where the turbulent *Schmidt* number for the continuous field, Sh_c^t, is set to 1.

2.7.2.8 Force causing rejection of droplet deposition at the wall

Consider very strong evaporation of a film. The deposition mass flow rate of droplets is $\left(\rho w\right)_{32}$ with a velocity $w_{32} = \left(\rho w\right)_{32} / \rho_3$, which is perpendicular to the wall. The film evaporation emits a vapor with velocity that has a component opposing the droplet deposition velocity $w_{1,evaporation} = \dot{q}'' / \rho_1 \Delta h$. Therefore, the droplet in the proximity to the wall experiences an additional drag force that opposes its movement towards the wall

$$\mathbf{f}_{cd}^{dw} = \rho_c \frac{1}{D_d}\frac{3}{4} c_{cd}^{dw} \left|w_{1,evaporation} - w_{32}\right| \left(w_{1,evaporation} - w_{32}\right)\mathbf{n}_w .$$

As we can see this force is important a) for high pressure because the continuum density is high, b) for high heat fluxes, and c) for low turbulence in the vapor phase.

2.8 Working form for the dispersed and continuous phase

Thus the momentum equation of a dispersed velocity field takes the form

$$\frac{\partial}{\partial\tau}\left(\alpha_l\rho_l\mathbf{V}_l\,\gamma_v\right)+\nabla\cdot\left(\alpha_l^e\rho_l\mathbf{V}_l\,\mathbf{V}_l\,\gamma\right)+\nabla\cdot\left[\alpha_l^e\left(\rho_l\overline{\mathbf{V}_l'\mathbf{V}_l'}\right)\gamma\right]+\alpha_l^e\gamma\nabla p_l+\alpha_l\gamma_v\rho_l\mathbf{g}$$

$$+\left(p_l-p_m+\delta_l\sigma_{lm}\kappa_l\right)\nabla\left(\alpha_l^e\gamma\right)-\Delta p_m^{l\sigma^*}\nabla\left(\alpha_l^e\gamma\right)$$

$$-\gamma_v\alpha_l\rho_m\begin{Bmatrix}c_{ml}^{vm}\left[\dfrac{\partial}{\partial\tau}\Delta\mathbf{V}_{ml}+\left(\mathbf{V}_l\cdot\nabla\right)\Delta\mathbf{V}_{ml}\right]\\[2ex]-c_{ml}^{L}\Delta\mathbf{V}_{ml}\times\left(\nabla\times\mathbf{V}_m\right)+\dfrac{1}{D_l}\dfrac{3}{4}c_{ml}^{d}\left|\Delta\mathbf{V}_{ml}\right|\Delta\mathbf{V}_{ml}\end{Bmatrix}$$

$$=\gamma_v\sum_{\substack{k=1\\k\neq l}}^{3,w}\left(\mu_{kl}\mathbf{V}_k-\mu_{lk}\mathbf{V}_l\right). \tag{2.195}$$

In the case of isotropic turbulence we have

$$\frac{\partial}{\partial\tau}\left(\alpha_l\rho_l\mathbf{V}_l\,\gamma_v\right)+\nabla\cdot\left(\alpha_l^e\rho_l\mathbf{V}_l\,\mathbf{V}_l\,\gamma\right)-\tilde{\mathbf{S}}_l+\frac{2}{3}\nabla\left(\gamma\alpha_l^e\rho_l k_l\right)+\alpha_l^e\gamma\nabla p_l+\alpha_l\gamma_v\rho_l\mathbf{g}$$

$$+\left(p_l-p_m+\delta_l\sigma_{lm}\kappa_l-\Delta p_m^{l\sigma^*}\right)\nabla\left(\alpha_l^e\gamma\right)$$

$$-\gamma_v\alpha_l\rho_m\begin{Bmatrix}c_{ml}^{vm}\left[\dfrac{\partial}{\partial\tau}\Delta\mathbf{V}_{ml}+\left(\mathbf{V}_l\cdot\nabla\right)\Delta\mathbf{V}_{ml}\right]\\[2ex]-c_{ml}^{L}\Delta\mathbf{V}_{ml}\times\left(\nabla\times\mathbf{V}_m\right)+\dfrac{1}{D_l}\dfrac{3}{4}c_{ml}^{d}\left|\Delta\mathbf{V}_{ml}\right|\Delta\mathbf{V}_{ml}\end{Bmatrix}$$

$$=\gamma_v\sum_{\substack{k=1\\k\neq l}}^{3,w}\left(\mu_{kl}\mathbf{V}_k-\mu_{lk}\mathbf{V}_l\right). \tag{2.195b}$$

The momentum equation of the continuous phase so far takes the following form:

$$\frac{\partial}{\partial\tau}\left(\alpha_m\rho_m\mathbf{V}_m\gamma_v\right)+\nabla\cdot\left(\alpha_m^e\rho_m\mathbf{V}_m\mathbf{V}_m\gamma\right)$$

$$-\tilde{\mathbf{S}}_m+\frac{2}{3}\nabla\left(\gamma\alpha_m^e\rho_m k_m\right)-\nabla\cdot\left(\alpha_m^e\gamma\eta_m\left[2\mathbf{D}_m-\frac{2}{3}\left(\nabla\cdot\mathbf{V}_m\right)\mathbf{I}\right]\right)+\alpha_m^e\gamma\nabla p_m$$

$$+\alpha_m\gamma_v\rho_m\mathbf{g}+\Delta p_m^{l\sigma^*}\nabla\left(\alpha_l^e\gamma\right)-\Delta p_m^{w\sigma^*}\nabla\gamma$$

$$+\gamma_v\alpha_l\rho_m\left\{\begin{array}{l} c_{ml}^{vm}\left[\dfrac{\partial}{\partial\tau}\Delta\mathbf{V}_{ml}+\left(\mathbf{V}_l\cdot\nabla\right)\Delta\mathbf{V}_{ml}\right] \\ \\ -c_{ml}^{L}\Delta\mathbf{V}_{ml}\times\left(\nabla\times\mathbf{V}_m\right)+\dfrac{1}{D_l}\dfrac{3}{4}c_{ml}^{d}\left|\Delta\mathbf{V}_{ml}\right|\Delta\mathbf{V}_{ml} \end{array}\right\}$$

$$+\gamma_v\rho_m\left[c_w^{vm}\frac{1}{2}\frac{\partial\mathbf{V}_m}{\partial\tau}-c_{mw}^{L}\mathbf{V}_m\times\left(\nabla\times\mathbf{V}_m\right)+\frac{1}{D_w}\frac{3}{4}c_{mw}^{d}\left|\mathbf{V}_m\right|\mathbf{V}_m\right]$$

$$=\gamma_v\sum_{\substack{k=1\\k\neq m}}^{3,w}\left(\mu_{km}\mathbf{V}_k-\mu_{mk}\mathbf{V}_m\right). \tag{2.196}$$

In the case of isotropic turbulence, we have

$$\frac{\partial}{\partial\tau}\left(\alpha_m\rho_m\mathbf{V}_m\gamma_v\right)+\nabla\cdot\left(\alpha_m^e\rho_m\mathbf{V}_m\mathbf{V}_m\gamma\right)+\nabla\cdot\left[\alpha_m^e\gamma\left(\rho_m\overline{\mathbf{V}_m'\mathbf{V}_m'}-\mathbf{T}_m\right)\right]+\alpha_m^e\gamma\nabla p_m$$

$$+\alpha_m\gamma_v\rho_m\mathbf{g}+\Delta p_m^{l\sigma^*}\nabla\left(\alpha_l^e\gamma\right)-\Delta p_m^{w\sigma^*}\nabla\gamma$$

$$+\gamma_v\alpha_l\rho_m\left\{\begin{array}{l} c_{ml}^{vm}\left[\dfrac{\partial}{\partial\tau}\Delta\mathbf{V}_{ml}+\left(\mathbf{V}_l\cdot\nabla\right)\Delta\mathbf{V}_{ml}\right] \\ \\ -c_{ml}^{L}\Delta\mathbf{V}_{ml}\times\left(\nabla\times\mathbf{V}_m\right)+\dfrac{1}{D_l}\dfrac{3}{4}c_{ml}^{d}\left|\Delta\mathbf{V}_{ml}\right|\Delta\mathbf{V}_{ml} \end{array}\right\}$$

$$+\gamma_v\rho_m\left[c_w^{vm}\frac{1}{2}\frac{\partial\mathbf{V}_m}{\partial\tau}-c_{mw}^{L}\mathbf{V}_m\times\left(\nabla\times\mathbf{V}_m\right)+\frac{1}{D_w}\frac{3}{4}c_{mw}^{d}\left|\mathbf{V}_m\right|\mathbf{V}_m\right]$$

$$=\gamma_v\sum_{\substack{k=1\\k\neq m}}^{3,w}\left(\mu_{km}\mathbf{V}_k-\mu_{mk}\mathbf{V}_m\right). \tag{2.196b}$$

The relation between the two bulk pressures is given by the momentum jump condition. With the assumptions made in Section 2.6.2.1, the momentum jump condition, Eq. (2.23), reduces to

$$\left(\rho w\right)_{ml}^2\left(\frac{1}{\rho_l}-\frac{1}{\rho_m}\right)+p_l^{m\sigma,\tau}-p_m^{l\sigma,\tau}-\sigma_{ml}\kappa_m=0. \tag{2.197}$$

We exchange the subscripts *l* and *m* because the surface tension is assumed to belong to the liquid phase. After time averaging we obtain

$$(\rho w)_{ml}^2 \left(\frac{1}{\rho_l} - \frac{1}{\rho_m} \right) + p_l^{m\sigma} - p_m^{l\sigma} + \sigma_{ml} \kappa_l = 0 \,, \tag{2.198}$$

or in terms of bulk pressure

$$p_l - p_m + \sigma_{ml} \kappa_l = \Delta p_m^{l\sigma} + (\rho w)_{ml}^2 \left(\frac{1}{\rho_m} - \frac{1}{\rho_l} \right). \tag{2.199}$$

Actually, the pressure difference $\Delta p_m^{l\sigma}$ varies over the surface and some surface-averaged value

$$\frac{1}{F_{l\sigma}} \left| \int\limits_{F_{l\sigma}} \Delta p_m^{l\sigma} \mathbf{n}_l dF \right| = \frac{Vol}{F_{l\sigma}} \left| \frac{1}{Vol} \int\limits_{F_{l\sigma}} \Delta p_m^{l\sigma} \mathbf{n}_l dF \right| \tag{2.200}$$

may be used. There is no experience in this field and future investigations are necessary. Approximations are thinkable for predominant surface tension and low mass transfer

$$p_l - p_m + \sigma_{ml} \kappa_l \approx 0 \,, \tag{2.201}$$

or for predominant mass transfer

$$p_l - p_m + \sigma_{ml} \kappa_l \approx (\rho w)_{ml}^2 \left(\frac{1}{\rho_m} - \frac{1}{\rho_l} \right). \tag{2.202}$$

Note that for spheres $\kappa_l = 1/R_l + 1/R_l = 2/R_l$. Remember that if the radius is inside the field the curvature is negative.

Now let us as a practical illustration of the application of the theory analyze the eigenvalues for bubble flow without mass transfer in a one-dimensional horizontal channel with constant cross-section section, assuming noncompressible phases and neglecting the diffusion terms. The governing system then simplifies to

$$p = p_2 \,, \tag{2.203}$$

$$p_1 = p + \sigma_{12} \kappa_2 \,, \tag{2.204}$$

$$\alpha_1 \frac{\partial w_1}{\partial z} + \alpha_2 \frac{\partial w_2}{\partial z} + (w_1 - w_2) \frac{\partial \alpha_1}{\partial z} = 0 \tag{2.205}$$

$$\frac{\partial \alpha_1}{\partial \tau} + \alpha_1 \frac{\partial w_1}{\partial z} + w_1 \frac{\partial \alpha_1}{\partial z} = 0 \tag{2.206}$$

$$\alpha_1 (\rho_1 + \rho_2 c_{21}^{vm}) \left(\frac{\partial w_1}{\partial \tau} + w_1 \frac{\partial w_1}{\partial z} \right) - \alpha_1 \rho_2 c_{21}^{vm} \left(\frac{\partial w_2}{\partial \tau} + w_1 \frac{\partial w_2}{\partial z} \right) + \alpha_1 \frac{\partial p}{\partial z} - \Delta p_2^{1\sigma *} \frac{\partial \alpha_1}{\partial z}$$
$$= \alpha_1 \rho_2 \frac{1}{D_1} \frac{3}{4} c_{21}^d |\Delta w_{21}| \Delta w_{21} \,, \tag{2.207}$$

$$-\alpha_1\rho_2 c_{21}^{vm}\left(\frac{\partial w_1}{\partial\tau}+w_1\frac{\partial w_1}{\partial z}\right)+\left(\alpha_2+\alpha_1 c_{21}^{vm}+c_w^{vm}\right)\rho_2\frac{\partial w_2}{\partial\tau}+\left(\alpha_2 w_2+\alpha_1 c_{21}^{vm}w_1\right)\rho_2\frac{\partial w_2}{\partial z}$$
$$+\alpha_2\frac{\partial p}{\partial z}+\Delta p_2^{1\sigma^*}\frac{\partial\alpha_1}{\partial z}=-\frac{3}{4}\rho_2\left(\alpha_1\frac{1}{D_1}c_{21}^{d}\left|\Delta w_{21}\right|\Delta w_{21}+\frac{1}{D_w}c_{2w}^{d}\left|w_2\right|w_2\right) \tag{2.208}$$

In matrix notation we have

$$\begin{pmatrix}0&0&0&0\\0&1&0&0\\0&0&\alpha_1\left(\rho_1+\rho_2 c_{21}^{vm}\right)&-\alpha_1\rho_2 c_{21}^{vm}\\0&0&-\alpha_1\rho_2 c_{21}^{vm}&\left(\alpha_2+\alpha_1 c_{21}^{vm}+c_w^{vm}\right)\rho_2\end{pmatrix}\frac{\partial}{\partial\tau}\begin{pmatrix}p\\\alpha_1\\w_1\\w_2\end{pmatrix}$$
$$+\begin{pmatrix}0&w_1-w_2&\alpha_1&\alpha_2\\0&w_1&\alpha_1&0\\\alpha_1&-\Delta p_2^{1\sigma^*}&\alpha_1\left(\rho_1+\rho_2 c_{21}^{vm}\right)w_1&-\alpha_1\rho_2 c_{21}^{vm}w_1\\\alpha_2&\Delta p_2^{1\sigma^*}&-\alpha_1\rho_2 c_{21}^{vm}w_1&\left(\alpha_2 w_2+\alpha_1 c_{21}^{vm}w_1\right)\rho_2\end{pmatrix}\frac{\partial}{\partial z}\begin{pmatrix}p\\\alpha_1\\w_1\\w_2\end{pmatrix}$$
$$=\begin{pmatrix}0\\0\\\alpha_1\rho_2\frac{1}{D_1}\frac{3}{4}c_{21}^{d}\left|\Delta w_{21}\right|\Delta w_{21}\\-\frac{3}{4}\rho_2\left(\alpha_1\frac{1}{D_1}c_{21}^{d}\left|\Delta w_{21}\right|\Delta w_{21}+\frac{1}{D_w}c_{2w}^{d}\left|w_2\right|w_2\right)\end{pmatrix}. \tag{2.209}$$

The reader unfamiliar with the analysis of the type of a system of partial differential equations by first computing the eigenvalues, eigenvectors, and canonical forms, is recommended to first read Section 11 before continuing here.

The characteristic equation for determining the eigenvalues is then

$$\begin{pmatrix}0&w_1-w_2&\alpha_1&\alpha_2\\0&w_1-\lambda&\alpha_1&0\\\alpha_1&-\Delta p_2^{1\sigma^*}&\alpha_1\left(\rho_1+\rho_2 c_{21}^{vm}\right)\left(w_1-\lambda\right)&-\alpha_1\rho_2 c_{21}^{vm}\left(w_1-\lambda\right)\\\alpha_2&\Delta p_2^{1\sigma^*}&-\alpha_1\rho_2 c_{21}^{vm}\left(w_1-\lambda\right)&\begin{bmatrix}\alpha_2 w_2+\alpha_1 c_{21}^{vm}w_1\\-\lambda\left(\alpha_2+\alpha_1 c_{21}^{vm}+c_w^{vm}\right)\end{bmatrix}\rho_2\end{pmatrix}=0. \tag{2.210}$$

or

$$\alpha_2\left(c_{21}^{vm}+\alpha_2\frac{\rho_1}{\rho_2}\right)(w_1-\lambda)^2+\alpha_1\left(w_2-\lambda\right)\left[\alpha_2 w_2+\alpha_1 c_{21}^{vm} w_1-\lambda\left(\alpha_2+\alpha_1 c_{21}^{vm}+c_w^{vm}\right)\right]$$

$$-\alpha_1\alpha_2\left(w_1-w_2\right)c_{21}^{vm}\left(w_1-\lambda\right)+\alpha_2\frac{\Delta p_2^{1\sigma^*}}{\rho_2}=0 \tag{2.211}$$

or

$$a\lambda^2-2b\lambda+c=0 \tag{2.212}$$

where

$$a=\alpha_2\left(\alpha_1-\alpha_2\frac{\rho_1}{\rho_2}\right)+\left(\alpha_1^2-\alpha_2\right)c_{21}^{vm}+\alpha_1 c_w^{vm}>0\,, \tag{2.213}$$

$$b=\frac{1}{2}\left\{\left[\alpha_1 w_2+\left(\alpha_1^2-2\alpha_2-\alpha_1\alpha_2\right)w_1\right]c_{21}^{vm}+\alpha_1\left(2\alpha_2+c_w^{vm}\right)w_2-2w_1\alpha_2^2\frac{\rho_1}{\rho_2}\right\}, \tag{2.214}$$

$$c=\left(\alpha_1 w_1 w_2+\alpha_2^2 w_1^2\right)c_{21}^{vm}+\alpha_1\alpha_2 w_2^2+\alpha_2^2\frac{\rho_1}{\rho_2}w_1^2+\alpha_2\frac{\Delta p_2^{1\sigma^*}}{\rho_2}\,, \tag{2.215}$$

with two real solutions

$$\lambda_{1,2}=\frac{b\pm\sqrt{b^2-ac}}{a} \tag{2.216}$$

for

$$b^2>ac \tag{2.217}$$

which is, in fact, the stability criterion for bubbly flow.

2.9 General working form for dispersed and continuous phases

In this section, we write a single equation valid for both disperse and continuous phases. First we compare the terms in the two equations

$$\mathbf{f}_{d\alpha}=\left(p_d-p_c+\delta_d\sigma_{dc}\kappa_d-\Delta p_c^{d\sigma^*}\right)\nabla\left(\alpha_d^e\gamma\right), \tag{2.218}$$

and

$$\mathbf{f}_{c\alpha}=\Delta p_c^{d\sigma^*}\nabla\left(\alpha_d^e\gamma\right), \tag{2.219}$$

and realize that in both cases the force is a function of the gradient of the disperse volume fraction multiplied by different multipliers. With this notation, we have

$$\begin{aligned}
&\frac{\partial}{\partial\tau}\left(\alpha_l\rho_l\mathbf{V}_l\gamma_v\right)+\nabla\cdot\left(\alpha_l^e\rho_l\gamma\left\{\mathbf{V}_l\mathbf{V}_l-\nu_l^*\left[\nabla\mathbf{V}_l+\left(\nabla\mathbf{V}_l\right)^T-\frac{2}{3}\left(\nabla\cdot\mathbf{V}_l\right)\mathbf{I}\right]\right\}\right)\\
&+\alpha_l^e\gamma\nabla p_l+\alpha_l\rho_l\mathbf{g}\gamma_v-\Delta p_l^{w\sigma^*}\nabla\gamma+\mathbf{f}_{l\alpha}\\
&-\gamma_v\sum_{\substack{m=1\\m\neq l}}^{3}\left\{\begin{array}{l}\overline{c}_{ml}^{d}\left|\Delta\mathbf{V}_{ml}\right|\Delta\mathbf{V}_{ml}\\ \\ +\overline{c}_{ml}^{L}\left(\mathbf{V}_l-\mathbf{V}_m\right)\times\left(\nabla\times\mathbf{V}_m\right)+\overline{c}_{ml}^{vm}\left[\dfrac{\partial}{\partial\tau}\Delta\mathbf{V}_{ml}+\left(\mathbf{V}_l\cdot\nabla\right)\Delta\mathbf{V}_{ml}\right]\end{array}\right\}\\
&+\gamma_v\left[\overline{c}_{lw}^{d}\left|\mathbf{V}_l\right|\mathbf{V}_l+\rho_l c_{lw}^{vm}\frac{\partial\mathbf{V}_l}{\partial\tau}-\rho_l c_{lw}^{L}\mathbf{V}_l\times\left(\nabla\times\mathbf{V}_l\right)\right]=\gamma_v\sum_{m=1}^{3,w}\left(\mu_{ml}\mathbf{V}_m-\mu_{lm}\mathbf{V}_l\right).
\end{aligned}\tag{2.220}$$

Note that

$$\Delta p_d^{w\sigma^*}=0,\tag{2.221}$$

$$\Delta p_c^{w\sigma^*}\neq 0.\tag{2.222}$$

Similarly

$$c_{dw}^{d},c_{dw}^{vm},c_{dw}^{L}=0,\tag{2.223}$$

and

$$c_{cw}^{d},c_{cw}^{vm},c_{cw}^{L}\neq 0,\tag{2.224}$$

if the continuum is in a contact with the wall. For easy programming, a couple of simple drag, lift, and virtual mass coefficients combined as follows are introduced for each field

$$\overline{c}_{ml}^{d}=\overline{c}_{lm}^{d}=\frac{3}{4}\left(\alpha_m\rho_l c_{lm}^{d}/D_m+\alpha_l\rho_m c_{ml}^{d}/D_l\right),\tag{2.225}$$

$$\overline{c}_{ml}^{L}=\overline{c}_{lm}^{L}=\alpha_m\rho_l c_{lm}^{L}+\alpha_l\rho_m c_{ml}^{L},\tag{2.226}$$

$$\overline{c}_{ml}^{vm}=\overline{c}_{lm}^{vm}=\alpha_m\rho_l c_{lm}^{vm}+\alpha_l\rho_m c_{ml}^{vm}.\tag{2.227}$$

If field l is disperse and surrounded by the continuous m-field, the coefficient c_{ml} is not equal to zero and c_{lm} is equal to zero, and vice versa. In other words if the second subscript refers to a disperse field, the local size of dispersion is positive and the coefficients are not equal to zero. For application in computer codes the following general notation is recommended:

$$\mathbf{f}_l = \sum_{\substack{m=1 \\ m\neq l}}^{3,w} \overline{c}_{ml}^{d} \mathbf{f}_{ml} \tag{2.228}$$

to take into account the fact that a control volume may contain two dispersed fields carried by one continuous field. This approach together with implicit discretization of the momentum equations, their strong coupling through a special numerical procedure, and the comparison with data for three-phase bubble flow was presented by *Kolev* et al. (1991). In Volume II the reader will find additional information on practical computation of drag forces in multiphase flows.

Equation (2.220) is the rigorously derived local volume and time average momentum balance for multiphase flows in heterogeneous porous structures conditionally divided into three velocity fields.

The nonconservative form of the momentum conservation equation in component notation is given in Appendix 2.3. In the same appendix some interesting single-phase analytical solutions are given. They can be used as benchmarks for testing the accuracy of the numerical solution methods.

2.10 Some practical simplifications

Equation (2.220) has been used since 1984 in the IVA1 to IVA6 computer codes *Kolev* (1985, 1986a, 1986b, 1987, 1991a, 1991b, 1993a, 1993b, 1993c, 1993d, 1994, 1996, 1999) with the following simplifications:

$$p_l - p_m + \frac{2\sigma_{lm}}{R_l} - \Delta p_m^{l\sigma^*} \approx 0\,, \tag{2.229}$$

$$p_l \approx p_m = p\,, \tag{2.230}$$

$$v_l^t \approx 0\,. \tag{2.231}$$

Assumption (2.229) is quite close to the local volume and time average interfacial jump condition at the interface and, therefore, does not lead to any problems for slow interfacial mass transfer.

Assumption (2.230) leads to the so-called *single-pressure model*. It should be emphasized that the most important interfacial pressure forces, which are considerably larger in magnitude than the error introduced by the single-pressure assumption, have already been taken into account. This assumption likewise does not lead to any problems. In this type of single-pressure model the hyperbolicy is

preserved due to the stabilizing viscous, drag, and virtual mass terms. Neglect of the viscous, drag and virtual mass terms leads to unphysical models.

Assumption (2.231) was dictated by a lack of knowledge. When information for ν_l^t becomes available, this can easily be included, as the viscous terms have already been taken into account.

The resulting simplified form of Eq. (2.220) is, therefore,

$$\frac{\partial}{\partial\tau}\left(\alpha_l\rho_l\mathbf{V}_l\,\gamma_v\right)+\nabla\cdot\left(\alpha_l^e\rho_l\gamma\left\{\mathbf{V}_l\,\mathbf{V}_l\,-\nu_l^*\left[\nabla\mathbf{V}_l+\left(\nabla\mathbf{V}_l\right)^T-\frac{2}{3}\left(\nabla\cdot\mathbf{V}_l\right)\mathbf{I}\right]\right\}\right)$$

$$+\alpha_l^e\gamma\nabla p\;+\alpha_l\rho_l\mathbf{g}\gamma_v$$

$$-\gamma_v\sum_{\substack{m=1\\m\neq l}}^{3}\left\{\begin{array}{l}\overline{c}_{ml}^{\,d}\left|\Delta\mathbf{V}_{ml}\right|\cdot\Delta\mathbf{V}_{ml}\\[2ex]+\overline{c}_{ml}^{\,L}\left(\mathbf{V}_l-\mathbf{V}_m\right)\times\left(\nabla\times\mathbf{V}_m\right)+\overline{c}_{ml}^{\,vm}\left[\dfrac{\partial}{\partial\tau}\Delta\mathbf{V}_{ml}+\left(\mathbf{V}_l\cdot\nabla\right)\Delta\mathbf{V}_{ml}\right]\end{array}\right\}$$

$$+\gamma_v\left[\overline{c}_{lw}^{\,d}\left|\mathbf{V}_l\right|\cdot\mathbf{V}_l+\rho_l c_{lw}^{vm}\frac{\partial\mathbf{V}_l}{\partial\tau}-\rho_l c_{lw}^{L}\mathbf{V}_l\times\left(\nabla\times\mathbf{V}_l\right)\right]$$

$$=\gamma_v\sum_{m=1}^{3,w}\left(\mu_{ml}\mathbf{V}_m-\mu_{lm}\mathbf{V}_l\right). \tag{2.232}$$

The form of Eq. (2.232) is sometimes called *conservative* in order to distinguish it from the *nonconservative* form. The nonconservative form is derived by applying the chain rule to the first two terms and inserting the mass-conservation equation (1.45). The resulting equation,

$$\alpha_l\rho_l\left[\gamma_v\frac{\partial\mathbf{V}_l}{\partial\tau}+\left(\mathbf{V}_l\,\gamma\nabla\right)\mathbf{V}_l\right]-\nabla\cdot\left\{\alpha_l^e\rho_l\gamma\nu_l^*\left[\nabla\mathbf{V}_l+\left(\nabla\mathbf{V}_l\right)^T-\frac{2}{3}\left(\nabla\cdot\mathbf{V}_l\right)\mathbf{I}\right]\right\}$$

$$+\alpha_l^e\gamma\nabla p\;+\alpha_l\rho_l\mathbf{g}\gamma_v$$

$$-\gamma_v\sum_{\substack{m=1\\m\neq l}}^{3}\left\{\begin{array}{l}\overline{c}_{ml}^{\,d}\left|\Delta\mathbf{V}_{ml}\right|\cdot\Delta\mathbf{V}_{ml}\\[2ex]+\overline{c}_{ml}^{\,L}\left(\mathbf{V}_l-\mathbf{V}_m\right)\times\left(\nabla\times\mathbf{V}_m\right)+\overline{c}_{ml}^{\,vm}\left[\dfrac{\partial}{\partial\tau}\Delta\mathbf{V}_{ml}+\left(\mathbf{V}_l\cdot\nabla\right)\Delta\mathbf{V}_{ml}\right]\end{array}\right\}$$

$$+\gamma_v\left[\overline{c}_{lw}^{\,d}\left|\mathbf{V}_l\right|\cdot\mathbf{V}_l+\rho_l c_{lw}^{vm}\frac{\partial\mathbf{V}_l}{\partial\tau}-\rho_l c_{lw}^{L}\mathbf{V}_l\times\left(\nabla\times\mathbf{V}_l\right)\right]$$

$$= \gamma_v \left\{ \sum_{m=1}^{3} \left[\mu_{ml} \left(\mathbf{V}_m - \mathbf{V}_l \right) \right] + \mu_{wl} \left(\mathbf{V}_{wl} - \mathbf{V}_l \right) + \mu_{lw} \left(\mathbf{V}_{lw} - \mathbf{V}_l \right) \right\}, \tag{2.233}$$

contains some extremely interesting information, namely:

(a) mass sinks of the velocity field *l* have no influence on the velocity change (an exception is the controlled flow suction from the structure through the structure interface), and
(b) mass sources from a donor field whose velocities differ from the velocity of the receiving field influence the velocity change.

To facilitate the direct use of the vector equation (2.333), we give its scalar components for the most frequently used cylindrical, $\kappa = 1$, and Cartesian, $\kappa = 0$, coordinate systems.

r direction

$$\frac{\partial}{\partial \tau}\left(\alpha_l \rho_l u_l \gamma_v\right) + \frac{1}{r^\kappa}\frac{\partial}{\partial r}\left[r^\kappa \alpha_l \rho_l \left(u_l u_l - \nu_l^* \frac{\partial u_l}{\partial r} \right) \gamma_r \right]$$

$$+ \frac{1}{r^\kappa}\frac{\partial}{\partial \theta}\left[\alpha_l \rho_l \left(v_l u_l - \nu_l^* \frac{1}{r^\kappa}\frac{\partial u_l}{\partial \theta} \right) \gamma_\theta \right]$$

$$- \frac{\kappa}{r^\kappa}\alpha_l \rho_l \left[v_l v_l - \frac{2}{r^\kappa}\nu_l^* \left(\frac{\partial v_l}{\partial \theta} + u_l \right) \right] \gamma_\theta + \frac{\partial}{\partial z}\left[\alpha_l \rho_l \left(w_l u_l - \nu_l^* \frac{\partial u_l}{\partial z} \right) \gamma_z \right]$$

$$+ \alpha_l \gamma_r \frac{\partial p}{\partial r} + \left(\alpha_l \rho_l g_r + f_{lu} \right) \gamma_v = \gamma_v \sum_{m=1}^{3,w} \left(\mu_{ml} u_{ml} - \mu_{lm} u_l \right) + f_{vlu}, \tag{2.234}$$

where

$$f_{vlu} = \frac{1}{r^\kappa}\frac{\partial}{\partial r}\left(r^\kappa \alpha_l \rho_l \nu_l^* \frac{\partial u_l}{\partial r} \gamma_r \right) + \frac{1}{r^\kappa}\frac{\partial}{\partial \theta}\left[\alpha_l \rho_l \nu_l^* r^\kappa \frac{\partial}{\partial r}\left(\frac{v_l}{r^\kappa} \right) \gamma_\theta \right]$$

$$+ \frac{\partial}{\partial z}\left(\alpha_l \rho_l \nu_l^* \frac{\partial w_l}{\partial z} \gamma_z \right) - \frac{2}{3}\frac{1}{r^\kappa}\left\{ \frac{\partial}{\partial r}\left[r^\kappa \left(\alpha_l \rho_l \nu_l^* \nabla \cdot \mathbf{V}_l \right) \gamma_r \right] - \left(\alpha_l \rho_l \nu_l^* \nabla \cdot \mathbf{V}_l \right) \gamma_\theta \right\}; \tag{2.235}$$

θ direction

$$\frac{\partial}{\partial \tau}\left(\alpha_l \rho_l v_l \gamma_v\right) + \frac{1}{r^\kappa}\frac{\partial}{\partial r}\left[r^\kappa \alpha_l \rho_l \left(u_l v_l - \nu_l^* \frac{\partial v_l}{\partial r} \right) \gamma_r \right]$$

$$+ \frac{1}{r^\kappa}\frac{\partial}{\partial \theta}\left[\alpha_l \rho_l \left(v_l v_l - \nu_l^* \frac{1}{r^\kappa}\frac{\partial v_l}{\partial \theta} \right) \gamma_\theta \right]$$

$$+\frac{\kappa}{r^{\kappa}}\alpha_l\rho_l\left[v_l u_l - r^{\kappa}\nu_l^*\frac{\partial}{\partial r}\left(\frac{v_l}{r^{\kappa}}\right)-\nu_l^*\frac{1}{r^{\kappa}}\frac{\partial u_l}{\partial\theta}\right]\gamma_\theta+\frac{\partial}{\partial z}\left[\alpha_l\rho_l\left(w_l v_l-\nu_l^*\frac{\partial v_l}{\partial z}\right)\gamma_z\right]$$

$$+\alpha_l\gamma_\theta\frac{1}{r^{\kappa}}\frac{\partial p}{\partial\theta}+\left(\alpha_l\rho_l g_\theta+f_{lv}\right)\gamma_v=\gamma_v\sum_{m=1}^{3,w}\left(\mu_{ml}v_{ml}-\mu_{lm}v_l\right)+f_{vlv}, \tag{2.236}$$

where

$$f_{vlv}=\frac{1}{r^{\kappa}}\frac{\partial}{\partial r}\left[\alpha_l\rho_l\nu_l^*\left(\frac{\partial u_l}{\partial\theta}-v_l\right)\gamma_r\right]+\frac{1}{r^{\kappa}}\frac{\partial}{\partial\theta}\left[\alpha_l\rho_l\nu_l^*\frac{1}{r^{\kappa}}\left(\frac{\partial v_l}{\partial\theta}+2u_l\right)\gamma_\theta\right]$$

$$+\frac{\partial}{\partial z}\left(\alpha_l\rho_l\nu_l^*\frac{1}{r^{\kappa}}\frac{\partial w_l}{\partial\theta}\gamma_z\right)-\frac{2}{3}\frac{1}{r^{\kappa}}\frac{\partial}{\partial\theta}\left[\left(\alpha_l\rho_l\nu_l^*\nabla\cdot\mathbf{V}_l\right)\gamma_\theta\right]; \tag{2.237}$$

z direction

$$\frac{\partial}{\partial\tau}\left(\alpha_l\rho_l w_l\gamma_v\right)+\frac{1}{r^{\kappa}}\frac{\partial}{\partial r}\left[r^{\kappa}\alpha_l\rho_l\left(u_l w_l-\nu_l^*\frac{\partial w_l}{\partial r}\right)\gamma_r\right]$$

$$+\frac{1}{r^{\kappa}}\frac{\partial}{\partial\theta}\left[\alpha_l\rho_l\left(v_l w_l-\nu_l^*\frac{1}{r^{\kappa}}\frac{\partial w_l}{\partial\theta}\right)\gamma_\theta\right]+\frac{\partial}{\partial z}\left[\alpha_l\rho_l\left(w_l w_l-\nu_l^*\frac{\partial w_l}{\partial z}\right)\gamma_z\right]$$

$$+\alpha_l\gamma_z\frac{\partial p}{\partial z}+\left(\alpha_l\rho_l g_z+f_{lw}\right)\gamma_v=\gamma_v\sum_{m=1}^{3,w}\left(\mu_{ml}w_{ml}-\mu_{lm}w_l\right)+f_{vlw}, \tag{2.238}$$

where

$$f_{vlw}=\frac{1}{r^{\kappa}}\frac{\partial}{\partial r}\left(r^{\kappa}\alpha_l\rho_l\nu_l^*\frac{\partial u_l}{\partial z}\gamma_r\right)+\frac{1}{r^{\kappa}}\frac{\partial}{\partial\theta}\left(\alpha_l\rho_l\nu_l^*\frac{\partial v_l}{\partial z}\gamma_\theta\right)+\frac{\partial}{\partial z}\left(\alpha_l\rho_l\nu_l^*\frac{\partial w_l}{\partial z}\gamma_z\right)$$

$$-\frac{2}{3}\frac{\partial}{\partial z}\left[\left(\alpha_l\rho_l\nu_l^*\nabla\cdot\mathbf{V}_l\right)\gamma_z\right]. \tag{2.239}$$

Here

$$\nabla\cdot\mathbf{V}_l=\left[\frac{1}{r^{\kappa}}\frac{\partial}{\partial r}\left(r^{\kappa}u_l\right)+\frac{1}{r^{\kappa}}\frac{\partial v_l}{\partial\theta}+\frac{\partial w_l}{\partial z}\right]. \tag{2.240}$$

Note that all interfacial forces are designated with $\mathbf{f}_l$ with components f_{lu}, f_{lv}, and f_{lw}.

The viscous terms have been rearranged in order to obtain a *convection-diffusion form* for the left-hand side of the momentum equations. The residual terms are pooled into the momentum source terms $\mathbf{f}_v$. This notation is justified for two reasons. First, for a single-phase flow in a pool (unrestricted flows) and a constant density, the source terms $\mathbf{f}_v$ are equal to zero, which *intuitively leads to the idea that the main viscous influence is outside the* $\mathbf{f}_v$ *source terms*. This argument led some authors to derive an explicit discretization for the $\mathbf{f}_v$ source terms for

single-phase flow applications, see *Trent* and *Eyler* (1983), or even to neglect these source terms. Second, methods with known mathematical properties for the discretization of convection-diffusion equations have already been developed, and these can be applied directly.

Note that for Cartesian coordinates the convective components contain spatial derivatives. In the case of cylindrical coordinates the convective part contains in addition two components not containing spatial derivatives. The component

$$centrifugal\ force = -\frac{\kappa}{r^{\kappa}} \alpha_l \rho_l v_l v_l \gamma_\theta \tag{2.241}$$

is known in the literature as centrifugal force. It gives the effective force component in the r direction resulting from fluid motion in the θ direction. The component

$$Coriolis\ force = \frac{\kappa}{r^{\kappa}} \alpha_l \rho_l v_l u_l \gamma_\theta \tag{2.242}$$

is known in the literature as the *Coriolis* force. It is an effective force component in the θ direction when there is flow in both the r and θ directions. This results in the components of the viscous stress tensor, $\tau_{l,\theta\theta}$ and $\tau_{l,r\theta}$ corresponding to these forces and acting in the opposite directions.

2.11 Conclusion

The positive experience with Eqs. (2.334)–(2.340) in the development of the IVA code *Kolev* (1985, 1993e, 1996, 1999) allows one to recommend these equations for general use. One should keep in mind for application purposes that both sides of the equations are local volume and time averages.

Understanding of the local volume and time average momentum equations is a prerequisite for understanding the second law of thermodynamics and its extremely interesting application to yield a simple description of this highly complicated system. As a next step in this direction, a rigorous formulation of the equations reflecting the second law of thermodynamics for this multiphase, multicomponent system has been successfully derived. The result of this derivation has formed the subject of a Chapter 5, see also *Kolev* (1995), and a comment to this publication (*Kolev* 1997).

Appendix 2.1

Substituting in the momentum conservation equation and performing time averaging,

$$\overline{\left\langle p_l^{\tau} \right\rangle^{le}} = p_l ,$$

$$\overline{\left\langle p_m^{\tau} \right\rangle^{me}} = p_m ,$$

$$\overline{\alpha_l \gamma_v \left\langle \rho_l \right\rangle^{l} \mathbf{V}_l} = \alpha_l \gamma_v \rho_l \mathbf{V}_l ,$$

$$\overline{\alpha_l \gamma_v \left\langle \rho_l \right\rangle^{l} \mathbf{V}_l'} = 0 ,$$

$$\overline{\alpha_l^e \gamma \left\langle \rho_l \right\rangle^{l} \mathbf{V}_l \mathbf{V}_l} = \alpha_l^e \gamma \rho_l \mathbf{V}_l \mathbf{V}_l ,$$

$$\overline{\alpha_l^e \gamma \left\langle \rho_l \right\rangle^{l} \mathbf{V}_l' \mathbf{V}_l} = 0 ,$$

$$\overline{\alpha_l^e \gamma \left\langle \rho_l \right\rangle^{l} \mathbf{V}_l' \mathbf{V}_l'} = \alpha_l^e \gamma \rho_l \overline{\mathbf{V}_l' \mathbf{V}_l'} ,$$

$$\overline{\nabla \cdot \left(\alpha_l^e \gamma \left\langle \mathbf{T}_l^{\tau} \right\rangle^{le} \right)} = \nabla \cdot \left(\alpha_l^e \gamma \mathbf{T}_l \right) ,$$

$$\overline{\alpha_l^e \gamma \nabla \cdot \left\langle p_l^{\tau} \right\rangle^{le}} = \alpha_l^e \gamma \nabla \cdot p_l ,$$

$$\overline{\alpha_l \gamma_v \left\langle \rho_l \right\rangle^{l} \mathbf{g}} = \alpha_l \gamma_v \rho_l \mathbf{g} ,$$

$$\sum_{m=1}^{3} \left(\overline{\mu_{ml}^{\tau} \left\langle \mathbf{V}_m^{\tau} \right\rangle^{me}} - \overline{\mu_{lm}^{\tau} \left\langle \mathbf{V}_l^{\tau} \right\rangle^{le}} \right) \approx \sum_{m=1}^{3} \left(\mu_{ml} \mathbf{V}_m - \mu_{lm} \mathbf{V}_l \right) ,$$

and

$$+ \left(p_l - p_m + \delta_l \sigma_{lm} \kappa_l \right) \left(\nabla \left(\alpha_l^e \gamma \right) + \frac{1}{Vol} \int_{F_{lw}} \mathbf{n}_l dF \right) - \delta_l \frac{1}{Vol} \int_{F_{l\sigma}} \left(\nabla_t \sigma_{lm} \right) dF$$

$$+ \frac{1}{Vol} \int_{F_{l\sigma}} \left(\Delta p_m^{l\sigma} \mathbf{I} - \mathbf{T}_m^{l\sigma} \right) \cdot \mathbf{n}_l dF + \frac{1}{Vol} \int_{F_{lw}} \left(\Delta p_l^{w\sigma} \mathbf{I} - \mathbf{T}_l^{w\sigma} \right) \cdot \mathbf{n}_l dF$$

$$= \gamma_v \sum_{m=1}^{3,w} \left(\mu_{ml} \mathbf{V}_m - \mu_{lm} \mathbf{V}_l \right)$$

$$\overline{\int_{F_{l\sigma}} \left\{ \left(-\Delta p_m^{l\sigma} \mathbf{I} + \mathbf{T}_m^{l\sigma} \right) \cdot \mathbf{n}_l - \nabla_t \sigma_{lm} \right\} dF + \int_{F_{lw}} \left(-\Delta p_l^{w\sigma} \mathbf{I} + \mathbf{T}_l^{w\sigma} \right) \cdot \mathbf{n}_l dF}$$

$$= \int_{F_{l\sigma}} \left\{ \left(-\Delta p_m^{l\sigma} \mathbf{I} + \mathbf{T}_m^{l\sigma} \right) \cdot \mathbf{n}_l - \nabla_t \sigma_{lm} \right\} dF + \int_{F_{lw}} \left(-\Delta p_l^{w\sigma} \mathbf{I} + \mathbf{T}_l^{w\sigma} \right) dF$$

one obtains Eq. (2.50a).

Appendix 2.2

The normal velocity difference can be obtained by splitting the relative velocity vector at the interface $\Delta\mathbf{V}_{lm}$ into a component that is parallel to $\mathbf{n}_l$

$$\Delta\mathbf{V}_{lm}^{n} = proj_{\mathbf{n}_l}\Delta\mathbf{V}_{lm} = \left(\frac{\Delta\mathbf{V}_{lm}\cdot\mathbf{n}_l}{\mathbf{n}_l\cdot\mathbf{n}_l}\right)\mathbf{n}_l = \left(\Delta\mathbf{V}_{lm}\cdot\mathbf{n}_l\right)\mathbf{n}_l,$$

with a magnitude

$$\left|\Delta\mathbf{V}_{lm}^{n}\right| = \left|\Delta\mathbf{V}_{lm}\cdot\mathbf{n}_l\right| = \sqrt{\left[n_{lx}\left(u_l-u_m\right)\right]^2+\left[n_{ly}\left(v_l-v_m\right)\right]^2+\left[n_{lz}\left(w_l-w_m\right)\right]^2}$$

and a component orthogonal to $\mathbf{n}_l$,

$$\Delta\mathbf{V}_{lm}^{t} = \Delta\mathbf{V}_{lm} - proj_{\mathbf{e}_l}\Delta\mathbf{V}_{lm} = \Delta\mathbf{V}_{lm} - \left(\Delta\mathbf{V}_{lm}\cdot\mathbf{n}_l\right)\mathbf{n}_l$$
$$= \left[\Delta u_{lm} - n_{lx}\left(\Delta\mathbf{V}_{lm}\cdot\mathbf{n}_l\right)\right]\mathbf{i} + \left[\Delta v_{lm} - n_{ly}\left(\Delta\mathbf{V}_{lm}\cdot\mathbf{n}_l\right)\right]\mathbf{j} + \left[\Delta w_{lm} - n_{lz}\left(\Delta\mathbf{V}_{lm}\cdot\mathbf{n}_l\right)\right]\mathbf{k}$$

Appendix 2.3

The nonconservative form of Eqs. (2.195) is

r direction:

$$\alpha_l\rho_l\left(\gamma_v\frac{\partial u_l}{\partial\tau}+\gamma_r\frac{1}{2}\frac{\partial u_l^2}{\partial r}+v_l\gamma_\theta\frac{1}{r^\kappa}\frac{\partial u_l}{\partial\theta}+w_l\gamma_z\frac{\partial u_l}{\partial z}\right)$$
$$-\frac{1}{r^\kappa}\frac{\partial}{\partial r}\left(r^\kappa\alpha_l\rho_l\nu_l^*\frac{\partial u_l}{\partial r}\gamma_r\right)-\frac{1}{r^\kappa}\frac{\partial}{\partial\theta}\left(\alpha_l\rho_l\nu_l^*\frac{1}{r^\kappa}\frac{\partial u_l}{\partial\theta}\gamma_\theta\right)-\frac{\partial}{\partial z}\left(\alpha_l\rho_l\nu_l^*\frac{\partial u_l}{\partial z}\gamma_z\right)$$
$$-\frac{\kappa}{r^\kappa}\alpha_l\rho_l\left[v_lv_l-\frac{2}{r^\kappa}\nu_l^*\left(\frac{\partial v_l}{\partial\theta}+u_l\right)\right]\gamma_\theta+\alpha_l\gamma_r\frac{\partial p}{\partial r}+\left(\alpha_l\rho_l g_r+f_{lu}\right)\gamma_v$$
$$=\gamma_v\left\{\sum_{m=1}^{3}\left[\mu_{ml}\left(u_m-u_l\right)\right]+\mu_{wl}\left(u_{wl}-u_l\right)-\mu_{lw}\left(u_{lw}-u_l\right)\right\}+f_{vlu};$$

θ direction:

$$\alpha_l\rho_l\left(\gamma_v\frac{\partial v_l}{\partial\tau}+u_l\gamma_r\frac{\partial v_l}{\partial r}+\gamma_\theta\frac{1}{2}\frac{1}{r^\kappa}\frac{\partial v_l^2}{\partial\theta}+w_l\gamma_z\frac{\partial v_l}{\partial z}\right)$$
$$-\frac{1}{r^\kappa}\frac{\partial}{\partial r}\left(r^\kappa\alpha_l\rho_l\nu_l^*\frac{\partial v_l}{\partial r}\gamma_r\right)-\frac{1}{r^\kappa}\frac{\partial}{\partial\theta}\left(\alpha_l\rho_l\nu_l^*\frac{1}{r^\kappa}\frac{\partial v_l}{\partial\theta}\gamma_\theta\right)-\frac{\partial}{\partial z}\left(\alpha_l\rho_l\nu_l^*\frac{\partial v_l}{\partial z}\gamma_z\right)$$

$$+\frac{\kappa}{r^{\kappa}}\alpha_l\rho_l\left[v_l u_l - r^{\kappa}\nu_l^*\frac{\partial}{\partial r}\left(\frac{v_l}{r^{\kappa}}\right)-\nu_l^*\frac{1}{r^{\kappa}}\frac{\partial u_l}{\partial\theta}\right]\gamma_\theta+\alpha_l\gamma_\theta\frac{1}{r^{\kappa}}\frac{\partial p}{\partial\theta}+\left(\alpha_l\rho_l g_\theta+f_{lv}\right)\gamma_v.$$

$$=\gamma_v\left\{\sum_{m=1}^{3}\left[\mu_{ml}\left(v_m-v_l\right)\right]+\mu_{wl}\left(v_{wl}-v_l\right)-\mu_{lw}\left(v_{lw}-v_l\right)\right\}+f_{vlv};$$

z direction:

$$\alpha_l\rho_l\left(\gamma_v\frac{\partial w_l}{\partial\tau}+u_l\gamma_r\frac{\partial w_l}{\partial r}+v_l\gamma_\theta\frac{1}{r^{\kappa}}\frac{\partial w_l}{\partial\theta}+\gamma_z\frac{1}{2}\frac{\partial w_l^2}{\partial z}\right)$$

$$-\frac{1}{r^{\kappa}}\frac{\partial}{\partial r}\left(r^{\kappa}\alpha_l\rho_l\nu_l^*\frac{\partial w_l}{\partial r}\gamma_r\right)-\frac{1}{r^{\kappa}}\frac{\partial}{\partial\theta}\left(\alpha_l\rho_l\nu_l^*\frac{1}{r^{\kappa}}\frac{\partial w_l}{\partial\theta}\gamma_\theta\right)-\frac{\partial}{\partial z}\left(\alpha_l\rho_l\nu_l^*\frac{\partial w_l}{\partial z}\gamma_z\right)$$

$$+\alpha_l\gamma_z\frac{\partial p}{\partial z}+\left(\alpha_l\rho_l g_z+f_{lw}\right)\gamma_v$$

$$=\gamma_v\left\{\sum_{m=1}^{3}\left[\mu_{ml}\left(w_m-w_l\right)\right]+\mu_{wl}\left(w_{wl}-w_l\right)-\mu_{lw}\left(w_{lw}-w_l\right)\right\}+f_{vlw}.$$

Some simple single-phase test cases: For testing numerical solutions it is important to provide a set of simple benchmarks having analytical solutions. Some of them are presented here.

Rigid body steady rotation problem: This test problem presents a hollow cylinder with symmetric flow in the azimuth direction, see Fig. A2.3-1. No axial and radial flow exists. The mass conservation equation gives $\frac{\partial v}{\partial\theta}=0$. The r direction momentum equation simplifies to $\rho\frac{v^2}{r}=\frac{\partial p}{\partial r}$, and the θ direction momentum equation gives $\frac{\partial p}{\partial\theta}=0$. For constant rotational frequency ω, $\left(v(r)=\mathrm{r}\omega\right)$, the analytical solution of the radial momentum equation is $p-p_0=\frac{1}{2}\rho\omega^2\left(r^2-r_0^2\right)$ or $p-p_0=\frac{1}{2}\rho\left[v(r)\right]^2\left[1-\left(\frac{r_0}{r}\right)^2\right]$.

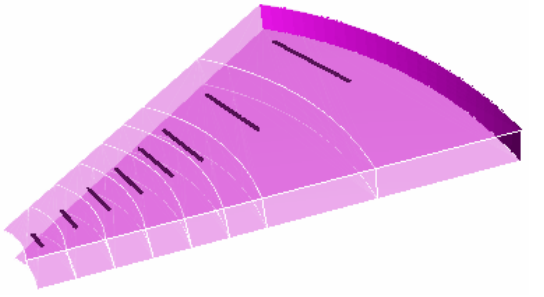

Fig. A2.3-1 Geometry of the test problem *rigid body steady rotation*

Pure radial symmetric flow: This test problem presents a hollow cylinder with symmetric flow in the radial direction, see Fig. A2.3-2.

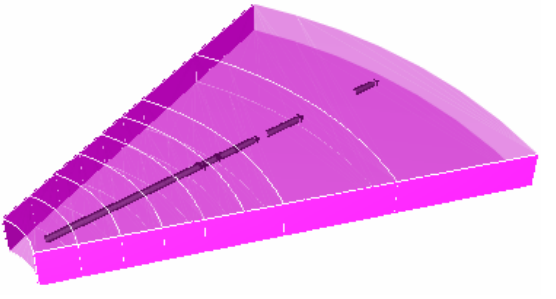

Fig. A2.3-2 Geometry of the test problem *pure radial symmetric flow*

No axial and azimuthal flow exists. The mass conservation equation gives $\frac{\partial}{\partial r}(ru)=0$. The r direction momentum equation simplifies to $\rho\frac{1}{2}\frac{\partial u^2}{\partial r}=-\frac{\partial p}{\partial r}$, and the θ direction momentum equation gives $\frac{\partial p}{\partial \theta}=0$. From the mass conservation we have $u=u_0\frac{r_0}{r}$. The analytical solution of the radial momentum equation is the well-known *Bernoulli* equation $p-p_0=-\frac{1}{2}\rho\left(u^2-u_0^2\right)$ or

$$p-p_0=\frac{1}{2}\rho u_0^2\left[1-\left(\frac{r_0}{r}\right)^2\right].$$

Radial-azimuthal symmetric flow: This test problem presents a hollow cylinder with symmetric flow in the radial and azimuthal directions – it is, in fact, a superposition of the previous two cases, rigid body steady rotation and pure radial symmetric flow, see Fig. A2.3-3. No axial flow exists. The mass conservation eq-

uation gives $\frac{\partial}{\partial r}(ru)=0$. The r direction momentum equation simplifies to $\rho\left(\frac{1}{2}\frac{\partial u^2}{\partial r}-\frac{v^2}{r}\right)=-\frac{\partial p}{\partial r}$, and the θ-direction momentum equation gives $\rho u\left(\frac{\partial v}{\partial r}+\frac{v}{r}\right)=-\frac{1}{r}\frac{\partial p}{\partial \theta}$. From the mass conservation we have $u=u_0\frac{r_0}{r}$. From the azimuthal symmetry, $\frac{\partial p}{\partial \theta}=0$, the θ direction momentum equation gives $\frac{\partial v}{\partial r}+\frac{v}{r}=0$ or $v=v_0\frac{r_0}{r}$. Taking into account the both solutions of the mass and of the θ momentum equation the radial momentum equation gives $\rho\frac{1}{r}\left(u^2+v^2\right)=\frac{\partial p}{\partial r}$ or $\rho\left(u_0^2+v_0^2\right)r_0^2\frac{1}{r^3}=\frac{\partial p}{\partial r}$ or

$$p-p_0=\rho\left(u_0^2+v_0^2\right)r_0^2\frac{1}{2}\left(\frac{1}{r_0^2}-\frac{1}{r^2}\right).$$

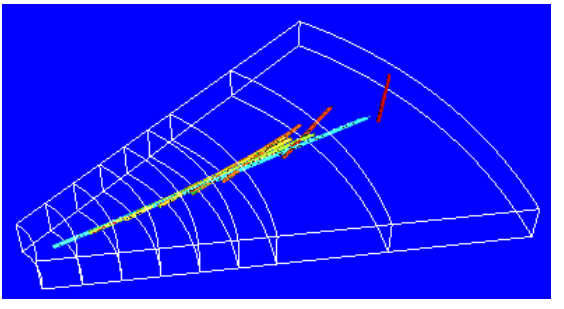

Fig. A2.3-3 Geometry of the test problem *radial-azimuthal symmetric flow*

Trajectory of particles in a known gas field: Consider flow of particles with very small concentrations in a known gas velocity field. Compute the trajectory of a particle with mass m_i taking into account only the drag force and assuming the validity of *Stokes'* law. Such a task was usually solved in the past for computing trajectories of particles in cyclone separators. If in such computations, the trajectory ends in the particle capturing devices, this class characterized by particle size and starting coordinate is considered as removed from the gas flow. The three simplified momentum equations are then

$$\rho_i\frac{\pi D_{3,i}^3}{6}\left(\frac{du_{3,i}}{d\tau}-\frac{v_{3,i}^2}{r}\right)=3\pi\eta_1 D_{3,i}\left(u_1-u_{3,i}\right),\quad \frac{du_{3,i}}{d\tau}=\frac{v_{3,i}^2}{r}+\frac{18\eta_1}{\rho_i D_{3,i}^2}\left(u_1-u_{3,i}\right),$$

$$\rho_i\frac{\pi D_{3,i}^3}{6}\left(\frac{dv_{3,i}}{d\tau}+\frac{v_{3,i}u_{3,i}}{r}\right)=3\pi\eta_1 D_{3,i}\left(v_1-v_{3,i}\right),\quad \frac{dv_{3,i}}{d\tau}=-\frac{v_{3,i}u_{3,i}}{r}+\frac{18\eta_1}{\rho_i D_{3,i}^2}\left(v_1-v_{3,i}\right),$$

$$\rho_i \frac{\pi D_{3,i}^3}{6} \frac{dw_{3,i}}{d\tau} = 3\pi\eta_1 D_{3,i}\left(w_1 - w_{3,i}\right), \quad \frac{dw_{3,i}}{d\tau} = \frac{18\eta_1}{\rho_i D_{3,i}^2}\left(w_1 - w_{3,i}\right).$$

For constant gas velocity and particle size the analytical solution is provided by *Crowe* and *Patt* (1974)

$$w_{3,i} = w_1 - \left(w_1 - w_{3,i,a}\right)\exp\left(-\Delta\tau/\Delta\tau_{13}\right),$$

$$u_{3,i} = u_1 - \left(u_1 - u_{3,i,a}\right)\exp\left(-\Delta\tau/\Delta\tau_{13}\right) + \left[1 - \exp\left(-\Delta\tau/\Delta\tau_{13}\right)\right]\Delta\tau_{13}\, v_{3,i}^2/r,$$

$$v_{3,i} = v_1 - \left(v_1 - v_{3,i,a}\right)\exp\left(-\Delta\tau/\Delta\tau_{13}\right) - \left[1 - \exp\left(-\Delta\tau/\Delta\tau_{13}\right)\right]\Delta\tau_{13}\, v_{3,i} u_{3,i}/r,$$

where

$$\Delta\tau_{13} = \left(\rho_3 D_{3i}^2\right)/\left(18\eta_1\right)$$

is the *Stokes* relaxation time constant. Knowing the initial position and the velocity, the position after the time interval $\Delta\tau$ can be computed by using the *Euler* method.

The Kreith and Sonju solution for the decay of turbulent swirl in a pipe: *Kreith* and *Sonju* (1965) analyzed steady turbulent swirl in a pipe. After making several reasonable simplifying assumptions the authors arrived at the following form of the tangential momentum equation:

$$w\frac{\partial v}{\partial z} = \left(\nu + \nu^t\right)\left(\frac{\partial^2 v}{\partial r^2} + \frac{1}{r}\frac{\partial v}{\partial r} - \frac{v}{r^2}\right),$$

or in nondimensional form

$$\frac{\partial \overline{v}}{\partial \overline{z}} = \frac{\overline{v}}{\mathrm{Re}}\left(\frac{\partial^2 \overline{v}}{\partial \overline{r}^2} + \frac{1}{\overline{r}}\frac{\partial \overline{v}}{\partial \overline{r}} - \frac{\overline{v}}{\overline{r}^2}\right),$$

where $\overline{v} = v/w_{\max}$, $\overline{r} = r/R$, $\overline{v} = \left(\nu + \nu^t\right)/\nu$, $\overline{z} = z/R$, and $\mathrm{Re} = wR/\nu$. The authors solved this equation by separation of the variables for the following boundary conditions: $v = 0$ at $r = 0$ and $r = \mathrm{R}$, $v(r, 0) = f(r)$ at $z = 0$. The initial condition was gained from experimental data for the initial distribution of the tangential velocity behind a tape swirler

$$\overline{v}\left(\overline{r}, 0\right) = \left[6.3\overline{r} - 0.013\left(1.1 - \overline{r}\right)^{-2.68}\right]/\overline{\Delta z}_{ts},$$

where $\overline{\Delta z}_{ts} = \Delta z_{ts}/R$, Δz_{ts} is the length of the tape swirler making a complete 360° rotation.

$$\overline{v}\left(\overline{r}, \overline{z}\right) = \frac{7.78}{\overline{H}} J_1\left(3.832\overline{r}\right)\exp\left(-16.7\frac{\overline{\nu}\,\overline{z}}{\mathrm{Re}}\right) - \frac{5.26}{\overline{H}} J_1\left(7.016\overline{r}\right)\exp\left(-55.7\frac{\overline{\nu}\,\overline{z}}{\mathrm{Re}}\right)$$

$$+ \frac{3.93}{\overline{H}} J_1\left(10.174\overline{r}\right)\exp\left(-117.9\frac{\overline{\nu}\,\overline{z}}{\mathrm{Re}}\right) - \frac{3.16}{\overline{H}} J_1\left(13.324\overline{r}\right)\exp\left(-203.7\frac{\overline{\nu}\,\overline{z}}{\mathrm{Re}}\right) + \ldots$$

J_1 is the *Bessel*'s function of the first kind of order one. From experimental data the relation $\overline{v} = 1 + 2.03\times10^{-3}\,\mathrm{Re}^{0.86}$ was recommended for $4\times10^4 < \mathrm{Re} < 1\times10^6$. Experimental data for Re = 18 000 and 61 000 validate the approximate solution.

The data indicate the initial swirl decay to be about 20% at $\overline{z} = 100$. There are authors trying to represent the decay by a single exponential function. From the data collected by *Steenberger* (1995) it is visible that the decay coefficient is a decreasing function with increasing Reynolds number as manifested by the above solution. Note the practical importance of this solution. Having the rotation introduced by twisted tapes in the cylinder particle trajectories can be computed and, therefore, the efficiency of separation devices can be judged.

References

Albring, W.: Angewandte Strömungslehre. Theodor Steinkopff, Dresden (1970)

Anderson, T.B., Jackson, R.: A fluid mechanical description of fluidized beds. Ind. Eng. Fundam. 6, 527 (1967)

Antal, S.P., Lahey Jr., R.T., Flaherty, J.E.: Analysis of phase distribution in a fully developed laminar bubbly two-phase flow. Int. J. Multiphase Flow 17(5), 635–652 (1991)

Auton, R.T.: The lift force on a spherical body in rotating flow. J. Fluid Mechanics 183, 199–218 (1987)

Barnea, D., Taitel, Y.: Interfacial and structural stability. Int. J. Multiphase Flow 20(suppl.), 387–414 (1994)

Bataille, J., Lance, M., Marie, J.L.: Bubble turbulent shear flows. In: ASME Winter Annular Meeting, Dallas (November 1990)

Bernemann, K., Steiff, A., Weinspach, P.M.: Zum Einfluss von längsangeströmten Rohrbündeln auf die großräumige Flüssigkeitsströmung in Blasensäulen. Chem. Ing. Tech. 63(1), 76–77 (1991)

Biberg, D.: An explicit approximation for the wetted angle in two-phase stratified pipe flow. The Canadian Journal of Chemical Engineering 77, 1221–1224 (1999)

Biesheuvel, A., van Wijngaarden, L.: Two-phase flow equations for a dilute dispersion of gas bubbles in liquid. J. Fluid Mechanics 168, 301–318 (1984)

Biesheuvel, A., Spoelstra, S.: The added mass coefficient of a dispersion of spherical gas bubbles in liquid. Int. J. Multiphase Flow 15, 911–924 (1989)

Bournaski, E.: Numerical simulation of unsteady multiphase pipeline flow with virtual mass effect. Int. J. Numer. Meth. Eng. 34, 727–740 (1992)

Boussinesq, J.: Essai sur la théorie des eaux courantes. Mem. Pŕs. Acad. Sci. 23, 46 (1877)

Brackbill, J.U., Kothe, D.B., Zemach, C.: A continuum method for modeling surface tension. J. Comput. Phys. 100, 335–354 (1992)

Brauner, N., Maron, D.M.: Stability analysis of stratified liquid–liquid flow. Int. J. Multiphase Flow 18(1), 103–121 (1992)

Crowe, C.T., Pratt, D.T.: Analysis of the flow field in cyclone separators. Comp. Fluids 2, 249–260 (1974)

Cook, T.L., Harlow, F.H.: VORT: A computer code for bubble two-phase flow. Los Alamos National Laboratory documents LA-10021-MS (1983)

Cook, T.L., Harlow, F.H.: Virtual mass in multi-phase flow. Int. J. Multiphase Flow 10(6), 691–696 (1984)

de Crecy, F.: Modeling of stratified two-phase flow in pipes, pumps and other devices. Int. J. Multiphase Flow 12(3), 307–323 (1986)

Deich, M.E., Philipoff, G.A.: Gas dynamics of two phase flows, Energoisdat, Moskva (1981)

Delhaye, J.M.: Basic equations for two-phase flow. In: Bergles, A.E., et al. (eds.) Two-Phase Flow and Heat Transfer in Power and Process Industries. Hemisphere Publishing Corporation, McGraw-Hill Book Company, New York (1981)

Delhaye, J.M., Giot, M., Riethmuller, M.L.: Thermohydraulics of two-phase systems for industrial design and nuclear engineering. Hemisphere Publishing Corporation, McGraw Hill Book Company, New York (1981)

Drazin, P.G., Reid, W.H.: Hydrodynamic Stability. Cambridge Univ. Press, Cambridge (1981)

Drew, D.A., Lahey Jr., R.T.: The virtual mass and lift force on a sphere in rotating and straining flow. Int. J. Multiphase Flow 13(1), 113–121 (1987)

Erichhorn, R., Small, S.: Experiments on the lift and drag of spheres suspended in a Poiseuille flow. J. Fluid Mech. 20(3), 513 (1969)

Gray, W.G., Lee, P.C.Y.: On the theorems for local volume averaging of multi-phase system. Int. J. Multi-Phase Flow 3, 222–340 (1977)

Helmholtz, H.: Über diskuntinuirliche Flüssigkeitsbewegungen, Monatsberichte der Königlichen Akademie der Wissenschaften zu Berlin, pp. 215–228 (1868)

Hetstrony, G.: Handbook of multi-phase systems. Hemisphere Publ. Corp., McGraw-Hill Book Company, Washington, New York (1982)

Hirt, C.W., Nichols, B.D.: Volume of fluid (VOF) method for dynamics of free boundaries. J. of Comp. Physics 39, 201–225 (1981)

Ho, B.P., Leal, L.G.: Internal migration of rigid spheres in two-dimensional unidirectional flows. J. Fluid Mech. 78(2), 385 (1976)

Hwang, G.J., Schen, H.H.: Tensorial solid phase pressure from hydrodynamic interaction in fluid-solid flows. In: Proc. of the Fifth International Topical Meeting on Reactor Thermal Hydraulics, NURETH-5, Salt Lake City, UT, USA, September 21-24, vol. IV, pp. 966–971 (1992)

Ishii, M.: Thermo-fluid dynamic theory of two-phase flow. Eyrolles, Paris (1975)

Ishii, M., Michima, K.: Two-fluid model and hydrodynamic constitutive relations. NSE 82, 107–126 (1984)

Jeffrey, D.: Condition to a random suspension of spheres. Proc. R. Soc. London A335, 355–367 (1973)

Kendoush, A.A.: Modification of the classical theory of the virtual mass of an accelerated spherical particle. In: Proc. of the FEDSM 2006, 2006 ASME Joint US-European Fluids Engineering Summer Meeting, Miami, FL, July 17-20 (2006)

Klausner, J.F., Mei, R., Bernhard, D., Zeng, L.Z.: Vapor bubble departure in forced convection boiling. Int. J. Heat Mass Transfer 36, 651–662 (1993)

Kolev, N.I.: Two-phase two-component flow (air-water steam-water) among the safety compartments of the nuclear power plants with water cooled nuclear reactors during lose of coolant accidents, PhD Thesis, Technical University Dresden (1977)

Kolev, N.I.: Transiente Dreiphasen-Dreikomponenten Strömung, Teil 1: Formulierung des Differentialgleichungssystems, KfK 3910 (March 1985)

Kolev, N.I.: Transiente Dreiphasen-Dreikomponenten Strömung, Teil 3: 3D-Dreifluid-Diffusionsmodell, KfK 4080 (1986a)

Kolev, N.I.: Transient three-dimensional three-phase three-component non equilibrium flow in porous bodies described by three-velocity fields. Kernenergie 29(10), 383–392 (1986b)

Kolev, N.I.: A three field-diffusion model of three-phase, three-component Flow for the transient 3D-computer code IVA2/001. Nuclear Technology 78, 95–131 (1987)

Kolev, N.I.: IVA3: A transient 3D three-phase, three-component flow analyzer. In: Proc. of the Int. Top. Meeting on Safety of Thermal Reactors, Portland, Oregon, July 21-25, pp. 171–180 (1991a); Also presented at the 7th Meeting of the IAHR Working Group on Advanced Nuclear Reactor Thermal-Hydraulics, Kernforschungszentrum Karlsruhe, August 27-29 (1991)

Kolev, N.I.: A three-field model of transient 3D multi-phase, three-component flow for the computer code IVA3, Part 1: Theoretical basics: conservation and state equations, Numerics. KfK 4948, Kernforschungszentrum Karlsruhe (September 1991b)

Kolev, N.I., Tomiyama, A., Sakaguchi, T.: Modeling of the mechanical interaction between the velocity fields in three-phase flow. Experimental Thermal and Fluid Science 4(5), 525–545 (1991)

Kolev, N.I.: The code IVA3 for modeling of transient three-phase flows in complicated 3D geometry. Kerntechnik 58(3), 147–156 (1993)

Kolev, N.I.: IVA3 NW: Computer code for modeling of transient three-phase flow in complicated 3D geometry connected with industrial networks. In: Proc. of the Sixth Int. Top. Meeting on Nuclear Reactor Thermal Hydraulics, Grenoble, France, October 5-8 (1993)

Kolev, N.I.: Berechnung der Fluiddynamischen Vorgänge bei einem Sperrwasser-Kühlerrohrbruch, Projekt KKW Emsland, Siemens KWU Report R232/93/0002 (1993)

Kolev, N.I.: IVA3-NW A three phase flow network analyzer. Input description, Siemens KWU Report R232/93/E0041 (1993)

Kolev, N.I.: IVA3-NW components: relief valves, pumps, heat structures, Siemens KWU Report R232/93/E0050 (1993)

Kolev, N.I.: IVA4: Modeling of mass conservation in multi-phase multi-component flows in heterogeneous porous media. Kerntechnik 59(4-5), 226–237 (1994a)

Kolev, N.I.: The code IVA4: Modelling of momentum conservation in multi-phase multi-component flows in heterogeneous porous media. Kerntechnik 59(6), 249–258 (1994b)

Kolev, N.I.: The code IVA4: Second law of thermodynamics for multi phase flows in heterogeneous porous media. Kerntechnik 60(1), 1–39 (1995)

Kolev, N.I.: Three Fluid Modeling with Dynamic Fragmentation and Coalescence Fiction or Daily practice? In: 7th FARO Experts Group Meeting Ispra, October 15-16 (1996); Proceedings of OECD/CSNI Workshop on Transient Thermal-Hydraulic and Neutronic Codes Requirements, Annapolis, MD, November 5–8 (1996); 4th World Conference on Experimental Heat Transfer, Fluid Mechanics and Thermodynamics, ExHFT 4, Brussels, June 2-6 (1997); ASME Fluids Engineering Conference & Exhibition, The Hyatt Regency Vancouver, British Columbia, June 22-26 (1997); Invited Paper; Proceedings of 1997 International Seminar on Vapor Explosions and Explosive Eruptions (AMIGO-IMI), Aoba Kinen Kaikan of Tohoku University, Sendai-City, Japan, May 22-24 (1997)

Kolev, N.I.: Comments on the entropy concept. Kerntechnik 62(1), 67–70 (1997)

Kolev, N.I.: Verification of IVA5 computer code for melt-water interaction analysis, Part 1: Single phase flow, Part 2: Two-phase flow, three-phase flow with cold and hot solid spheres, Part 3: Three-phase flow with dynamic fragmentation and coalescence, Part 4: Three-phase flow with dynamic fragmentation and coalescence – alumna experiments. In: CD Proceedings of the Ninth International Topical Meeting on Nuclear Reactor Thermal Hydraulics (NURETH-9), San Francisco, CA, October 3-8 (1999); Log. Nr. 315

Kreith, F., Sonju, O.K.: The decay of turbulent swirl in pipe. J. Fluid Mech. 2, part 2, 257–271 (1965)

Krepper, E., Lucas, D., Prasser, H.-M.: On the modeling of bubbly flow in vertical pipes. Nucl. Eng. Des. 235, 597–611 (2005)

Krepper, E., Egorov, Y.: CFD-Modeling of subcooled boiling and application to simulate a hot channel of fuel assembly. In: 13th Int. Conference on Nuclear Engineering, Beijing, China, May 16-20 (2005)

Lahey Jr., R.T.: Void wave propagation phenomena in two-phase flow. AIChE Journal 31(1), 123–135 (1991)

Lahey Jr., R.T.: The analysis of phase separation and phase distribution phenomena using two-fluid models. NED 122, 17–40 (1990)

Lahey Jr., R.T., Lopez de Bertodano, M., Jones Jr., O.C.: Phase distribution in complex geometry conditions. Nucl. Eng. Des. 141, 177–201 (1993)

Lance, M., Bataille, J.: Turbulence in the liquid phase of a uniform bubbly air-water flow. J. Fluid Mech. 22, 95–118 (1991)

Lamb, M.A.: Hydrodynamics. Cambridge University Press, Cambridge (1945)

Lamb, H.: Hydrodynamics. Dover, New York (1945)

Laurien, E., Niemann, J.: Determination of the virtual mass coefficient for dense bubbly flows by direct numerical simulation. In: 5th Int. Conf. on Multiphase Flow, Yokohama, Japan, paper no 388 (2004)

Lopez de Bertodano, M.: Turbulent bubbly two-phase flow in triangular duct, PhD Thesis, Renssaelaer Polytechnic Institute, Troy, NY (1992)

Mamaev, W.A., Odicharia, G.S., Semeonov, N.I., Tociging, A.A.: Gidrodinamika gasogidkostnych smesey w trubach, Moskva (1969)

Mei, R.: An approximate expression for the shear lift force on spherical particle at finite Reynolds number. Int. J. Multiphase Flow 18(1), 145–147 (1992)

Mei, R., Klausner, J.F.: Shear lift force on spherical bubbles. Int. J. Heat Fluid Flow 15, 62–65 (1995)

Milne-Thomson, L.M.: Theoretical Hydrodynamics. MacMillan & Co. Ltd., London (1968)

Mokeyev, G.Y.: Effect of particle concentration on their drag induced mass. Fluid. Mech. Sov. Res. 6, 161 (1977)

Naciri, A.: Contribution à l'étude des forces exercées par un liquide sur une bulle de gaz: portance, masse ajoutée et interactions hydrodynamiques, Doctoral Dissertation, École Central de Lyon, France (1992)

Nigmatulin, R.I.: Spatial averaging in the mechanics of heterogeneous and dispersed systems. Int. J. Multiphase Flow 4, 353–385 (1979)

Nigmatulin, R.T.: Spatial averaging in the mechanics of heterogeneous and dispersed systems. Int. J. of Multiphase Flow 5, 353–389 (1979)

No, H.C., Kazimi, M.S.: Effects of virtual mass of the mathematical characteristics and numerical stability of the two-fluid model. In: NSE, vol. 89, pp. 197–206 (1985)

Pougatch, K., Salcudean, M., Chan, E., Knapper, B.: Modeling of compressible gas–liquid flow in convergent-divergent nozzle. Chemical Engineering Science 63, 4176–4188 (2008)

Prandtl, L.: Essentials of Fluid Dynamics, p. 342. Blackie & Son, Glasgow (1952)

Ransom, V.H., et al.: RELAP5/MOD2 Code manual, vol 1: Code structure, system models, and solution methods, NUREG/CR-4312, EGG-2396. rev. 1 (March 1987)

Ruggles, A.E., et al.: An investigation of the propagation of pressure perturbation in bubbly air/water flows. Trans. ASME J. Heat Transfer 110, 494–499 (1988)

Schlichting, H.: Boundary layer theory. McGraw-Hill, New York (1959)
Sha, T., Chao, B.T., Soo, S.L.: Porous-media formulation for multi-phase flow with heat transfer. Nuclear Engineering and Design 82, 93–106 (1984)
Shi, J.-M., Burns, A.D., Prasser, H.-M.: Turbulent dispersion in poly-dispersed gas–liquid flows in a vertical pipe. In: 13th Int. Conf. on Nuclear Engineering, ICONE, Beijing, China, May 16-20, vol. 13 (2005)
Slattery, J.C.: Flow of visco-elastic fluids through porous media. AIChE J. 13, 1066 (1967)
Slattery, J.C.: Interfacial transport phenomena. Springer, Heidelberg (1990)
Slattery, J.C.: Advanced transport phenomena. Cambridge University Press, Cambridge (1999)
Staffman, P.G.: The lift on a small sphere in a slow shear flow. J. Fluid Mech. 22, Part 2, 385–400 (1965)
Staffman, P.G.: Corrigendum to "The lift on a small sphere in a slow shear flow". J. Fluid Mech. 31, 624 (1968)
Steenberger, W.: Turbulent flow in a pipe with swirl, PhD thesis Eindhoven University of Technology (1995)
Stokes, G.G.: On the theories of the internal friction of fluids in motion and of the equilibrium and motion of elastic solids. Trans. Cambridge Phil. Soc. 8, 287–305 (1845)
Stuhmiller, J.H.: The influence of the interfacial pressure forces on the character of the two-phase flow model. In: Proc. of the 1977 ASME Symp. on Computational Techniques for Non-Equilibrium Two-Phase Phenomena, pp. 118–124 (1977)
Thomas Jr., G.B., Finney, R.L., Weir, M.D.: Calculus and analytic geometry, 9th edn. Addison-Wesley Publishing Company, Reading (1998)
Tomiyama, A.: Struggle with computational bubble dynamics. In: Proc. of the 3rd Int. Conf. on Multiphase Flow ICMF-1998, France (1998)
Tomiyama, A., et al.: Transverse migration of single bubbles in simple shear flows. Chem. Eng. Sci. 57, 1849–1858 (2002)
Trent, D.S., Eyler, L.L.: Application of the TEMPTEST computer code for simulating hydrogen distribution in model containment structures, PNL-SA-10781, DE 83 002725 (1983)
Truesdell, C.: Essays in the history of mechanics. Springer, New York (1968)
van Wijngaarden, L.: Hydrodynamic interaction between the gas bubbles in liquid. J. Fluid Mechanics 77, 27–44 (1976)
van Wijngaarden, L.: On pseudo turbulence. Theor. Comp. Fluid Dyn. 10, 449–458 (1998)
Vasseur, P., Cox, R.G.: The lateral migration of spherical particles in two-dimensional shear flows. J. Fluid Mech. 78, Part 2, 385–413 (1976)
Wang, S.K., Lee, S.J., Jones, O.C., Lahey Jr., R.T.: 3-D turbulence structure and phase distribution measurements in bubbly two-phase flows. Int. J. Multiphase Flow 13(3), 327–343 (1987)
Wellek, R.M., Agrawal, A.K., Skelland, A.H.P.: Shapes of liquid drops moving in liquid media. AIChE J. 12, 854 (1966)
Whitaker, S.: Diffusion and dispersion in porous media. AIChE Journal 13, 420 (1967)
Whitaker, S.: Advances in theory of fluid motion in porous media. Ind. Engrg. Chem. 61(12), 14–28 (1969)
Whitaker, S.: A Simple geometrical derivation of the spatial averaging theorem. Chem. Eng. Edu., 18–21, 50-52 (1985)

Winatabe, T., Hirano, M., Tanabe, F., Kamo, H.: The effect of the virtual mass force term on the numerical stability and efficiency of the system calculations. Nucl. Eng. Des. 120, 181–192 (1990)

Wallis, G.B.: One-dimensional two-phase flow. McGraw-Hill, New York (1969)

Yamamotto, Y., Potthoff, M., Tanaka, T., Kajishima, Tsui, Y.: Large-eddy simulation of turbulent gas-particcle flow in a vertical channel: effect of considering inter-particle collisions. J. Fluid Mech. 442, 303–334 (2001)

Zuber, N.: On the dispersed two-phase flow in the laminar flow regime. Chem. Eng. Science 49, 897–917 (1964)

Zun, I.: The transferees migration of bubbles influenced by walls in vertical bubbly flow. Int. J. Multiphase Flow 6, 583–588 (1980)